

Aus der Medizinischen Klinik und Poliklinik IV
Klinikum der Ludwig-Maximilian-Universität München



Complement C5a blockade is sufficient to resolve crystalline thrombotic microangiopathy

Dissertation
zum Erwerb des Doktorgrades der Humanbiologie
an der Medizinischen Fakultät der
Ludwig-Maximilians-Universität zu München

vorgelegt von

Danyang Zhao

aus
Heilongjiang, China

Jahr
2024

Mit Genehmigung der Medizinischen Fakultät der
Ludwig-Maximilians-Universität München

Erstes Gutachten: Prof. Dr. Hans-Joachim Anders
Zweites Gutachten: PD Dr. Sebastian Clauß
Drittes Gutachten: Prof. Dr. Alexander Bartelt

Dekan: Prof. Dr. med. Thomas Gudermann

Tag der mündlichen Prüfung: 17.07.2024

Table of Contents

Declaration	iv
Zusammenfassung.....	v
1. Introduction	1
1.1 Innate system.....	1
1.2 The complement system.....	2
1.2.1 Activation of complement system	4
1.2.2 Complement membrane attack complex	5
1.2.3 Complement Factor 3	6
1.2.4 Complement Factor 5a.....	6
1.3 Complement system and kidney thrombotic microangiopathy.....	7
1.3.1 Thrombotic microangiopathy.....	7
1.3.2 Clinical presentations of atypical hemolytic uremic syndrome	9
1.3.3 Therapy for atypical hemolytic uremic syndrome	9
1.3.4 Safety concerns with C5 inhibition	10
1.4 Acute kidney injury and acute kidney disease.....	10
1.4.1 Pathophysiology of ischemia-induced acute kidney injury	12
1.4.2 Impact of the complement system in acute kidney injury	15
1.5 Complement-related therapy in acute kidney injury	16
1.6 Cholesterol crystal embolism	17
1.6.1 Clinical manifestation of cholesterol crystal embolism.....	17
1.6.2 Treatment of cholesterol crystal embolism.....	18
2. Research hypothesis	19
3. Material and Methods.....	20
3.1 Materials.....	20
3.2 Experimental Procedures.....	27
3.2.1 Animals	27
3.2.2 Animal models	27
3.2.3 Measurement of arterials obstructions	29
3.2.4 C5a-C5aR axis in cholesterol crystal-induced thrombotic microangiopathy.....	31
3.2.5 Preemptive therapy of C5a inhibitor on cholesterol crystal embolism-induced thrombotic microangiopathy.....	32
3.2.6 Therapeutic window of C5a inhibition on cholesterol crystal embolism-driven thrombotic microangiopathy.....	33
3.2.7 Mechanism of C5a inhibitor on cholesterol crystal embolism-induced thrombotic microangiopathy.....	34
3.3 Preparation of cholesterol crystal working solution	36
3.4 Primary and Secondary endpoints.....	36
3.5 Periodic acid Schiff (PAS) staining	37
3.6 Immunostaining	39

3.6.1 Neutrophil infiltration analysis.....	40
3.6.2 CD31 staining	40
3.6.3 Alpha-smooth muscle actin (α -SMA) / fibrinogen staining	41
3.7 TUNEL staining	41
3.8 RNA isolation and quantitative real-time PCR.....	41
3.8.1 Total RNA Isolation.....	41
3.8.2 RNA reverse transcription.....	42
3.8.3 Quantitative real-time PCR	42
3.9 Mouse neutrophil isolation and flow cytometry	43
3.10 Flow chamber assay.....	43
3. 11 Statistical analyses.....	44
4. Results	45
4.1 C3 deficiency entirely abrogated thrombotic microangiopathy	45
4.1.1 Cholesterol crystal-induced acute kidney injury and infarct size with C3-Deficiency.....	45
4.1.2 Cholesterol crystal embolism-related arterial occlusion with C3-deficiency	46
4.1.3 Neutrophil infiltration and endothelium injury in crystalline thrombotic microangiopathy with C3-deficiency.....	48
4.1.4 Kidney injury caused by cholesterol crystal-related thrombotic microangiopathy with C3-deficiency	50
4.1.5 Thrombotic microangiopathy-related cell death in mice with C3-deficiency	51
4.2 C5a/C5aR axis in crystalline thrombotic microangiopathy.....	52
4.2.1 C5a/C5aR axis improved kidney function and reduced infarct size in crystalline thrombotic microangiopathy.....	52
4.2.2 The C5a/C5aR mediated cholesterol crystal embolism-related arterial occlusion.....	54
4.2.3 The C5a/C5aR mediated endothelial injury and immune cell infiltration	55
4.2.4 C5a/C5aR diminished cell death in crystalline thrombotic microangiopathy	57
4.2.5 C5a/C5aR inhibition mitigated CCE-induced kidney injury.....	58
4.3 C5a inhibition resolved established thrombotic microangiopathy	59
4.3.1 Early treatment of C5a inhibitor improved kidney function in established thrombotic microangiopathy.....	59
4.3.2 Administration of C5a inhibitor at early thrombotic microangiopathy alleviated thrombus formation	60
4.3.3 Early treatment of C5a inhibitor ameliorated endothelial injury and immune cell migration in established thrombotic microangiopathy.....	61
4.3.4 Early treatment of C5a inhibitor protected kidney from cell death in established thrombotic microangiopathy.....	62
4.3.5 Role of C5a in kidney injury.....	63
4.4 Mechanism-of-action of C5a inhibition.....	64
4.4.1 Role of C5a in endothelial cells injury caused by cholesterol crystals	64
4.4.2 Role of C5a in neutrophil migration initiated by cholesterol crystals	67
4.4.3 Role of C5a in platelet activation and platelet-interaction with neutrophils.....	68
5. Discussion	71

5.1 Ablation of the complement system attenuates kidney thrombotic microangiopathy and its consequences	71
5.2 Targeting the C5a/C5aR axis reduces kidney damage during crystalline thrombotic microangiopathy.....	73
5.3 Mechanism-of-action of C5a inhibition.....	74
5.4 Delayed therapy of C5a inhibition still alleviates kidney injury.....	77
6. Summary	82
7. References	83
8.Acknowledgement	99

Declaration

I hereby acknowledge and express my gratitude to the authors and researchers whose work and ideas have been cited and referenced in this thesis. I declare that all the original work present in this thesis was conducted by myself from 10/2019 until 09/2023 under the supervision of Prof. Dr. Hans Joachim Anders, Nephrologisches Zentrum, Medizinische Klinik und Poliklinik IV, Innenstadt Klinikum der Universität München. This work has not been submitted in part or full to any other university or institute for any degree or diploma, any sources of information, data, or ideas not directly cited have been duly referenced.

Part of the work was supported by others, as follows: Prof. Paola Romagnani, University of Florence, Italy, and her team performed single cell RNAseq for the complement system components.

Parts of this work were in revision in the journal of Kidney International.

Date:

Place: Munich, Germany

Signature:

Danyang Zhao

Zusammenfassung

Thrombotische Mikroangiopathien (TMA) sind seltene, aber schwere Schädigungen kleiner Gefäße, die häufig die Nieren betreffen. Die Therapie mit C5-Inhibitoren ist wirksam, kann jedoch aufgrund der Blockade des gesamten terminalen Komplementwegs mit schweren infektiösen Komplikationen einhergehen. Es hat sich gezeigt, dass die C5aR-Blockade bei systemischer Vaskulitis wirksam ist und gleichzeitig infektiöse Komplikationen vermeidet, die bei C5-Antagonisten bei thrombotischer Mikroangiopathie (TMA) auftreten. Wir vermuteten daher, dass die selektivere Blockade der C5a/C5aR-Achse ausreichen würde, um TMA zu kontrollieren. Die Injektion von Cholesterin-Mikrokristallen in die linke Nierenarterie von Wildtyp-Mäusen löste innerhalb weniger Stunden eine diffuse TMA aus, gefolgt von einem plötzlichen Abfall der glomerulären Filtrationsrate und einer ischämischen Nierennekrose nach 24 Stunden. Genetische Defizienz von entweder C3-Konvertase oder C5aR verhinderte die TMA, den GFR-Verlust und die ischämische Nekrose nach 24 Stunden im gleichen Umfang wie die präventive Behandlung mit einem C5a-Antagonisten.

Wir induzierten die gleiche CC-TMA bei Mäusen mit genetischem Mangel an C5aR1 und erzielten ähnliche Ergebnisse wie mit C3-Mangel in Bezug auf AKI, verringerte intravaskuläre TMA-Arterienobstruktionläsionen, geringe ischämische Nekrose, verringerten CD31-Verlust im Mikrogefäßsystem und Infiltration kleiner Neutrophilen Menge und Niere. All diese Konsequenzen deuten stark darauf hin, dass C5aR der dominierende Effektorrezeptor in den Pathomechanismen der durch Cholesterinkristalle induzierten thrombotischen Mikroangiopathie ist, C5aR/CD88 einen Transmembranrezeptor mit hoher Affinität an C5a bindet. Bei einer Vielzahl von Zelltypen im gesamten menschlichen Körper und hauptsächlich bei Immunzellen führt die Aktivierung von CD88 zu erhöhten intrazellulären Kalziumspiegeln und einer weiteren Aktivierung intrazellulärer Signalwege in Verbindung mit einer Reihe von funktionellen Reaktionen. Aus diesem Grund ist die Deletion des C5a-Rezeptors 1 zu einer geringen Migration von Immunzellen zu Verletzungsstellen führt und die folgenden Kaskaden weiter reduziert, die den Nierenrestzelltod und die

Entzündungsreaktion beschleunigen, da es sich bei der CC-induzierten TMA nicht nur um den Verschluss der Arterien durch Cholesterinkristalle handelt, sondern vor allem um eine Reihe von Reaktionen, die durch die Cholesterinkristallembolien verursacht werden. Durch die Aufhebung kann verhindert werden, dass die Niere durch die Rekrutierung von Immunzellen und eine induzierte Entzündungsreaktion geschädigt wird. Als nächstes bewerteten wir die Wirksamkeit von AON-D21, einem L-konfigurierten gemischten RNA/DNA-Aptamer, das murines C5a mit günstiger In-vivo-Pharmakokinetik und Pharmakodynamik im Hinblick auf unser Studiendesign bindet und neutralisiert. Im Vergleich zum inaktiven Kontroll-L-Aptamer revAON-D21, das aus der inversen Sequenz besteht, verbesserte der aktive Inhibitor AON-D21 die GFR signifikant, hob Niereninfarkte auf, reduzierte intravaskuläre TMA-Läsionen und unterdrückte den Zustrom von Neutrophilen bei den behandelten Mäusen. Allerdings war die Wirkung auf die Erhaltung von CD31+-Endothelzellen weniger ausgeprägt. Somit scheint die C5a/C5aR-Achse das Haupteffektorelement der Komplementaktivierung in kristalliner TMA zu sein, was mit Daten übereinstimmt, die aus Mausmodellen der Vaskulitis durch anti-neutrophile zytoplasmatische Antikörper erhalten wurden, eine Autoimmunerkrankung in Form einer mikrovaskulären Schädigung, die mit komplementbedingter Gewebenekrose einhergeht.

Ein selektiverer therapeutischer Ansatz könnte ein günstigeres Sicherheitsprofil aufweisen. Daher reicht die selektive Blockade von C5a/C5aR aus, um etablierte TMA abzuschwächen. Dies könnte man auch beim Menschen bewirken, möglicherweise mit einem besseren Sicherheitsprofil im Vergleich zur C5-Hemmung.

1. Introduction

1.1 Innate system

The immune system serves to protect the body against damage by external antigens or intruders, primarily comprising microbes like bacteria, viruses, parasites, fungi, and agents of injury or diseases. There are distinct immune organs in the human immune system including adenoids, thymus, tonsils, bone marrow, intestine, spleen, and lymph nodes [1]. Defense against foreign invaders is classified into two forms: the innate immunity and the adaptive immunity, its components are shown in Figure 1.

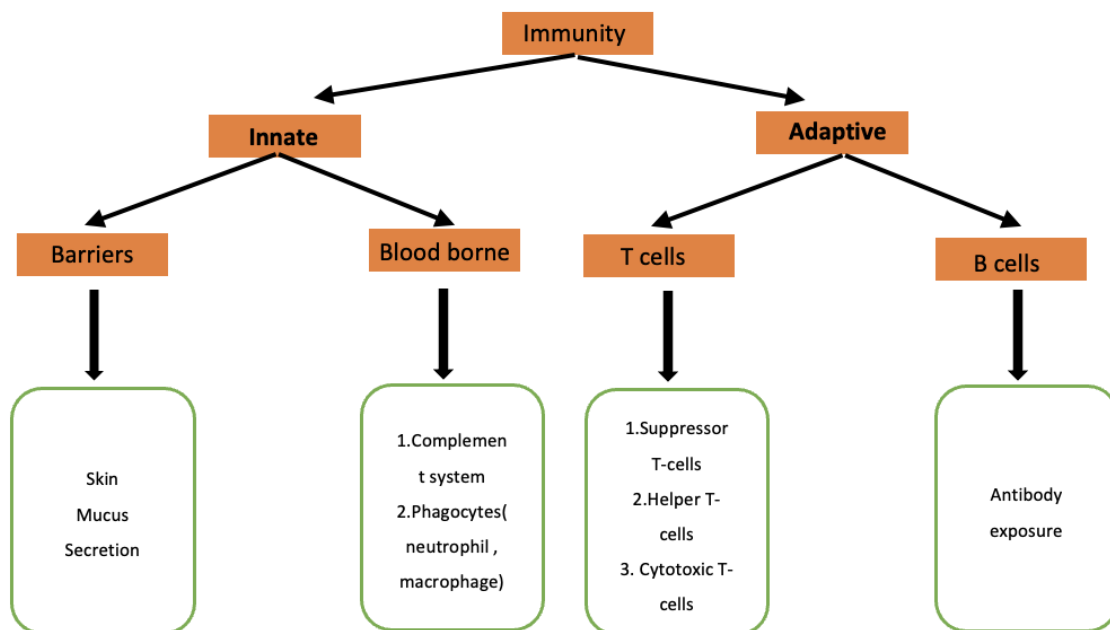


Figure 1: Basic components of human Immune system: Human immune system consists of two main systems including the innate system and the adaptive system. The innate system is activated rapidly upon pathogens encountered. Skin, and mucus secretion play barriers roles in the innate system. The complement system and neutrophils from the innate system are the first defense for invader like pathogens. The adaptive immune system occurs upon following the same stimulation. Antibody, T cells, B cells induce a strong adaptive immune reaction.

The innate immunity is the first line of defense that is rapidly activated upon encountering pathogens and is responsible for providing immediate protection within minutes or hours [2]. Its host defense is explained as its mature form by the host germ-line gene [3]. Innate immunity cannot develop antigen-specific immune memory or identification of identical pathogens upon subsequent encounters. Innate immunity can be divided into two primary

components: the humoral components (cytokines, immunoregulatory lipid mediators, and the complement system) and the cellular aspect (including granulocytes, macrophages, and natural killer cells).

In the conventional approach, the innate and adaptive immune systems are distinguished based on their distinct specificity and memory capabilities. Yet, in recent times, cells within the innate immune system seem capable of acquiring memory-like traits following temporary stimulation, culminating in an amplified reaction upon subsequent encounters. This occurrence is referred to as trained immunity. Trained immunity is marked by a generalized heightened reactivity, facilitated through substantial metabolic and epigenetic reconfiguration [4, 5]. Thus, the innate immune system can remember the first invaders, giving rise to a functional alteration upon following the same stimulation [6].

1.2 The complement system

The complement system as a part of the innate immune system plays an important role in host defense. Activation of the complement system leads to the removal of foreign or senescent cells, cell debris, bacteria, and dying cells, the disposal of immune complexes, and the promotion of chemotaxis of immune cells. There are a lot of components in the complement system, which make itself be related to different functions of immune or residual cells. And the complement components also participate in inflammation development and disease pathophysiological progression. Complement factors are present in the plasma, tissue, or cells. To avoid host tissue damage, the subsequent cascade of enzymatic reactions is tightly regulated to assure that the complement effectors are initiated only at specific locations requiring host defense against pathogens [7]. There are more than 20 plasma glycoproteins synthesized in the liver, but some also by macrophages as well as fibroblasts [2]. Throughout the course, numerous factors and split products are generated. These products can modify vascular permeability and aid in the acute inflammatory reaction. Ultimately, the membrane attack complex is assembled, inducing cellular rupture of target cells, and facilitating the clearance of infectious agents [5]. The complement system can be activated via three pathways: the classical pathway, the lectin pathway via mannose-binding lectin, and the alternative pathway (Figure 2).

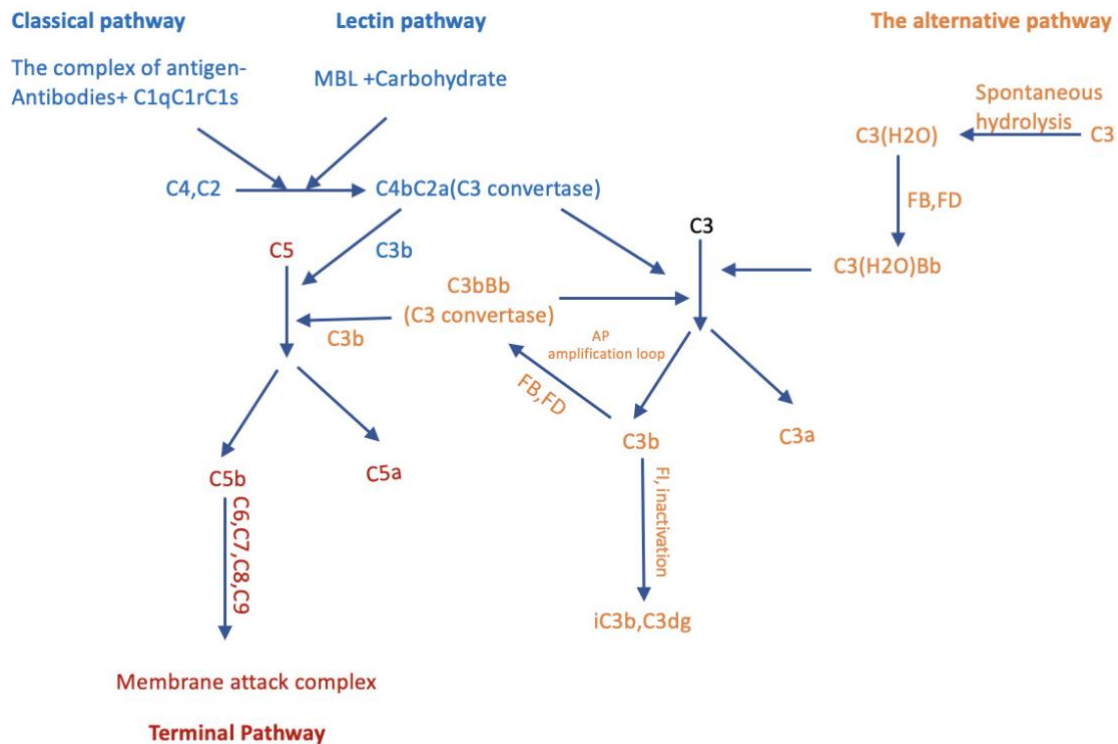


Figure 2. Schematic drawing of complement system: Complement system is made of three pathways: the classical pathway, the lectin pathway, and the alternative pathway. Different stimulations initiate different pathways: antigen-antibody complex in the classical pathway, carbohydrate in the lectin pathway and spontaneous activation at low rate in the alternative pathway. After initiation of complement system in a different way, the common procedure of C3 convertase continues to cleave C3 into C3a and C3b, and further downstream occurs and assembles the membrane attack complex.

The complement system links the innate and adaptive immune system to safeguard the host against infectious agents [8]. While in cases of viral infections, the activation of the complement system facilitates the neutralization of viral particles and the elimination of virus-infected cells, which may promote unintended harm. Excessive complement activation inside the microvasculature can trigger an inflammatory reaction, activation of platelets and neutrophils. These may lead to microangiopathy and increase the tendency of blood coagulation [9]. Furthermore, an interactive connection is present between immune activation and the processes of clot development. Specifically, the complement system can influence platelet stimulation and consequent clot formation [10, 11]. Excessive inflammation, including the heightened activation of the complement system, plays a central role in the pathobiology of severe COVID-19. This hyperinflammation triggers an inflammatory cascade, resulting in microangiopathy, the activation of platelets and neutrophils, and ultimately leading to blood coagulation [12]. Apart from COVID-19, complement components

(particularly C1q, C4b-binding protein, properdin, mannose-binding lectin and Factor H) are also able to carry out as soluble pattern recognition receptors for a couple of viruses, for instance, murine leukemia Virus, Human immunodeficiency virus under different mechanism [13].

1.2.1 Activation of complement system

The complement system is initiated by numerous factors, like antigen-antibody complexes or directly interactions between complement proteins and pathogens. Once activated, the complement cascade starts with the activation of certain complement elements. This activation can occur through the classical, the alternative, or the lectin pathway, depending on the specific stimulators (Figure 2).

The classical pathway is primarily initiated by the binding of antibodies (IgG or IgM) to antigens on the surface of pathogens. Antibodies produced by B cells connect with specific antigens, that create immune complexes. C1, which is the first complement protein involved in the classical pathway, forms a complex of three subunits: C1q, C1r, and C1s. C1q binds to the Fc region of antibodies that are part of immune complexes. The binding of C1q to antigen-antibody complexes causes a conformational change of C1r and C1s, resulting in their activation. Furthermore, activated C1s cleaves C4 and C2 into smaller fragments (C4a, C4b, C2a, C2b). The cleaved segment C4b binds to the pathogen surface and C2a fastens C4b forming C3 convertase. C3 convertase catalyzes C3 into C3a and C3b (Figure 3). C3a acts as an opsonin, and C3b continues to the subsequent cascades [14]. In patients with diabetes, mainly kidney C1q deposition in the glomerular vascular hilus is correlated with the occurrence of kidney diseases [15]. Lately, studies using transcriptomics have been extensively used to detect relative genes with disease pathogenesis. Those studies found that C1q and C3 activation in glomeruli might speed up the progression of diabetic nephropathy, which further proves that the classical pathway has an impact on the kidney disease progression [16].

The lectin pathway is triggered by the binding of mannose-binding lectins, a pattern-recognition receptor, or ficolin to carbohydrate on the surface of pathogens. This pathway provides a way to monitor pathogens that lack antibody-mediated recognition. Mannose-binding lectins-associated serine proteases are activated after mannose-binding lectins or ficolin to carbohydrate combined with pathogens. Parallel to the classical pathway, activated

Mannose-binding lectins-associated serine proteases cleave C4 and C2, forming C3 convertase (C4b2a). The C3 convertase triggers the splitting of C3 into C3a and C3b (Figure 2).

The alternative pathway is active consistently at a low rate and serves as a surveillance mechanism. It is spontaneously activated by hydrolysis of C3, leading to form C3b and C3a. C3b exposes a reactive thioester bond [17]. With the assistance of complement factor D, complement factor B which binds to C3 is split into subunit Ba and Bb segments. Subunit CBb keeps related with C3b, leading to the formation of the alternative pathway C3 convertase (C3bBb). Subsequently, C3 convertase cleaves more C3 into C3a and C3b, and C3b rebinds to Bb and generates more C3 convertase, this process is called the amplification loop. In essence, the amplification of the alternative pathway serves as a rapid-response mechanism, turning a small initial trigger into a robust and extensive immune reaction. By generating a cascade of enzymatic reactions and producing an ever-increasing number of C3b molecules, the alternative pathway significantly contributes to the immune system's ability to neutralize and eliminate invading pathogens effectively.

1.2.2 Complement membrane attack complex

The complement terminal pathway, also known as the membrane attack pathway, is the final step in the complement system's activation cascade. It accumulates and forms the membrane attack complex, which is a set of complement proteins that work together to create pores in the cell membranes of pathogens, which result in cell lysis and destruction [18]. After the activation of earlier complement pathways (classical, lectin, or alternative), C3b molecules are deposited on the pathogen's surface and bind with C4b2a or C3bBb, and further produce C5 convertase (C4b2a3b in classical pathway or lectin pathway, C3bBb3b in alternative pathway). C5 convertase cleaves complement protein C5 into two fragments, C5a and C5b. C5a is a potent inflammatory mediator that attracts immune cells to the site of infection. C5b is the initiating molecule for the terminal pathway. C5b initiates the assembly of the membrane attack complex on the pathogen's surface. C6 detects a labile binding site in C5b (half-life: 2min) followed by C7 association that makes the complex lipophilic. C8 binds to the C5b-C6-C7 complex membrane, this process defines the initial membrane insertion event, the compound of C5b-C6-C7-C8 serves as a receptor for C9 and catalyzes C9 oligomerization, and finally forms membrane attack complexes, the complement components associate through sideways alignment of the central membrane attack complexes-perforin domain [19].

1.2.3 Complement Factor 3

The complement system has a broad significance within the innate immune response. A multitude of novel functions within this system have been uncovered, going beyond its original bactericidal purpose, and complementing the actions of antibodies [20]. C3 is the central molecule of the complement cascade and produces mostly in the liver. C3 presents in the circulation at a concentration of more than 1 mg/ml, small amounts of C3 remain in tissues or within cells [21]. Native C3 presents in blood at an inactive state, upon pathogen inflammation or cell damage, it can be activated and generate biological active segments such as C3a, C3b, iC3b, and C3d. Apart from biological function in blood, the intracellular C3 form has been reported lately. This intracellular C3 can be taken up from extracellular environment as C3 (H₂O) [22], be produced by cells using the same starting point as the secreted C3 form [23, 24], or be originated from an alternate variant, creating a shorter, cytoplasmic form devoid of disulfide bonds and glycosylation [25]. C3 glomerulopathy with predominant C3 deposit, paroxysmal nocturnal hemoglobinuria, and immunoglobulin associated MPGN with combined C3 and Ig are C3-related diseases in the clinic. Up to now, there is still no effective treatment for those diseases [26, 27]. Therefore, it's necessary to seek a proper therapy for C3-related disorders.

1.2.4 Complement Factor 5a

C5a, also known as complement component 5a, is a small protein fragment that has a crucial role in the immune system's response to infections and inflammation. C5a is particularly known for its role as a potent chemoattractant and anaphylatoxin by binding to its receptor C5aR. This means it can attract and guide immune cells, to the site of infection or inflammation, such as neutrophils and macrophages [28, 29]. Additionally, C5a can induce the release of histamine from mast cells, leading to vasodilation (widening of blood vessels) and increased permeability of blood vessel walls [30]. However, in some cases, an excessive or uncontrolled release of C5a as well as C5a-bound C5aR can lead to harmful effects, contributing to inflammatory disorders including sepsis, asthma and acute respiratory distress syndrome, autoimmune diseases, and hypersensitivity reactions [31].

1.3 Complement system and kidney thrombotic microangiopathy

1.3.1 Thrombotic microangiopathy

Thrombotic microangiopathy (TMA) is a range of severe diseases characterized by thrombocytopenia, microangiopathic hemolytic anemia and organ failure. The TMA microvascular occlusive disorders with the systemic or intrarenal accumulation of platelets and thrombocytopenia [37]. One of the most prevalent classifications is that proposed by George [35], which divided TMA into primary (genetic and acquired) and secondary TMA illustrated in Figure 4. Secondary TMA can be triggered in the context of distinct disease process, for instance transplantation, pregnancy, cancer, or HIV infection [36]. Hemolytic-uremic Syndrome predominantly impacts kidney, and endothelial injury with platelet activation and accumulation and leads to microvascular thrombosis formation, kidney impairment, and further end-organ failure [39].

Thrombotic thrombocytopenic purpura (TTP) is a TMA and systemic disease with extensive von Willebrand Factor (vWF)-platelet clots in arterioles and capillaries resulting in thrombocytopenia, microangiopathic hemolytic anemia, and neurologic symptoms [40, 41], TTP was first described to explain the accumulation of von Willebrand factor released from endothelial cells in the plasma of patients with chronic relapsing thrombotic thrombocytopenic purpura in 1982 [38]. Those (vWF)-platelet clots come from mutate ADAMTS13 enzyme which cut vWF into segments.

Atypical Hemolytic-Uremic Syndrome (aHUS) is another type of TMA predominantly affecting the kidney secondary to the complement system, it is partially caused by a genetical defect in complement-related factors or acquired autoantibodies to complement regulators, and 50-60 % of all cases are relevant to genetical disorders of complement-associated components [43]. Many rare genetic variants were identified in five complement genes, namely CFH, CFI, MCP, C3, and CFB. These variants can regulate or participate in the complement system by either disrupting or enhancing the function of those gene encode proteins [44]. Around 10 % of all cases are caused by Shiga-like toxin-producing *Escherichia coli* (STEC) [45]. Usually there is not only a single cause or the genetic cases at birth. Once the complement system is initiated, People with susceptibility of complement activation cannot stop the complement system like normal people. The autoimmune disruption is either transient or permanent. Therefore, nowadays clinical problem is to reach a certain threshold

of the complement activation as the different combination of genetic or environmental susceptibility of the complement disorder.

STEC-HUS mainly impacts children and has a better prognosis. However, an increasing incidence of STEC-HUS in adults was observed, normally with severe clinical manifestations and elevated mortality rates. Stx1 and Stx2 are exotoxins that interact with targeting cells by binding the corresponding receptors on the surface of cells, which predominantly express on the kidney endothelial cells, interfering protein synthesis and cell death. Stx1 and Stx2 aggravate inflammation reaction and induce reduction of endothelial thromboresistance, leading to microvascular thrombosis [42].

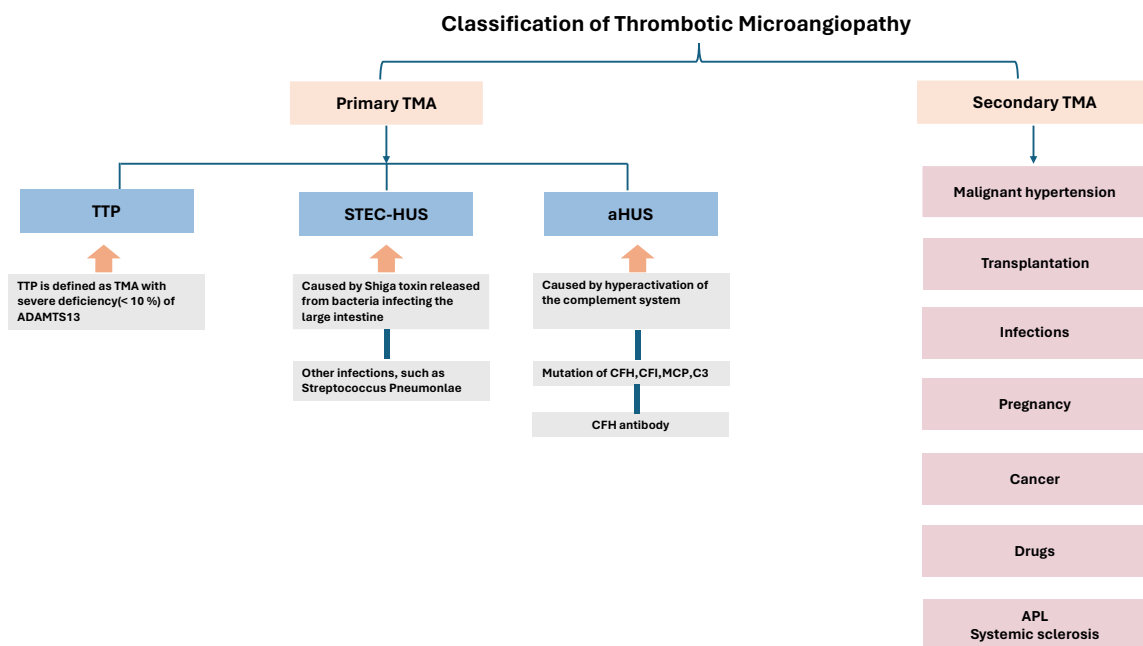


Figure 3: Classification of TMA. TMA is classified into primary TMA and secondary TMA according to different causes. Primary TMA comprise of TTP, STEC-HUS, and aHUS. TTP is defined with severe deficiency of ADAMTS13. STEC-HUS is mainly caused by Shiga toxin released from bacteria and other infections can also induce STEC-HUS, such as Streptococcus Pneumonia. Secondary TMA is triggered in the context of diverse conditions including transplantation, malignant hypertension, infections, cancer, drugs, systemic sclerosis, and APL. TMA: thrombotic microangiopathy; TTP: Thrombotic thrombocytopenic purpura; STEC-HUS: Shiga-like toxin-producing Escherichia coli-associated hemolytic uremic syndrome; CFH: complement factor H; CFI: complement factor I; MCP: membrane cofactor protein; C3: complement factor 3; APL: Acute promyelocytic leukemia.

1.3.2 Clinical presentations of atypical hemolytic uremic syndrome

The aHUS are defined by hemolytic anemia, thrombocytopenia, and kidney failure induced by platelet clots in the small blood vessels of the kidney and other organs. aHUS can manifest anytime from infancy to adulthood. Genetic aHUS constitute about 60 % of all aHUS cases. People with genetic aHUS often relapse even after making a full recovery from the initial episode; approximately 60 % of genetic aHUS cases advance to kidney failure. L. Bernd Zimmerhackl et al showed that 1 year after the onset of aHUS the clinical presentation of 23 % of all patients manifested significantly elevated arterial hypertension and chronic kidney disease in contrast to healthy groups [46].

1.3.3 Therapy for atypical hemolytic uremic syndrome

The management of aHUS has been improved with the clinical use of complement inhibitors. C5 blockade has emerged as the pivotal approach in the treatment of aHUS [47]. In the absence of efficacious intervention, roughly one-third of pediatric patients and approximately half of adult individuals diagnosed with aHUS. Those aHUS patients need dialysis therapy for the rest of their life although they can survive from the acute phase [48, 49]. The likelihood of a recurrent episode of the disease following kidney transplantation is 50 % - 80 %, resulting in an overall 5-year graft survival rate of 36 % (\pm 7 %) for patients with a recurrence. And 70 % (\pm 8 %) for those without a recurrent TMA [48]. The introduction of the complement C5 inhibitor eculizumab represents the onset of a fresh epoch for individuals diagnosed with aHUS in 2011 [50]. Eculizumab is a humanized, chimeric monoclonal antibody designed to target complement component C5. Its primary function is to hinder the cleavage of C5 into C5a and C5b, consequently decreasing the formation of C5b-C9 complexes, thus protecting against endothelial damage [51]. Based on two prospective phase 2 trials in which patients were diagnosed with aHUS, eculizumab treatment correlated with notable enhancements in the estimated GFR after 2 years of therapy. Furthermore, eculizumab demonstrated a positive impact on health-related quality of life. Throughout the further period, there was no evidence of cumulative therapy-related toxicity or severe infection-related adverse events, including meningococcal infections [51]. Preemptive eculizumab treatment proved remarkably efficacious in preventing the recurrence of post-transplant aHUS. Additionally, it is crucial to administer eculizumab upon diagnosis of recurrence to preserve kidney allograft function [52, 53]. Besides it is an efficacious and well-tolerated treatment in childhood with aHUS [54].

Meanwhile, the longer-acting C5 inhibitor ravulizumab has been approved for the treatment of paroxysmal nocturnal hemoglobinuria and aHUS [55, 56]. In pediatric patients with aHUS, the administration of ravulizumab every 4-8 weeks after changing from the treatment of eculizumab retained stable kidney function and hematologic parameters for 1 year [57]. Another complement-related protein that can be a potential target in treatment of complement-mediated HUS and systemic thrombophilia is properdin, inhibition of properdin in aHUS might be of therapeutic benefit [58]. eculizumab, however, is the first-line therapy for aHUS, but there are still infectious complications due to blockage of complement terminal pathway.

1.3.4 Safety concerns with C5 inhibition

Following the initial confirmation of eculizumab's effectiveness in the patients with PNH and aHUS, clinical assessments of complement activity and patient surveillance uncovered some anomalies that remain unexplained considering eculizumab's inhibitory action on C5 activation [59]. Eculizumab exhibits an extraordinarily high picomolar affinity for C5, characterized by remarkably slow off-rates. It was firmly anticipated that C5 bound by eculizumab would be incapable of activation to form functional membrane attack complexes [60]. It is noteworthy that a substantial proportion of PNH patients failed to maintain normal LDH or hemoglobin levels, despite experiencing a remarkable improvement [61]. Hepatotoxicity linked to anti-C5 inhibitor is a potentially significant adverse occurrence, which should be taken into consideration [62]. Due to the blockage of the complement terminal pathway, several infections that have been linked to the use of eculizumab in individuals with PNH/aHUS, anti-C5 inhibitor therapy can be associated with severe infectious complications such as meningitis, septic shock, and severe end-organ damage. The bacteria that cause the infection are *N. meningitidis*, *N. gonorrhoea*, *N. flavescens* (subflava), *N. cinerea*, *N. sicca*, *P. aeruginosa*, and *M. lacunata* [63].

1.4 Acute kidney injury and acute kidney disease

Acute kidney injury (AKI) is defined by a sudden increase in serum creatinine levels (an indicator of kidney excretory function) and a decrease in urinary output (oliguria, a quantitative sign of urine production) or both, and those parameters are limited to a duration of 7 days (table 1) [64]. AKI is part of a range of functional kidney situations called as acute

kidney disease and disorder (AKD) [65]. AKI is a syndrome, it constitutes a significant complication for patients hospitalized (occurring in 10-15 % of all hospitalizations) [66], and its prevalence can occasionally surpass 50 % for those in the intensive care unit [67]. The criterion of AKI now is giving way to more specific descriptions of multiorgan syndrome including sepsis-associated AKI [68], cardiac surgery-associated AKI [69], ischemic AKI [70], and drug-induced AKI [71].

Table 1 Criteria for defining AKI, AKD, CKD and NKD

	AKI	AKD	CKD	NKD
Duration	≤ 7days	< 3 months	> 3 months	NA
Functional criteria	Increase in sCr by ≥ 50% within 7 days or Increase in sCr by ≥ 0.3mg/dl (26.5umol/l) within 2 days or oliguria ≥ 6 hours	AKI or GFR < 60 ml/min/ 1.73m ² or decrease GFR by ≥ 35% over baseline or increase in sCr by ≥ 50% over baseline	GFR < 60 ml/min/ 1.73m ²	GFR ≥ 60 ml/min/ 1.73m ² , stable GFR(no decrease by 35% within 3 months), stable sCr(no increase by 50% within 3 months or increase by 0.3mg/dl within 2 days), no oliguria for ≥ 6hours
AND/OR	OR	OR	OR	AND
Structural criteria	Not defined	Elevated marker of kidney damage(albuminuria, haematuria or pyuria are most common)	Elevated marker of kidney damage(albuminuria is most common)	No marker of kidney damage

AKD, acute kidney diseases and disorders; AKI, acute kidney injury; CKD, chronic kidney disease; GFR, glomerular filtration rate; NKD, no kidney diseases; sCr, serum creatinine level. NKD implies no functional or structural criteria according to the definitions for AKI, AKD or CKD.

Sepsis-associated AKI(S-AKI) is a common complication of critically ill patients with substantial mortality and mobility. S-AKI is not easy to be recognized because most patients already developed when patients are diagnosed with sepsis. Even though sepsis stands as the most prevalent causal factor in AKI development, AKI originating from any source is linked to an elevated risk of sepsis emergence [72]. Sepsis possesses a multifaceted and unparalleled pathophysiology, rendering S-AKI a distinctive syndrome distinct from any other form of AKI. Targeting the precise moment of injury onset in sepsis proves exceedingly challenging, resulting in difficulties in timely intervention to forestall kidney damage [73]. However, lately, microvascular dysfunction, inflammation and metabolic reprogramming have been implicated

in preclinical studies [74]. Sepsis and AKI commonly coexist in the setting of critical illness, with 25-75 % of all sepsis-associated AKI or septic shock globally [75].

Cardiac surgery-associated AKI(CSA-AKI) is the most common complication among adult patients experiencing cardiac surgical procedures with higher mortality and morbidity. In intensive care, CSA-AKI is the second most prevailing AKI following S-AKI [76]. The pathophysiology of CSA-AKI is sophisticated and possibly linked to ischemic reperfusion injury, oxidative stress, inflammation and nephrotoxins. Until now, there is still no consensus on CSA-AKI. Furthermore, due to the distinct surgery types and different baseline characteristics, reported incidences remain variable between 3.1 % to 42 % based on KDIGO criteria [64]. CSA-AKI is significantly relevant to poor short- and long-term outcomes, so it is necessary to seek a medical intervention to prevent its development. Xiong C et al observed that the administration of Acetaminophen after cardiac surgery, an inhibitor of hemoprotein-catalyzed lipid peroxidation, was independently linked to a low risk of severe AKI in patients suffering from cardiac surgery which suggested that inhibition of oxidative stress might ameliorate kidney damage during CSA-AKI [77].

Ischemic acute kidney injury commonly occurs for several reasons, for instance cardiovascular surgery or diseases, uptake of vasoconstrictive drugs, with high mortality and morbidity, and it implicates the development of CKD and transient stage from CKD to kidney failure [78]. Human body can bear blood loss at a certain level, yet by the time circulation flow reduction is over the line, delivery of oxygen and metabolic substrates is inadequate, and cell injury further leads to kidney dysfunction. The first cell population that is affected during ischemic AKI is endothelial cells which play essential roles in circulation and kidney functions [79, 80]. Besides owing to endothelial cell injury, inflammation takes place accompanied by immune cell infiltration. During ischemic AKI a plenty of processes and cells are involved, thus seeking a safe and efficacy approach to improve kidney capacity after ischemia injury for short and long-term outcomes of individuals.

1.4.1 Pathophysiology of ischemia-induced acute kidney injury

Kidney ischemia-reperfusion (IR) injury represents a primary cause of perioperative AKI. In diverse clinical scenarios including major vascular, cardiac, and hepatic surgeries, along with conditions like shock, sepsis, trauma, and kidney transplantation. Kidney IR injury takes place due to the disruption of kidney blood flow (ischemia), succeeded by subsequent reperfusion

[81]. An insufficiency in local tissue oxygen and nutrient delivery coupled with the generation of harmful byproducts from damaged kidney cells (e.g., pro-inflammatory cytokines and damage-associated molecular patterns [DAMPs]) serves as the trigger for kidney tubular and endothelial cell damage, leading to subsequent kidney dysfunction [82]. Multiple pathophysiological mechanisms, including kidney tubular apoptosis, necrosis, and inflammation, contribute to the development of ischemic AKI.

Endothelial cells are a single layer covering the vascular surface, and they provide a physical barrier between blood and tissue, playing an essential role in sustaining intravascular homeostasis. Nevertheless, endothelial injury or endothelial cell death would lead to vascular barrier disruption, vascular constriction, diastolic dysfunction, vascular smooth muscle cell excessive proliferation and migration, inflammation, and thrombosis, which are tightly linked to a range of diseases, such as atherosclerosis, ischemic shock, and AKI [83]. For the kidney, apart from microvascular endothelium, glomerular endothelium is a distinct type of endothelia with specific structural and functional characteristics, which is highly covered by a rich glycocalyx, involves in the capacity of the glomerular filtration barrier and in the maintain podocyte structure [84]. Therefore, targeting kidney endothelial cell therapy may attenuate vascular damage and enhance the prognosis of ischemic AKI. P-selectin, a biomarker of endothelial cells in ischemic AKI, is validated and binds peptide-engineered extracellular vesicles with imaging and its function has been generated, and it can be used to provide a spatiotemporal diagnosis in the early stage of AKI. Therefore, P-selectin has been used to assist personalized therapy and displays superior nephroprotective effects [85]. In addition, endothelial-derived miR-17~92 activates a reparative signal in damaged kidney vasculature during kidney IRI by regulating angiogenic pathways [86].

Tubular epithelial cells or kidney tubules are the primary component of the kidney, tubules are susceptible to an array of injuries, which contain hypoxia [87], proteinuria, toxins, metabolic irregularities, and aging. The prevailing belief has been shown that tubules bear the tons of such injuries [88]. Kidney tubules are responsible for the reabsorption and secretion of diverse solutes. Thus, the damage to nephron tubules is a key mediator of AKI. Numerous typical injuries to the kidneys primarily affect the proximal tubular cells, which are exceptionally metabolically active. Proximal tubular cells represent the most energy-intensive cells within the kidney system [89]. They are more sensible for hypoxia during AKI, insufficient delivery of oxygen and nutrients to proximal tubular cells can lead to tubular epithelial cell

damage and induce inflammation. And conversely proximal tubular cells could also contribute to produce more inflammatory mediators. Anyway, a better understanding of the mechanism underlying tubular injury during ischemia-reperfusion AKI is necessary to develop therapeutics in this field.

Neutrophils account for 50-70 % of all circulating leukocytes in humans and 10-25 % of circulating leukocytes in mice [90]. Although neutrophil infiltration is detected in ischemic AKI, the precise function and kinetics of neutrophils transferring into the post-ischemic kidneys are still not fully clear [91, 92]. The regulation of neutrophil function is tightly controlled using three primary strategies: phagocytosis, degranulation, and the emission of neutrophil extracellular traps (NETs). NETs are expansive, extracellular, lattice-like formations comprising cytosolic and granular proteins, which assemble on a framework of relaxed chromatin¹. While the nucleus contributes the majority of DNA to NETs, these structures also contain mitochondrial DNA. NETs can attract, neutralize, and eliminate bacteria, fungi, viruses, and parasites, serving as a deterrent to the elimination of bacteria and fungi [93]. Some reports demonstrated that neutrophil recruitment accelerates kidney IR injury by distinct pathways such as the HMGB1-TLR4-IL-23-IL17A axis [94, 95]. In addition, histones and NETs generated by neutrophils are also key mediators to the progression of tubular necrosis and ischemic AKI [96]. Therefore, inhibiting neutrophil migration and infiltration could be another way to delay ischemic-induced AKI.

Macrophages display significant diversity and fulfill a broad range of diverse functions in protecting the host, regenerating tissue growth, maintaining equilibrium, and contributing to both tissue damage and the processes of healing and fibrosis [97]. Substantial available evidence suggests that signals originating within the microenvironment of the injured kidney play a pivotal role in governing the activation states of monocytes/macrophages. Following ischemia, the initial reperfusion phase is characterized by the predominance of neutrophil recruitment, the generation of reactive oxygen species (ROS), and the release of damage-associated molecular patterns (DAMP) from necrotic and damaged tubular cells [98]. These factors collectively contribute to an environment primed to facilitate the activation of resident mononuclear phagocytes and the transformation of recruited monocytes into proinflammatory macrophages [99]. The initial proinflammatory monocyte/macrophage phenotype transitions to macrophage phenotypes facilitate tubular repair and recovery from

AKI. For this reason, it is advisable to highlight the emphasis on macrophages when studying the transition from acute AKI to CKD.

Dendritic cells (DCs) originate either from the yolk sack or from hematopoiesis in the bone marrow. They coordinate both innate and adaptive immune responses [100]. DCs are mostly present throughout the entire body, including circulation, tissues like spleen, lung, and lymph nodes. Apart from macrophages, DC is other main type of mononuclear phagocytes and comprise the most abundant component in the intrarenal immune system. In a normal kidney, DCs coordinate effective immune responses, such as the recruitment of neutrophils to clear bacteria in pyelonephritis. Nevertheless, the pro-inflammatory activities of DCs can also contribute to tissue damage in various forms of AKI and chronic glomerulonephritis [101]. DCs recruit and activate effector T cells, which release harmful substances and maintain immune infiltration in the kidney's tubulointerstitial area. These actions are counteracted by specific subsets of DCs that facilitate the activation and persistence of regulatory T cells, aiding in the resolution of the immune response and promoting kidney repair. Numerous studies have explored the diverse roles of DCs in kidney health and disease. However, it has become apparent that existing tools and subset markers are insufficient for accurately distinguishing DCs from macrophages. Multifaceted transcriptomic analysis studies hold the promise of enhancing the classification of mononuclear phagocytes and providing a clearer understanding of DC development, different subsets, and their plasticity [101, 102].

1.4.2 Impact of the complement system in acute kidney injury

AKI presents a tough challenge characterized by elevated mortality and morbidity rates. Inflammatory reactions, containing both innate and adaptive immune responses, actively participate in the progression of AKI, particularly in ischemic conditions. Tubular cells and specific subcategories of immune cells assume pivotal roles in the genesis of inflammation. The complement system has been known to be triggered in immune complex glomerulonephritis for a long time, it has also been proved that the complement system is associated with a range of other kidney disorders in recent years. The participation of the complement system in the pathogenesis of so many kidney diseases suggests that the kidney might exhibit inherent susceptibility to injury mediated by complement. The formation of the C5b-9 complexes on the cell's plasma membrane results in the creation of transmembrane channels or alterations in membrane lipids, leading to a breakdown in membrane integrity.

While a single C5b-9 complex is sufficient to cause the lysis of erythrocytes, the lysis of nucleated cells necessitates multiple C5b-9 complexes. Lower concentrations of C5b-9 induce partial (sublethal or sublytic) damage in nucleated cells [103, 104]. C3 activation can be detected and characterized by immunostaining of kidney tissue, which implies the intrarenal complement activation. Studies in animal models observe an elevating deposition of C3 along the tubular basement membrane after ischemia-reperfusion [105]. However, C3 deposition is not seen in the peri-tubular capillaries or the glomeruli [106]. Recent research related to complement displays the treatment of opportunity for patients of kidney failure [107]. The complement system may play an adverse role in various stages of kidney transplantation, starting from donors who experienced brain or cardiac death, extending to the process of organ procurement, IRI, allograft rejection, and even the progression of chronic graft dysfunction [108]. Patients diagnosed with stage 3 AKI (as per KDIGO criteria) were paired with individuals lacking AKI, matched according to their illness severity scores [109]. The activation of complement through the alternative pathway has been observed in individuals during the initial stage of HUS associated with Shiga toxin-producing *Escherichia coli* infection. Experimental findings have underscored the involvement of complement proteins in regulating glomerular endothelial cells toward a pro-thrombotic state. Additionally, at the glomerular level, podocytes emerge as significant targets of complement activation induced by Shiga toxin. Consequently, glomerular damage resulting from podocyte malfunction and loss is a mechanism that may impact long-term kidney outcomes in this condition [110]. Complement factor H, as a key regulator of the complement alternative pathway, is linked to glomerular injury in genetic or acquired impairment as well as factor H-related proteins, which have unique and probably context-dependent effects on the resident kidney cell types (mesangial, glomerular endothelial, podocytes, and tubular epithelial) within the kidney [111].

In summary, overactivation of the complement system due to different genetic or acquired factors of complement components causes multiple forms of kidney disorders. Thus, specific therapy of certain complement abnormalities is a potential way to improve the prognosis of AKI.

1.5 Complement-related therapy in acute kidney injury

Complement system dysfunction due to genetic mutation or acquired impairment is associated with a broad array of kidney diseases, such as HUS, and IRI [112]. Several lines of

evidence have proved that complement activation is associated with the pathogenesis of kidney IR injury. Activated neutrophils and complement play a distinct and cooperative role in the onset of a progression of IRI because of C5a. In order to investigate the impact of a C1-inhibitor on the early inflammation to IRI and the following progression of fibrosis in mice, Juan S Danobeitia et al evaluated kidney injury and function, acute inflammatory response, and fibrosis as well as the survival rate at post-injury. Their observations indicate that intravenous administration of C1-inhibitor prior to ischemic injury provided a protective impact on the kidney from immunopathology and prevent fibrosis, which suggested that early intervention with complement blockade is a promising strategy for preventing fibrosis in IRI-induced AKI [113]. Most importantly, in mouse IRI model, knockout of C3, C3aR, or CFB all confer protection. A blocking antibody against CFB prevented C3b deposition in mouse kidneys. Likewise, C5 inhibition or knockout status for C5aR1 ameliorated kidney function and even upstream complement deposition. MAC formation appears to also play a role, as C6 deficient mice, which cannot generate MAC, are also protected from kidney IRI [114].

1.6 Cholesterol crystal embolism

Cholesterol crystal (CC) embolism (CCE) is a rare but serious complication of advanced atherosclerosis, it can affect almost every organ through microvascular obstructions and ischemic tissue necrosis. CCE originated from atheromatous plaques of abdominal aorta can affect lower limbs (“blue toe syndrome”) as well as solid organs such as kidney (AKI), pancreas (ischemic pancreatitis), and small intestines (intestinal ischemia). When the source of CC is plaques in the ascending aorta, ocular or cerebral embolism can occur as well as ischemic lesions in the upper limbs [115]. CCE can occur spontaneously or arise along intravascular catheter-based procedures, such as percutaneous coronary intervention [116]. 0.38 % of all the patients undergoing PCI were diagnosed with CCE [117].

1.6.1 Clinical manifestation of cholesterol crystal embolism

Usually, within 2 to 6 weeks following a vascular procedure, kidney dysfunction manifests along with distinctive skin manifestations. Although livedo reticularis and blue toes are considered classic symptoms, they are not definitive and may occasionally be absent. Vasculitis is a significant consideration for differential diagnosis. The confirmation of diagnosis typically requires a biopsy of the skin, muscle, or kidney. Alternatively, retinal cholesterol

emboli may be observed during fundoscopy. Treatment primarily revolves around managing symptoms, as corticosteroids lack proven effectiveness and may even pose risks. Administering statins to all patients is recommended due to their ability to stabilize plaques and reduce inflammation. However, randomized clinical trials in this area are scarce. The prognosis is generally unfavorable, with approximately 30-55 % of patients with kidney involvement eventually requiring kidney replacement therapy. Mortality rates are high, with 15-30 % of patients succumbing within the first year [118].

1.6.2 Treatment of cholesterol crystal embolism

Despite the utilization of various medications, such as corticosteroids and statin [119], in the management of CCE, there remains a lack of established treatment protocols. LDL apheresis was originally utilized for familial hypercholesterolemia. However, some evidence showed that LDL apheresis might help patients avoid the necessity for maintenance dialysis and was well tolerated in patients with CCE [120]. Additionally, CCE can lead to arterial obstruction and organ failure by forming crystal clots that contain fibrin, platelets, and extracellular DNA [121]. Therefore, appropriate blockage of clot-associated components could be a novel therapeutic approach for CCE.

2. Research hypothesis

I hypothesized that using a recently developed mouse model of injecting CC into a mouse left artery to induce TMA would be essential to unravel molecular mechanisms behind CCE-induced vessel obstruction, cell death, and kidney function affected by the complement system.

Correspondingly, the specific aims based on presumptions were:

1. C3 deficiency would preserve kidney function showed by improved GFR, less vessel obstruction and reduced kidney infarct size under the condition of CC-driven TMA.
2. C3 deficiency is used as a positive control and wild-type mice is used as a negative control to investigate whether the complement component C5a and its receptor axis contribute to the progression of TMA via C5aR deficiency mice and C5a-neutralizing L aptamer injection.
3. After validation of the C5a/C5aR axis in the CC-induced TMA mouse model, administration of C5a-neutralizing L aptamer will be utilized at different time points (3 hours, 6 hours, 9 hours, and 12 hours post-surgery) to explore the therapeutic window of C5a blockage.
4. In the end, to look into the potential underlying mechanism of C5a in CC-driven TMA, neutrophils and platelets will be isolated, in order to evaluating the function and neutrophils and platelets as well as endothelial cells with/without C5a-neutralizing L aptamer.

3. Material and Methods

3.1 Materials

Table 2: Instruments and Devices

Instrument	Designation	Manufacturer
Centrifuges	Centrifuge 5415C	Eppendorf, hamburg, DE
	Haraeus, Minifuge T	VWR internation, Darmstadt,DE
	Haraeus, Sepatech Biofugue A	Haraeus, Sepatech Biofugue A
Microscopes	Light microscope Leitz DM II	Leica Microsystems,Solms,DE
	Libra 120	Carl-Zeiss AG,Oberkochen,DE
	CCD-Camera	Trondle, Moorenweis, DE
	Light microscope Zeiss AxioPlan 2	Carl-Zeiss AG,Oberkochen,DE
	Axiocam HR	Carl-Zeiss AG,Oberkochen,DE
Fluorescence microscope	Leica DMI8	Leica Microsystem, Cambridge, UK
	Olympus BX50	Olympus Microscopy, Hamburg, DE
	Zeiss observer microscope	Carl-Zeiss AG,Oberkochen, DE
Confocal microscopy	LSM 510 microscope	Carl-Zeiss AG,Oberkochen, DE
	Leisa SP5 AOBS confocal microscopy	Leica Microsystems,Wetzlar, DE
Cell culture		
Cell incubator	Heracell Type B5060 EC-CO2	Haraeus, Sepatech, Osterode, DE
Cell counting chamber	Neubauer cell counting chamber	Roth, Karlsruhe, DE
Cell culture work bench	Sterile card hood class II, type A/B3	Baker Company, Stanford, ME, USA
Flow cytometry	FACS Canto II	BD, USA
	FACS Calibur	BD, USA
Tissue homogenizer	Ultra Turrax T 25	IKA GmbH, Staufen, DE
Microtome	Microtome HM 340 E	Microm, Heidelberg, DE
PCR cycler	Light Cycler 488	Roche Mannheim, Germany

Material and Methods

Instrument	Designation	Manufacturer
PCR cycler		Eppendorf, Germany
Cryomicrotome	Cryostat RM 2155	Leica Microsystems Bensheim, DE
	Cryostat CM 3000	Leica Microsystems Bensheim, DE
pH meter	pH meter WTW	WTW GmbH, Weiheim, DE
Thermomixer	Thermomixer 5436	Eppendorf AG, Hamburg, DE
	Thermocycler UNO II	Biometra, Gottingen, DE
Vortex mixer	Vortex Genie 2tm	Bender & Hobein, Zurich, CH
Workbench	Sterile workbench Microflow, Biological safety cabinet class II	Nunc GmbH, Wiesbaden, DE
Rotary mixer	Heavy-duty rotator	Bachofer Laboratoriumsgerate, Reutlingen, DE
Water bath	Water bath HI 1210	Leica Microsystems Bensheim, DE
Manual Pipette aid	Research Plus 30-300 ul	Eppendorf AG, Hamburg, DE
	Pipetman 2, 10, 20, 100, 200, 1000 ul	Gilson, Middleton, WI, USA
	Pipetus classic	Hirschmann Laborgerate, Eberstadt, DE
Miniaturized imager device	For GFR measurement	Mannheim Pharma & Diagnostics
Miniaturized Battery	For GFR imager device	Mannheim Pharma & Diagnostics
	Software for quantification of flow chamber	Bethesda, MD, USA

incorporated
analyze particle
module

Abb: FACS: Fluorescence-activated cell sorting

Table 3 :Disposable Instruments

Instrument	Designation	Manufacturer
Eppendorf tubes	1.5,2 ml	TPP Trasadingen, CH
Falcon tubes	5, 15 ,50 ml	BD Heidelberg, DE
Serological pipettes	5, 10 ,25 ml	BD Heidelberg, DE
Pipettes	Pipettes Pipetman	Gilson, Middleton, WI , USA
Pipettes tips	10, 200, 1000 ul type Gilson Pipette tip ep T.I.P.S	Peske,Aindling-Arnhofen, DE Eppendorf AG, Hamburg, DE
Embedding cassettes	Embedding cassettes ‘Biopsy’	ISOLAB, Wertheim, DE
Cell culture plates	6-, 12- ,24- ,96-well plate	TPP Trasadingen, CH
8-well plate		Ibidi, Martinsried, DE
Two-lane Organo Plate	400um * 220 um channels	BD, Drogheda, IE
Needles	20, 23, 25, 26, 30 Gauge 33 Gauge	BD, Drogheda, IE TSK Laboratory, Japan
Syringe	1,2,5,10 ml	Becton Dickinson GmbH, Heidelberg, DE
Microscope slides	Super frost Plus	Menzel – Glaser, Braunschweig, DE

Material and Methods

Cell culture dishes	10, 15 cm	TPP Trasadingen,Switzerland
Flow adhesion assay	Flow chamber system	Maastricht Instruments, Maastricht, The Netherlands
Culture-insert 2 well in u- Dish 35mm		Miltenyi biotec, DE

Table 4: Chemicals, Reagents, and Solutions

Product	Designation	Manufacturer
Ethanol		Merck, Darmstadt, DE
Formalin		Merck, Darmstadt, DE
HCl		Merck, Darmstadt, DE
NaCl		Merck, Darmstadt, DE
KCl		Merck, Darmstadt, DE
CaCl ₂		Merck, Darmstadt, DE
NaH ₂ PO ₄		Merck, Darmstadt, DE
NaHCO ₃		Merck, Darmstadt, DE
Glucose		Merck, Darmstadt, DE
Trisodium citrate		Merck, Darmstadt, DE
Tris-buffered saline		Merck, Darmstadt, DE
HEPES		Merck, Darmstadt, DE
Microfil injection compound		Flow-Tech, Carver, MA, USA
FITC-sinistrin		Mannheim Pharma &
Triton X-100		Diagnostics GmbH
TTC	Tetramethylbutylphenyl- polyethylene glycol	Merck, Darmstadt, DE
Cholesterol crystal		Merck, Darmstadt, DE
Cell death detection kit (TUNEL)	Terminal deoxynucleotidyl transferase dUTP nick end labeling	Roche, Manheim, DE

Material and Methods

SYTOX green assay	Extracellular DNA staining	Life Technologies, Eugene, OR, USA
LDH cytotoxicity assay	LDH: Lactate dehydrogenase	Roche, DE
Annexin V-FITC Kit		Miltenyi biotec, DE

Table 5: Antibodies for immunohistology and Drugs

Method	Name	Manufacturer
Immunohistology	CD31	Abcam, Cambridge, UK
	Ly6G	Bio-Rad Laboratories, Feldkirchen, DE
	Alpha smooth muscle actin (α-SMA)	Dako Deutschland GmbH, Hamburg, DE
	Fibrin	Abcam, Cambridge, UK
	CD41	Biozol, Eching, DE
	DAPI	Sigma Aldrich, Steinheim, DE
	FACS	Anti-mouse CD45
Anti-mouse CD11b		BD, USA
Anti-mouse Ly6c		BD, USA
Anti-mouse CD 11c		BD, USA
Counting beads		BD, USA
Drugs	Recombinant mouse C5a	Biotech, USA
	Recombinant mouse C3	Biotech, USA

Table 6: Primers for real-time PCR

Gene	Forward (5'-3')	Reverse (3'-5')
18s	GCAATTATCCCCATGAACG	AGGGCCTCACTAAACCATCC
ICAM1	AAACCAGACCCTGGAAGTGCAC	GCCTGGCATTTCAGAGTCTGCT
VCAM1	GCTATGAGGATGGAAGACTCTGG	ACTTGTGCAGCCACCTGAGATC
P-selectin	GTCCACGGAGAGTTTGGTGT	AAGTGGTGTTCGGACCAAAG
VAP	CTTCACCGACTTCATCAGCA	CCCGGAAATAGATGGAGTCA

Table 7: Medicine for anesthesia

Application	Drug	Concentration (mg/kg)	Cat number	Company	Treatment regimen
Narcosis	Medetomidine	0.5	07725752	Zoetis	Narcosis: Intraperitoneal injection, once prior to operation, surgical tolerance verified by toe reaction
	Midazolam	5	4921530	Ratiopharm	
	Fentanyl	0.05	2084366	Janssencilag	
Antagonist	Atipamezol	5	8-00732	CP-pharma	Antagonist: subcutaneous injection, once right after operation
	Flumazenil	0.1	4470990	Hexal	
Analgesia	Buprenophine	0.1	01498870	Bayer Vital	Analgesia: intraperitoneal injection, 30min right 30 min after antagonization, after injection every 8 hours for 3 consecutive days

Table 8: Reagents for Real-time PCR

Master mix (RNA reverse transcription)	Volume(ul)	Master mix (quantitative Real-time PCR)	Volume(ul)
5x buffer	4.5	Mix Sybgreen	10
0.1M DTT	1	Taq polymerase(5000u/ml)	0.16
25 mM dNTPs	0.45	Forward primer(10 uM)	0.6
Rnasin and ribonuclease inhibitor (40 u/μl)	0.5	Reverse Primer(10 uM)	0.6
Acrylamide (15 μg/ml)	0.25	cDNA	0.2
10x Hexanucleotide Mix	0.25	ddH ₂ O	8.44
Superscript II (200 u/μl)	0.5	Total	20
Sample (2 μg)	15		
Tota	22.45		

3.2 Experimental Procedures

3.2.1 Animals

Wild-type mice (C57BL/6N) as well as C5aR knockout and C3 knockout mice, were procured from Charles River (Sulzfeld, Germany). The mice were kept in polypropylene cages, maintained under SPF standard conditions at a temperature of $22 \pm 2^\circ\text{C}$, with a 12-hour light and dark cycle, and provided with unrestricted access to water and a standard chow diet (Sniff, Soest, Germany) for the duration of the study. Before use, cages, bedding, nesting material, food, and water were sterilized through autoclaving. All procedures involving animal handling and experimentation were approved by the Regierung von Oberbayern.

3.2.2 Animal models

To induce CC-driven TMA, 6-8 weeks wild-type male mice were under anesthesia by intraperitoneal injection of narcosis including medetomidine (0.5 mg/kg), midazolam (5 mg/kg), and fentanyl (0.05 mg/kg) under maintenance of the body's normal temperature through pre-operative heat supply within a warming chamber [122]. Following a median laparotomy procedure, a gentle procedure was taken to expose both the aorta and the left kidney artery. For the cannulation of the left kidney artery, a 33-Gauge needle was employed, traversing across the aorta gently, to facilitate the injection of varying volumes of a CC stock solution or normal saline, as indicated by the specific requirements of the experiment. The successful signal of this injection was visually confirmed through the observed decolorization of the kidney, as shown in Figure 4A. After the needle's removal, measures for bleeding control were carefully executed. These involved the application of gentle local pressure and the application of cyanoacrylate polymer for secure closure. Importantly, the right kidney artery remained undisturbed throughout the procedure, ensuring its integrity. In the end, the abdominal wall and skin were closed using standard absorbable sutures. After the surgical procedure, subcutaneous injections of atipamezole at a dosage of 2.5 mg/kg and flumazenil at a dosage of 0.5 mg/kg were administered to effectively antagonize the anesthesia. Additionally, subcutaneous injections of buprenorphine at a dosage of 1 mg/kg were administered every 8 hours to provide adequate pain control for the post-operative period.

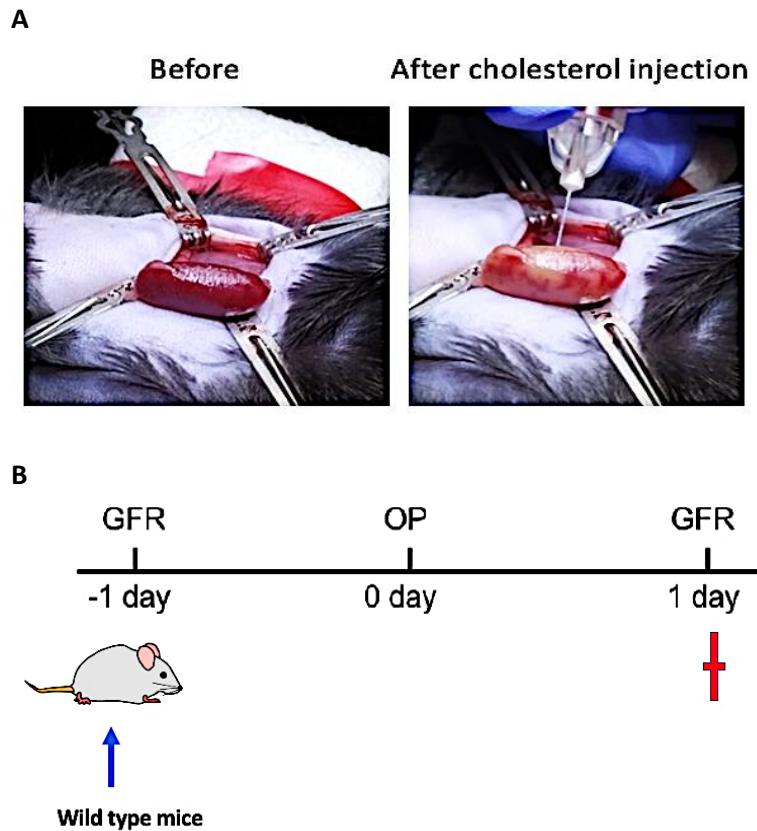


Figure 4: Schematic diagram of CCE-driven thrombotic angiopathy. (A): CC successful injection into the kidney vessel. Left panel: normal mouse kidney; Right panel: CC perfused kidney. **(B):** Thrombotic microangiopathy induction design.

To study CCE-induced TMA, 10 mg/kg CC were injected into the left kidney artery of male wild-type mice. 24 hours after CC injection, mice were terminated by cervical dislocation following GFR measurement. Kidney infarct area showed by TTC staining, kidney function evaluated via GFR, immune cell infiltration and endothelial cell injury quantified by histochemistry. The schematic diagram is displayed in Figure 4B. The characterization of AKI was conducted through a monitoring of kidney function over the entire study duration. This monitoring was accompanied by a detailed examination of associated pathological changes, which included tubular injury and the consequential loss of brush border integrity within the proximal tubule, interstitial edema, as well as a notable infiltration of immune cells, particularly neutrophils and macrophages, resulting in the secretion of inflammatory cytokines and subsequent thrombosis obstruction. Upon the conclusion of each experimental phase, an assessment of GFR was performed before sacrifice of the mice and the subsequent collection of the kidney tissue for further analysis. To preserve tissue integrity for histological

examination, the harvested kidneys were rapidly fixed in formalin before being embedded in paraffin, enabling a histological analysis of the kidney changes observed throughout the study.

In this study, we generated a method by an exposure to the CCE model in the murine kidney tissue. The surgical procedure was executed under the monitor of general anesthesia to ensure precision and minimal discomfort to the mice. For the induction of CCE, I initiated injection of a singular and unilateral injection of varying doses of CC through the left kidney artery of wild-type mice. In contrast, the control group was administered a PBS solution to serve as our baseline control. All mice were sacrificed after 24 hours following CC injection. But before farewell, I measured GFR to evaluate the kidney function before the sacrificial procedure.

In addition, I conducted an array of detailed additional analyses. The quantification of kidney infarct size was conducted by 2,3,5-triphenyltetrazolium chloride (TTC) staining, representing extent of tissue damage. Simultaneously, I evaluated kidney injury assessment via periodic acid-Schiff (PAS) scoring, discerning the extent of kidney impairment. Afterwards for immune cell infiltration, Ly6G+ immunostaining was employed to evaluate the immune response. The investigation also involved an assessment of vascular rarefaction and endothelial cell injury through CD31 sections, providing insights into the vascular landscape.

Lastly, I focused on arterial occlusion by thrombosis, employing α -smooth muscle actin (α SMA) and fibrinogen co-staining to quantify thrombotic obstructions. Thus, this study represented diverse aspects of the CCE model in murine kidney tissue, offering valuable insights into the pathophysiological mechanisms of thrombosis.

3.2.3 Measurement of arterials obstructions

To explore the crystal clot formation within the intrarenal arteries, wild-type mice were subjected to an intravenous injection of 10 mg/kg of CC, followed by their sacrifice 24 hours post-injection. To evaluate the extent of arterial obstruction, immunostaining for α SMA/fibrinogen was performed. The study was comprised of the establishment of distinct parameters. These parameters were assessed to account for variations in artery size (Figure 12C), classifying them into three categories: interlobar, arcuate, and interlobular. The assessment of these parameters accounted for a detailed analysis of the number of completely obstructed arteries, partially obstructed arteries, and those with none of any obstructions. This assessment was represented visually in Table 9. Apart from the arterial

obstruction, additional factors were taken into consideration. These included the measurement of kidney weight and infarct size. The evaluation of kidney infarct size was accomplished through TTC staining, while kidney injury was scored utilizing PAS staining. To measure immune cell infiltration within the kidney tissue, Ly6G+ immunostaining was applied. Furthermore, vascular rarefaction and potential endothelial cell injury were regularly examined via CD31 sections. Finally, the presence and extent of artery thrombosis occlusion were assessed utilizing α SMA/fibrinogen staining.

Table 9: Criteria of kidney arterial obstruction quantification

	Criteria of arterial obstruction	Interlobar (Number)	Arcuate (Number)	Interlobular (Number)
Total quantity		$A+B+C$	$A'+B'+C'$	$A''+B''+C''$
Arterial obstruction	No	A	A'	A''
	Partial	B	B'	B''
	Complete	C	C'	C''
The Ratio of obstructed arteries (%)	No	$A/(A+B+C)$	$A' / (A'+B'+C')$	$A''/(A''+B''+C'')$
	Partial	$B/(A+B+C)$	$B' / (A'+B'+C')$	$B''/(A''+B''+C'')$
	Complete	$C/(A+B+C)$	$C' / (A'+B'+C')$	$C''/(A''+B''+C'')$

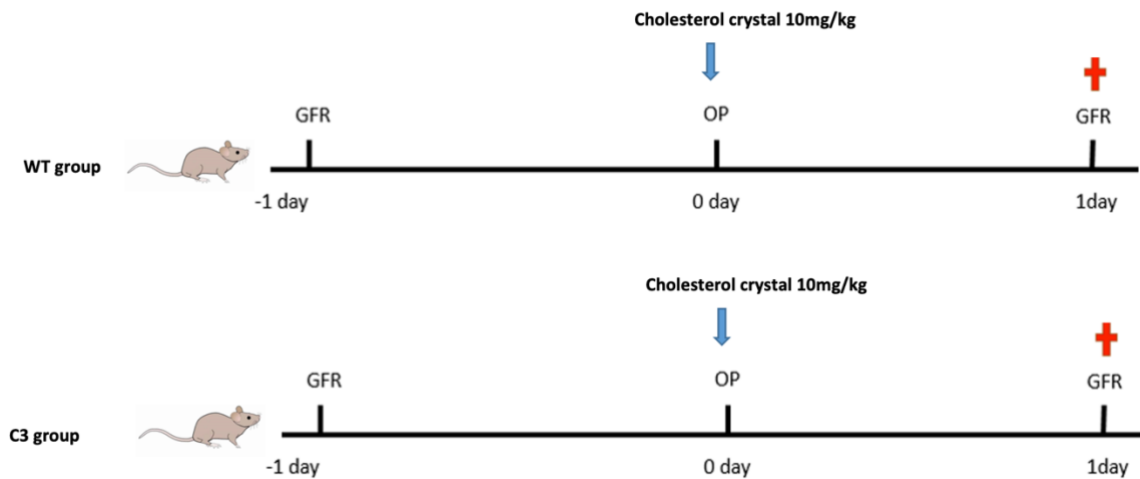


Figure 5: Schematic diagram of study design for complement system contribution on CCE-induced TMA. C3 knockout mice and wild-type mice were used in my experiment, GFR was measured for both mouse types, 24 hours later CC was injected in the left kidney artery of mice, and after 24 hours GFR was measured again following sacrifice.

3.2.4 C5a-C5aR axis in cholesterol crystal-induced thrombotic microangiopathy

To explore the impact of the complement component C5a within the context of CCE-induced TMA, C3 knockout mice were used as a positive control (Figure 5), C5aR knockout mice were used as a strategic experimental model. The parameters of the study contained the evaluation of GFR, urinary parameters, and blood collection in C5aR knockout mice, C3 knockout mice. Meanwhile, a negative control group comprising wild-type mice was employed. Before the induction of CCE all the mice were carried on the assessment of GFR, accompanied by the collection of urine and blood from C5aR knockout mice, C3 knockout mice, and the wild-type mice, who served as our experimental baseline (Figure 6). 24 hours later, I initiated the experimental phase by administering an intravenous dose of 10 mg/kg of CC into the left kidney artery of C5aR knockout mice, C3 knockout mice, and wild-type mice. Sacrifice was performed on all the mice after 24 hours following the injection of CC. Importantly, GFR measurements were conducted before their sacrifice, capturing an alteration of kidney function just before the experiment's conclusion. Following the sacrifice, an array of assessments was analyzed, including the analysis of kidney infarct dimensions through TTC staining, the scoring of kidney injuries utilizing PAS staining, the thorough evaluation of immune cell infiltration via the analysis of Ly6G+ immunostaining, a detailed exploration of

vascular rarefaction, and the potential existence of endothelial cell represented CD31 sections. Furthermore, the extent and occlusion of artery thrombosis were scored by using α SMA/fibrinogen staining.

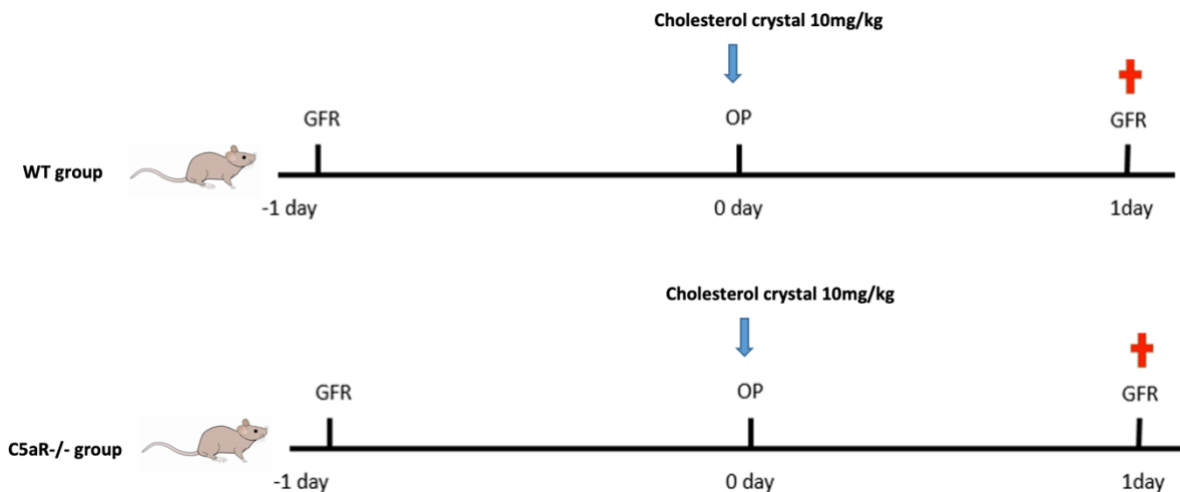


Figure 6: Schematic diagram of study design for complement factor C5a receptor effect on CCE-induced TMA. GFR was measured on wild-type and C5aR knockout mice 24 hours before TMA induction, 1 day later CC was injected into mice left artery, and after 24 hours GFR was measured again, and the organs were collected for future analysis.

3.2.5 Preemptive therapy of C5a inhibitor on cholesterol crystal embolism-induced thrombotic microangiopathy

To investigate the potential implication of complement factor 5a on CCE-induced TMA, AON-D21, a C5a neutralizing L-aptamer was utilized for intravenous injection in the experiments. One day before TMA induction, wild-type mice were performed to assess kidney function via GFR measurement (Figure 7). In the next day, the treatment group was received 10 mg/kg AON-D21 intravenous injection 1 hour before crystalline TMA; the control aptamer group was subjected to control aptamer revAON-D21 intravenous administration of 10 mg/kg 1 hour before TMA event; as for the control group, wild-type mice were without any intervention (Figure 7). 24 hours after induction of TMA, GFR measurement were evaluated to represent kidney function, afterwards kidney was collected and cut into pieces for further TTC staining, histochemistry, and TUNEL staining.

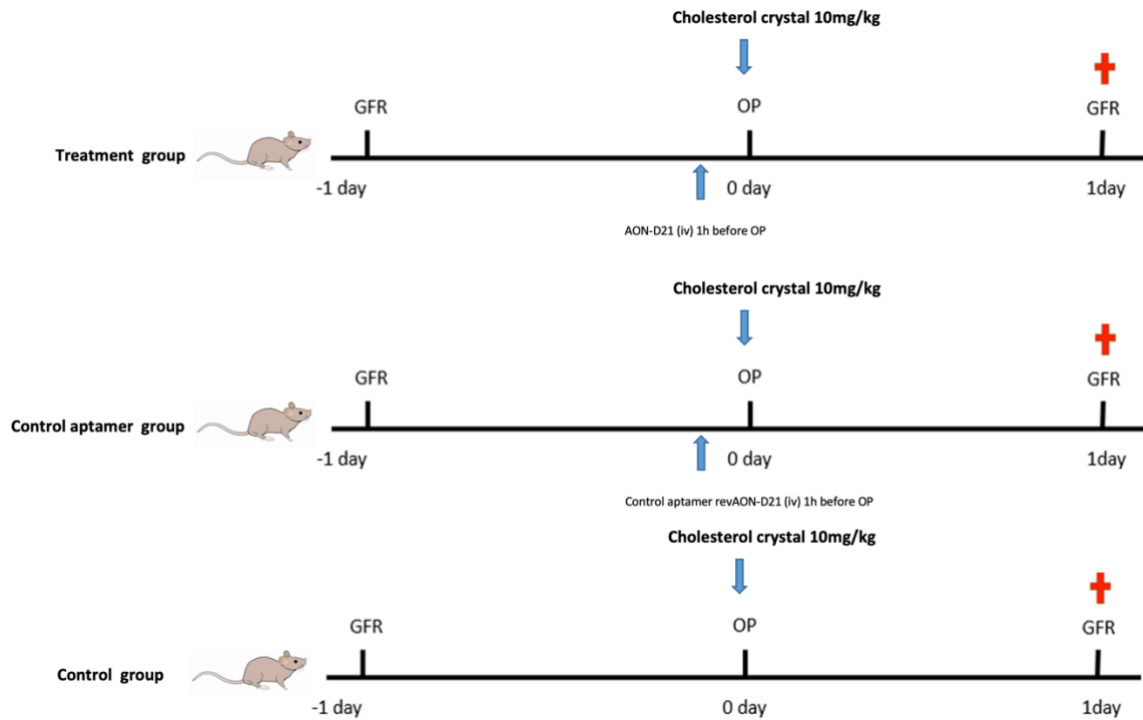


Figure 7: The preemptive therapy of C5a inhibition on crystalline TMA. Wild-type mice with no treatment, control aptamer as well as AON-D21 administration were administered in all wild-type mice 1 hour before surgery. GFR was measured for all the mouse, 24 hours later CC was injected in the left kidney artery of mice, and after 24 hours GFR was measured again following sacrifice.

I examined various staining and immunostaining techniques to assess different aspects of kidney health and vascular integrity. This included the analysis of kidney infarct size via TTC staining, scoring kidney injury via PAS staining, detecting immune cells infiltration through Ly6G+ immunostaining, evaluating vascular rarefaction, and discerning endothelial cells injury via CD31 sections, as well as assessing artery thrombosis occlusion using α SMA/fibrinogen staining.

3.2.6 Therapeutic window of C5a inhibition on cholesterol crystal embolism-driven thrombotic microangiopathy

To investigate the temporal effects of C5a blockage on the progression of CCE-induced thrombotic TMA, particularly after the conclusion of preemptive therapy and with a positive control involving the depletion of the complement system through the reduction of complement factor 3 levels, I initiated a temporal intervention on wild-type mice. These interventions involved the administration of a C5a inhibitor at distinct time intervals, specifically at 3 hours, 6 hours, 9 hours, and 12 hours following the induction of TMA (Figure

8). To provide a baseline for my study, I assessed GFR 24 hours before the TMA induction. On the day of the surgical procedure, I induced CCE to all the mice as part of our experimental protocol.

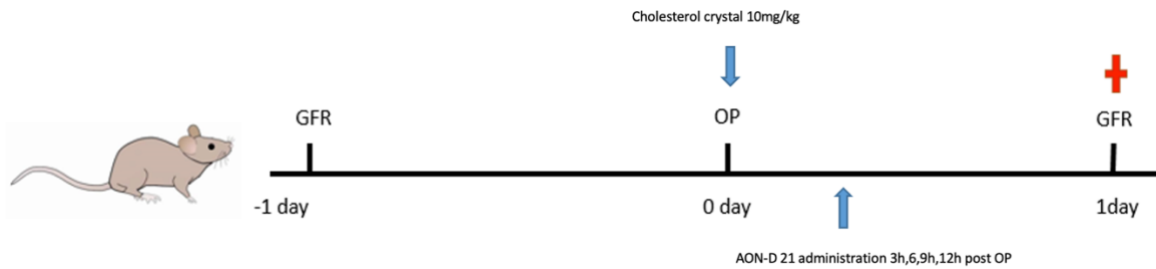


Figure 8: The window-of-opportunity of C5a inhibitor therapy on crystalline TMA. GFR was measured 24 hours before surgery, AON-D21 was administered at distinct time intervals (3h, 6h, 9h, 12h) after operation, and 24 hours post operation GFR was monitored again and collected organs for further analysis.

Subsequently, at various time points (3 hours, 6 hours, 9 hours, and 12 hours post-TMA induction), I administered the C5a inhibitor. A full 24 hours following the administration of the inhibitor, I conducted another round of GFR measurements, followed by the ultimate sacrifice of all the mice and collection of kidney tissues. The collected kidney tissues underwent a thorough histochemical evaluation to unravel different aspects of kidney function and vascular obstruction. This included the analysis of kidney infarct size using TTC staining, the scoring of kidney injuries via PAS staining, the detection of immune cell infiltration through Ly6G+ immunostaining, and the evaluation of potential endothelial cell injuries through CD31 sections. Additionally, I monitored the extent of artery thrombosis occlusion by employing α SMA/fibrinogen staining.

3.2.7 Mechanism of C5a inhibitor on cholesterol crystal embolism-induced thrombotic microangiopathy

To elucidate the mechanisms underlying the impact of C5a inhibition on the development of CCE-induced TMA, I conducted *in vitro* experiments, characterized by the cultivation of cells, mouse platelets as well as neutrophils. The cultured mouse glomerular endothelial cells (GenCs) served as an indicator of the endothelial injury, and their response to various stimuli was assessed. GenCs were cultivated in a flask using complete DMEM media enriched with 10 % fetal calf serum (FCS) and 1 % penicillin-streptomycin (PS). Upon reaching a confluence level of 80-90 %, the cells were gently detached by trypsin treatment for 2-3 minutes, and the

trypsin reaction was gently neutralized by addition of complete DMEM media. Following centrifugation, the cell pellet was carefully resuspended in 1 ml of complete DMEM, and the cell count was determined using a Neubauer chamber. The number of cells required for various experimental procedures was subsequently utilized. To stimulate the conditions of CCE, I added CC into the cellular milieu, followed by the addition of recombinant C5a protein and its corresponding inhibitor AON-D21. These dynamic procedures served as a method for assessing the presence of endothelial cells damage markers through real-time PCR analysis. Endothelial cells markers under consideration included ICAM1, VCAM1, and VAP-1.

Concurrently, to investigate the functional effect of C5a on neutrophils, I assessed a distinction of neutrophils between those derived from C5aR knockout mice and their wild-type counterparts. These isolated neutrophils underwent migration assay using a 24-well transwell system, where their migration capabilities were monitored, both in the presence and absence of C5a protein or the C5a inhibitor. This upper inserts of the 24-well transwell system were coated with fibrinogen. After 24 hours, I added chemoattractant recombinant C5a with or without AON-D21 into the lower chamber of the transwell plate. Neutrophils from C5aR knockout mice and wild-type mice were isolated and placed (2×10^5 cells/100 μ L) into the insert of the 24-well transwell precoated with fibrinogen and incubated for 1.5 hours at 37 °C. After that, I collected cells in the bottom chamber in FACS tube and resuspended with 300 μ L FACS buffer. Adding counting beads 50 μ L/sample was applied in each experiment sample before running FACS machine. The aspect of the study allowed us to gain a deeper understanding of the relationship between C5a signaling and neutrophil behavior.

Simultaneously, to further investigate the interaction of platelets and neutrophils, I extracted neutrophils from both C5aR knockout mice and wild-type mice. Mouse whole blood and bone marrow neutrophils were isolated from wild-type and C5aR knockout mice and used for an ex vivo flow adhesion assay in a flow chamber system. Rectangular cover slips (24 \times 60 mm) were coated with 50 μ g/mL fibrillar type I collagen and blocked with 1 % BSA in 1x PBS for 1 hour. Anticoagulated mouse whole blood samples were diluted 2:1 in Tyrode's buffer containing 1 mM CaCl_2 and incubated with 2.5 mg/mL CC or PBS for 10 minutes. The samples were then perfused over collagen-coated coverslips through a transparent flow chamber at a shear rate of 1000 s^{-1} . Afterwards, the system was washed with Tyrode's buffer without CaCl_2 , and adherent platelets were stained with an anti-CD41 antibody. In separate experiments, a second step flow adhesion assay was performed by perfusing wild-type mouse bone marrow

neutrophils through the chamber at 500 s^{-1} over collagen I-induced platelet-rich thrombi. Platelets and neutrophils were stained with an anti-CD41 antibody and an anti-Ly6G antibody, respectively. Nuclei were stained with DAPI. Confocal fluorescence images were obtained from 10 different areas per each sample using a Confocal Zeiss microscope. The mean area fraction of the immunofluorescence signals was quantified using the ImageJ software and the incorporated analyze particle module. This facet of the investigation aimed to elucidate the dynamic interplay between platelets and neutrophils and assess on potential collaborative or antagonistic interactions within this critical aspect of TMA development.

By conducting this exploration including cellular responses, immune cell behavior, and platelet dynamics, I aimed to unravel the complex mechanism of interactions underlying the influence of C5a inhibition in the context of CCE-induced TMA, thus extending our understanding of the pathological process.

3.3 Preparation of cholesterol crystal working solution

A pre-calculated quantity of CC powder was diluted in sterile phosphate-buffered saline to get a final dose of 2 mg/ml. The weight of the solution was recorded. To prevent blockage of the crystals and reduce crystal size, the CC solution was filtered several times by using different sizes of needles. The addition of CC powder was administrated to compensate for the loss of CC due to the filtration procedure. Repeated the above procedure several times until it got the correct concentration. In the end, the solution was autoclaved at $120\text{ }^{\circ}\text{C}$ and stored at $4\text{ }^{\circ}\text{C}$. The solution was warmed up to room temperature before use.

3.4 Primary and Secondary endpoints

Primary readout: Glomerular filtration rate (GFR)

To evaluate the excretory kidney function, all the mice were anesthetized with isoflurane, ensuring their complete sedation and immobilization. Subsequently, a miniaturized imager device, boasting the inclusion of light-emitting diodes and a photodiode carefully connected to a battery source, which was mounted on the cleanly shaved neck region of each mouse. This device was securely fixed using a double-sided adhesive patch, guaranteeing stable positioning throughout the procedure [123]. Before the administration of the intravenous injection, a baseline readout was recorded by the skin's background signal for 5 minutes. Only

after this pre-injection measurement, the intravenous injection of 150 mg/kg of FITC-sinistrin was administered. The subsequent recording of signals lasted over an approximate duration of 1.5 hours, capturing data for my study. Upon the conclusion of the data collection phase, the imager device was carefully removed, and the data underwent analysis by employing MPD Lab software. The calculation of GFR in microliters per minute ($\mu\text{l}/\text{min}$) was carried out by assessing the decrease in fluorescence intensity over time. This assessment was achieved through the application of a three-compartment model, while factoring in body weight and incorporating a conversion factor, thereby ensuring precision and accuracy in our GFR determination process [124].

Secondary readout: kidney infarct size

After 24 hours following the administration of CC injection, I continued to evaluate the kidney infarct size. This step was the retrieval of kidney samples, each of which was sectioned transversely into slices measuring 2 mm in thickness, all executed with the aid of a slicer. Afterwards, all the kidney samples were immersed in a solution composed of 1 % TTC, maintained at a stable temperature of 37°C for 15 minutes. Following this incubation period, the sections were subjected to further processing. To ensure that the structural integrity of the samples remained intact, the sections were fixed in a solution containing 4 % formalin for 2 hours at room temperature. This fixation phase was crucial in preserving the anatomical details and cellular structures within the kidney sections. To quantify the extent of infarction within each of the kidney sections, I used Image J to calculate the percentage of the kidney that was affected by the CC-induced infarction, thereby providing us with invaluable quantitative data to further our understanding of the experimental outcomes.

3.5 Periodic acid Schiff (PAS) staining

The paraffin-embedded kidney blocks, having undergone processing by specialized tissue processors, were sectioned to a thickness of 2 μm in preparation for PAS staining. These prepared sections underwent a systematic sequence of steps to ensure optimal staining conditions. To begin, the sections were subjected to a de-paraffinization process using xylene, with each immersion lasting 5 minutes and repeated twice. Following this, a rehydration process was involved with three cycles of 3-minute immersions in 100 % ethanol, two cycles of 3-minute immersions in 95 % ethanol, and a final 3-minute immersion in 70 % ethanol.

Following the rehydration, the sections were rinsed with distilled water, with each rinse lasting 5 minutes and repeated twice, to be ready for the subsequent PAS staining procedure. The PAS staining commenced with the incubation of kidney sections in a 2 % Periodic acid solution for 5 minutes, followed by a washing step with distilled water for an additional 5 minutes. Subsequently, the sections were immersed in Schiff reagent for 20 minutes at room temperature. After this incubation, a washing procedure with tap water was carried out, lasting 7 minutes. To complete the staining procedure, counterstaining was performed using a Hematoxylin solution for 2 minutes. After the Hematoxylin application, the sections underwent another washing phase with tap water for 5 minutes. The final steps involved the immersion of the stained kidney sections in 90 % ethanol, followed by a managed drying process. Ultimately, the sections were mounted with coverslips, thus concluding the PAS staining process and rendering the samples ready for detailed analysis.

3.5.1 Kidney injury assessment by PAS staining

The assessment of kidney injury in mice was conducted through an evaluation including both tubular and interstitial injury components. This evaluation included a semi-quantitative scoring system characterized by the consideration of five distinct parameters: tubular necrosis, tubular dilation, cast formation, loss of brush border, and interstitial edema. Each of these parameters was defined by a scale comprising ten different thresholds, as documented in Table 10 for reference. For the examination of kidney sections, a Leica DII light microscope was employed. The quantification of the observed data was expressed as the mean \pm standard deviation, represented as a percentage.

Table 10: Criteria for assessment of kidney injury

Parameters	Extent of damage	score	Estimated percentage
1.Tubular necrosis	None Slight	0	0
2.Tubular dilation		1	0-10
3.Lumen cast		2	10-20
4.Loss of brush border		3	20-30

5. Interstitial edema	Mild	4	30-40
		5	40-50
	medium	6	50-60
		7	60-70
		8	70-80
	Severe	9	80-90
		10	90-100
	Significant		

3.6 Immunostaining

For immunostaining, each kidney specimen was immediately subjected to fixation, immersing it in a solution containing 4 % formalin for 24 hours. Following fixation, the kidney samples underwent a process by the means of tissue processors (Leica system) and embedded the specimens within paraffin blocks. The paraffin-embedded kidney sections were slowly cut into a thickness of 2 mm. Subsequently, the sections underwent a de-paraffinization process, involving sequential immersions in xylene for 5 minutes and three cycles. The rehydration of the sections was equally thorough, immersing in 100 % ethanol for 3 minutes, removal, followed by two rounds of 95 % ethanol immersion for 3 minutes, and a final stage of 70 % ethanol immersion for 3 minutes. Afterwards, the sections were washed with PBS for 5 minutes, repeated twice to ensure the removal of residual substances. Next, I addressed the issue of endogenous peroxidase by using H₂O₂ and methanol, blocking its activity in a dark environment for 20 minutes. After this blockage, the sections were further washed in PBS for 5 minutes and repeated twice. The blockage of endogenous biotin was achieved by one drop of Avidin for 15 minutes, followed by Biotin for another 15 minutes, then a following wash with PBS for 5 minutes after each incubation. The sections were incubated with different first antibodies at 4 °C overnight in a wet environment. After this incubation, the sections were washed with PBS, lasting 5 minutes each and repeated twice. The next step was biotinylated secondary antibodies, which were applied to the sections for 30 minutes at room temperature, followed by another cycle of PBS washing, once again lasting 5 minutes and repeated twice.

Next the sections were incubated with substrate solution, which progressed for 30 minutes at room temperature in a wet environment, following a final 5-minute wash with PBS, then the sections were subjected to a rinsing stage in Tris buffer for 5 minutes. The DAB staining was carried out, followed by counterstaining with methyl green. To remove any excess stain and residual xylene, the sections were washed with 96 % ethanol, then dried before being mounted with VectaMount, thus preparing them for further analysis.

It is important to note that each immunostaining procedure was performed with a corresponding negative control and positive control. In these controls, the respective isotype antibodies were introduced instead of the primary antibodies, serving as an essential baseline for my experimental result.

3.6.1 Neutrophil infiltration analysis

Following the preparation of kidney tissue samples, each sample was incubated with a Ly6G+ antibody (1:800) diluted in 10 % skim milk powder in PBS and incubated at 4 °C overnight. Afterwards the samples were washed in wash buffer for 7 minutes, followed by a subsequent incubation with a biotinylated rabbit anti-rat IgG antibody (1:300) diluted in 10 % skim milk powder in PBS, incubated 30 minutes at room temperature. This procedure was aimed to identify and visualize the areas within the kidney tissue characterized by a marked influx of neutrophils. The regions exhibiting positive neutrophil infiltration were recognized as black, indicative of the presence of these immune cells. To quantify neutrophil infiltration within the kidney tissue, I used Image J to analyze the neutrophils infiltration by calculating the positive area of neutrophil infiltration divided by the total area of the kidney section. This approach allowed us to measure neutrophil infiltration and gain an understanding of the extent of neutrophil infiltration within the kidney tissue.

3.6.2 CD31 staining

Endothelium injury is an essential indicator of AKD. In my experiment, CD31 is served as a marker, specifically to elucidate endothelial cell injury. Following the pre-preparation procedures carried out on the kidney tissue sections, the kidney sections were incubated with CD31 antibody (1:300) at 4 °C overnight. Next, the samples were washed in wash buffer for 7 minutes, then incubated with a secondary antibody (anti-rat, 1:300) for 30 minutes at room

temperature. CD31 staining allowed us to visualize the presence and distribution of CD31 molecules on the surface of endothelial cells within the tissue.

3.6.3 Alpha-smooth muscle actin (α -SMA) / fibrinogen staining

α -SMA is an actin isoform that serves as an essential role in fibrogenesis, which can be found in smooth muscle cells, myofibroblasts and blood vessels [125]. As for fibrin, it is an insoluble clot or gel converted from fibrinogen with the action of serine protease thrombin, which is activated by a series of enzymatic reactions triggered by vessel wall injury [126].

Followed by the preparation of kidney tissue sections, the specimens were firstly incubated with a-fibrinogen antibody (1:2000) in 10 % skim milk powder in PBS for 30 minutes at room temperature. Then the sections were washed in a wash buffer for 7 minutes. In the next step, the specimens were incubated with a secondary antibody (anti-rabbit, 1:1000) for 30 minutes at room temperature. After fibrinogen staining, the samples were incubated with a-SMA (1:300) in 10 % skim milk powder in PBS at 4 °C overnight. In the end, the kidney sections were incubated with a secondary antibody (anti-mouse IgG2a, 1:300) in PBS for 30 minutes at room temperature.

Within my experiment, it is critical to recognize development of the clot formation. Therefore, α -SMA is employed to serve as an indicator of the blood vessel and on the other hand fibrin is utilized to provide insights on the thrombus formation. α -SMA staining presents a red color distinguishing from the black color stained by the anti-fibrinogen antibody. Total artery numbers in the kidney section were quantified by counting α -SMA, and clot formation was quantified by fibrinogen staining present in arterial vessel.

3.7 TUNEL staining

TdT-mediated dUTP-biotin nick end labeling (TUNEL) staining by a corresponding detection kit was conducted to identify dead cells in the kidney section. Kidney samples were assessed with a light microscope Leitz I and after photographed. The TUNEL positive cells were recognized and evaluated by the mean of using the Image J software.

3.8 RNA isolation and quantitative real-time PCR

3.8.1 Total RNA Isolation

GenCs were transferred using forceps into 2 ml of lysis buffer containing 1 % 2-mercaptoethanol, all within 5 ml falcons. Throughout this procedure, the constant cold environment was maintained by keeping the samples on ice. Each sample underwent a single round of homogenization by 20 seconds of processing with an Ultra-Turrax set at level 4. Following this, the homogenized samples were centrifuged at 6000 g for 5 minutes, after which the resulting supernatant was transferred into pristine RNase-free tubes. Next, a 700 μ l aliquot of each sample was selected and thoroughly mixed with an equal volume of 70 % ethanol. This mixing process ensured the preservation of the sample's integrity. The total RNA within the samples was then isolated using a Qiagen mRNA extraction kit, adhering to the provided instructions. The purified RNA was stored at -80 °C for future analyses.

3.8.2 RNA reverse transcription

The RNA samples were resuspended in RNase-free water. To promote the denaturation of any secondary RNA structures, the samples were incubated at 65 °C for 10 minutes. This denaturation step was stopped by reducing the temperature to 4 °C. Subsequently, the RNA samples were diluted to a final concentration of 2 μ g total RNA within a 22.45 μ l reaction volume. The master mix was incubated at 42 °C for 120 minutes and 85 °C for 5 minutes. The samples were then cooled to a stable 4 °C in long-term storage for future analytical utilization.

3.8.3 Quantitative real-time PCR

The quantitative real-time PCR analysis was conducted by using the SYBR Green Dye Detection System, integrated into the Light Cycler 480 platform. To prepare the cDNA samples for this real-time PCR assay, The cDNA samples were diluted in 1:100 dilution for real-time PCR. The prepared master mix underwent a controlled incubation process within the Light Cycler 480 system as follows: a pre-incubation phase was set at 95 °C for 5 minutes; the amplification phase was characterized by a sequence of temperature settings: 95 °C for 15 seconds, 60 °C for 15 seconds, and 68 °C for 20 seconds, running 40 regulated cycles; the melting curve analysis is set at 95 °C for 5 seconds, then at 65 °C for 60 seconds; Finally, the cooling phase was set at 40 °C for 30 seconds. The CT values were calculated and normalized by using the reference gene (18s rRNA) ensuring that the results were accurately adjusted for each sample.

3.9 Mouse neutrophil isolation and flow cytometry

Upper inserts of the 24-well transwell system were coated with fibrinogen, after 24 hours I added chemoattractant recombinant C5a with or without AON-D21 into the lower chamber of the transwell plate. Neutrophils from C5aR knockout mice and wild-type mice were isolated and placed neutrophils (2×10^5 cells/100 μ L) into inserts of the 24-well transwell system pre-coated with fibrinogen, incubated for 1.5 hours at 37 °C. After that, I collected cells in the bottom chamber in FACS tube and resuspended them with 300ul FACS buffer. The addition of counting beads 50 ul/sample was necessary for each experiment sample before the samples were placed into the FACS machine (Figure 9A).

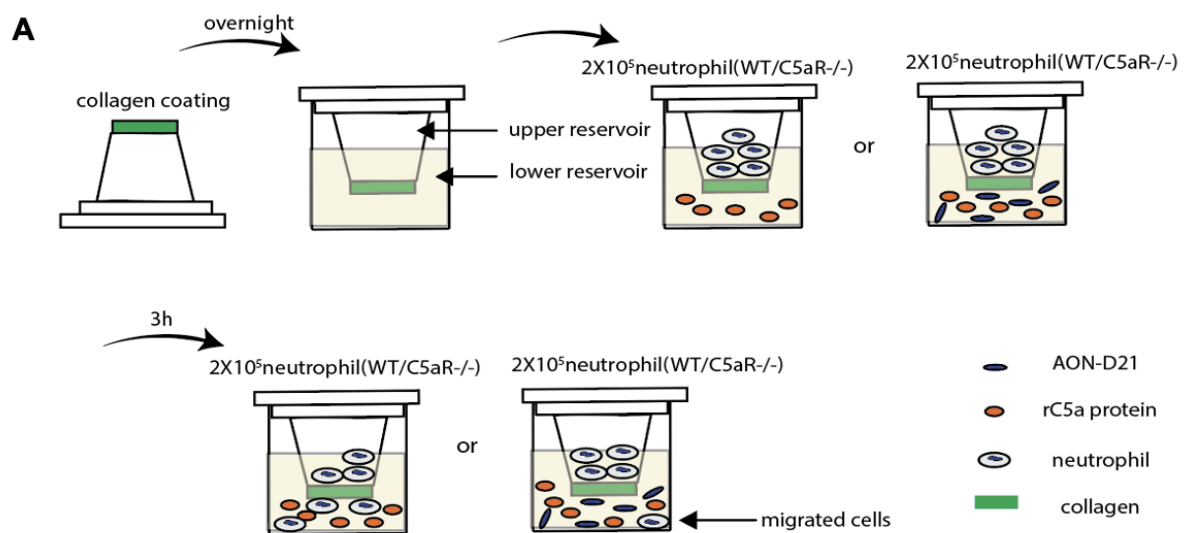


Figure 9: Schematic diagram of neutrophil migration assay. The upper chamber of the transwell assay was coated with collagen overnight, 2×10^5 neutrophils from C5aR^{-/-} or wild-type mice were added to the upper chamber, and in the lower chamber rC5a protein was used to be attractant to neutrophils, after 3h, the liquid from lower chamber went into flow chamber for the neutrophil migration.

3.10 Flow chamber assay

Mouse whole blood and bone marrow neutrophils were isolated from wild-type and C5aR knockout mice and used for an ex vivo flow adhesion assay in a flow chamber system. Rectangular coverslips (24 × 60 mm) were coated with 50 μ g/mL fibrillar type I collagen and blocked with 1 % BSA in 1x PBS for 1 hour. Anticoagulated mouse whole blood samples were diluted 2:1 in Tyrode's buffer containing 2 mM CaCl₂ and incubated with 2.5 mg/mL CC or PBS for 10 minutes. The samples were then perfused over collagen-coated coverslips through a

transparent flow chamber at a shear rate of 1000 s^{-1} . Afterwards, the system was washed with Tyrode's buffer without CaCl_2 , and adherent platelets were stained with an anti-CD41 antibody. In separate experiments, a second step flow adhesion assay was performed by perfusing wild-type mouse bone marrow neutrophils through the chamber at 500 s^{-1} over collagen I-induced platelet-rich thrombi. Platelets and neutrophils were stained with an anti-CD41 antibody and an anti-Ly6G antibody, respectively. Nuclei were stained with DAPI. Confocal fluorescence images were obtained from 10 different areas per each sample using a Confocal Zeiss microscope. The mean area fraction of the immunofluorescence signals was quantified using the ImageJ software and the incorporated analyze particle module (Bethesda, MD, USA).

3. 11 Statistical analyses

All statistical analyses were performed using GraphPad Prism 9.0 Software (GraphPad Software, San Diego, USA). Before each analysis, I assessed the normal distribution of the data (Shapiro-Wilk test), homo- and heteroscedasticity (Levene's test) and the presence of outliers (Grubb's test). Normally distributed and homoscedastic data were tested for statistical significance using a one-way ANOVA (3 or more groups) and t-test (2 groups). The post-hoc Bonferroni test was used for multiple comparisons. Heteroscedastic data was corrected using the Games-Howell post-hoc test. Not normally distributed data sets were compared using the Kruskal-Wallis test. A p-value of <0.05 was considered statistically significant.

4. Results

4.1 C3 deficiency entirely abrogated thrombotic microangiopathy

Crystalline thrombotic angiopathy in C3-deficient mice

C3 is a crucial element during the whole activation of the complement system. All upstream activated fragments intend to form C3 convertases (C4b2b in the classical or lectin pathway; C3bBb in the alternative pathway), finally trigger complement initiation. Therefore, C3 is the most important component factor within the complement system, deficiency of C3 represents the ablation of the entire complement system. In my experiment, C3 deficiency mice served as a positive control to demonstrate the impact of the complement system on crystalline TMA.

4.1.1 Cholesterol crystal-induced acute kidney injury and infarct size with C3-Deficiency

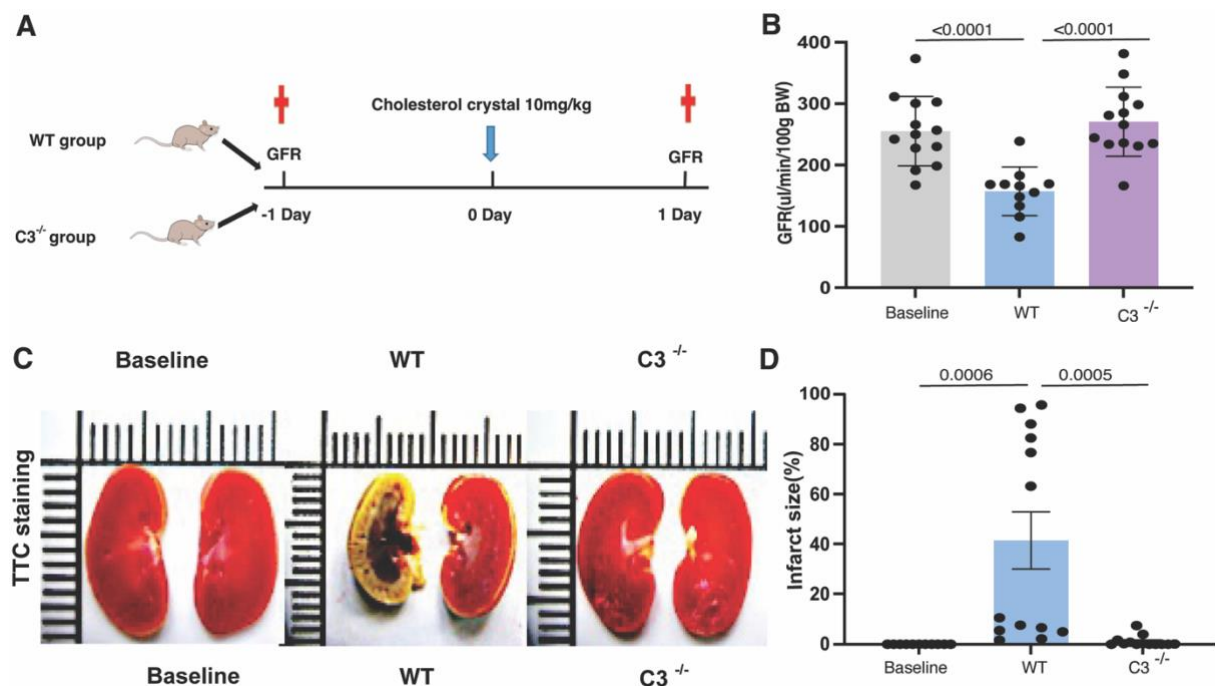


Figure 10: Crystalline TMA-induced kidney failure and cell death at 24 hours. (A) The schematic diagram of crystalline TMA induction experiment design. (B) GFR measurement at baseline, wild-type mice, C3 knockout mice. (C) Representative images of TTC staining at baseline, wild-type mice and C3 knockout mice. (D) Infarct size at baseline, wild-type mice and C3 knockout mice, all quantitative data are means \pm SEM and analyzed by one-way ANOVA following Dunn post-hoc test.

To induce TMA via CC, mice were subjected to an administrate of 10 mg/kg CC per mouse via injection of CC into the mouse left arterial vessel. This approach can prevent the discomfort of skin ulceration, peritonitis, etc when CC would be injected into the aorta. The successful

injection into the kidney artery was shown by the means of observing color switch from red to white.

To investigate the impact of the complement system on crystalline TMA, C3 was taken into consideration in my experiments as an inducer of complement system deletion. C3 is a crucial and central element in the complement system, without C3, there is no MAC formation, no complement factor 5 (C5), subunit C5a, C5b generation, and further cascades occurrence. C3 knockout mice and wild-type mice were subjected to CC administration. 24 hours before crystalline TMA induction, GFR was monitored in all the mice as a control. And 24 hours after CCE, infarct size as well as GFR were monitored. I observed that C3 deficiency mice displayed higher GFR value in comparison to the wild-type mice, and almost reached the same value level as the control group, which might give us a clue that the complement system plays an essential role in mitigating kidney function damage shown by GFR value (Figure 10A, B). After checking the kidney damage, to better establish a straight overview of kidney injury, TTC staining was used in this model. The results displayed that C3 deletion had less cell death (Figure 10C, D) compared with the wild-type group, nearly reached to the baseline standard. Therefore, those findings indicated that the complement system is a crucial part in development of crystalline TMA, as there are numerous amounts of proteins involved in the complement activation and progression, inhibition of complement system might be a better way to ameliorate early stage of TMA caused by CC.

4.1.2 Cholesterol crystal embolism-related arterial occlusion with C3-deficiency

Fibrin is vital for hemostasis and thrombosis, wound healing as well as several other biological functions and conditions that relate to extracellular matrix [127]. Fibrin and fibrinogen create and form a supporting framework during coagulation. In the early stage of thrombus formation, fibrinogen serves as an activator linked to regulate platelet aggregation.

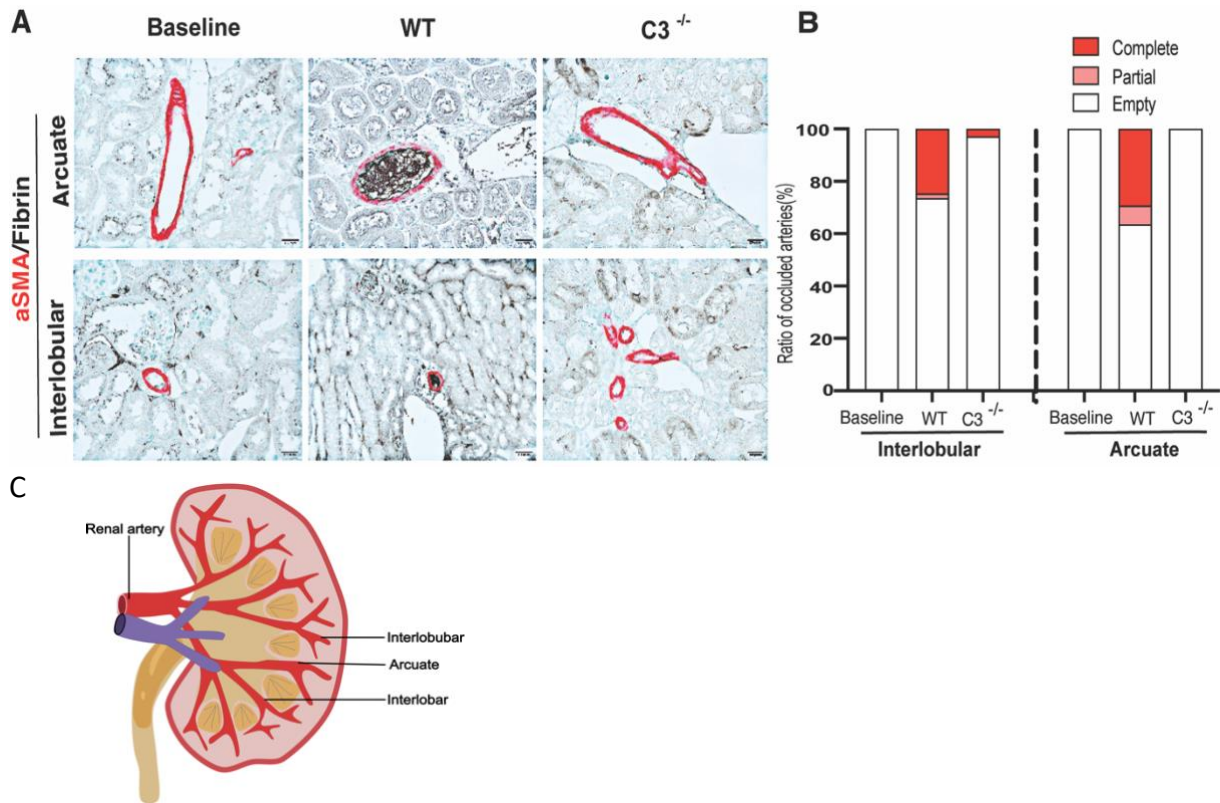


Figure 11: Arterial occlusion in crystalline TMA at 24 hours. (A) Representative histological image of kidney arterial occlusion, red color: α -SMA; black color: fibrinogen; scale bar: 50 μ m. **(B)** Quantitative result of arterial occlusion at baseline, wild-type and C3 knockout mice. **(C)** Schematic depiction of kidney vasculature; all quantitative data are means \pm SEM and analyzed by one-way ANOVA.

Afterwards, fibrinogen is turned into a fibrin matrix that provides the clot shape, stability, strength, and flexibility [128]. Fibrin formation from fibrinogen and subsequent stabilization of fibrin is a crucial process to maintain the integrity of the vascular system, which assists in preventing the lethal loss of vascular fluid in the occurrence of an injury [129]. Thus, fibrinogen staining could be a good way to represent the thrombosis formation. Anti- α -SMA antibody can react with many forms of smooth muscle cells in vessel walls, gut wall, and myometrium. it is an excellent marker for smooth muscle differentiation. Therefore, in my models, α -SMA staining is employed to serve as a marker for arterial vascular walls.

There are two types of kidney arterial vessels regarding the size of the kidney artery taken into quantification (Figure 11C): interlobular and arcuate arteries. Interlobular arteries, which have their origins in the arcuate arteries located within the depths of the kidney medulla, undertake a fascinating path as they ascend toward the cortex of the kidney. Along this ascending path, they divide into a series of smaller vessels, more commonly known as afferent

arterioles. It is these afferent arterioles that play a pivotal role in facilitating the distribution of oxygenated blood to the network of glomerular capillaries, a task crucial for the filtration of waste products and the regulation of essential substances in the kidney system. These afferent arterioles enable the glomerular capillaries to serve their purpose in filtering the blood and removing excess waste materials. This filtering process ultimately results in the formation of a modified arteriolar network, known as efferent arterioles. These efferent arterioles, while modified, can be efficiently channeled through the rest of the kidney circulatory system, contributing to the overall homeostasis of the body.

To better characterize the crystalline TMA, in the next step, kidney arterial occlusion was quantified. Kidney samples collected from wild-type mice as well as C3 knockout mice 24 hours after crystalline TMA induction were cut into small sections and staining with anti-fibrinogen and anti- α -SMA. Fibrinogen was shown in black color, and α -SMA was displayed in red color shown in (Figure 11A, B). In the wild-type group, no matter interlobular and arcuate arteries, all mice were near to reaching a 30 % arterial complete obstruction and 40 % of all kidney arteries displayed partial artery occlusion. In contrast to the wild-type group, C3 deficiency mice showed that there was nearly no kidney arterial obstruction in contrast to the wild-type group regardless of interlobular and arcuate arteries. Those findings are consistent with the results we found in the GFR monitor and TTC staining measurement.

4.1.3 Neutrophil infiltration and endothelium injury in crystalline thrombotic microangiopathy with C3-deficiency

To quantify the extent of TMA, I carried out to assessment of the immune cell infiltration as well as endothelium injury. CD31 and Ly6G+ staining was performed on kidney sections 24 hours after crystalline TMA induction. CD31 also known as platelet endothelial cell adhesion molecule (PECAM-1), which is traditionally found on endothelial cells, platelets, and macrophages. In immunohistochemistry, CD31 is mainly employed to demonstrate the presence of endothelial cells in tissue samples [130].

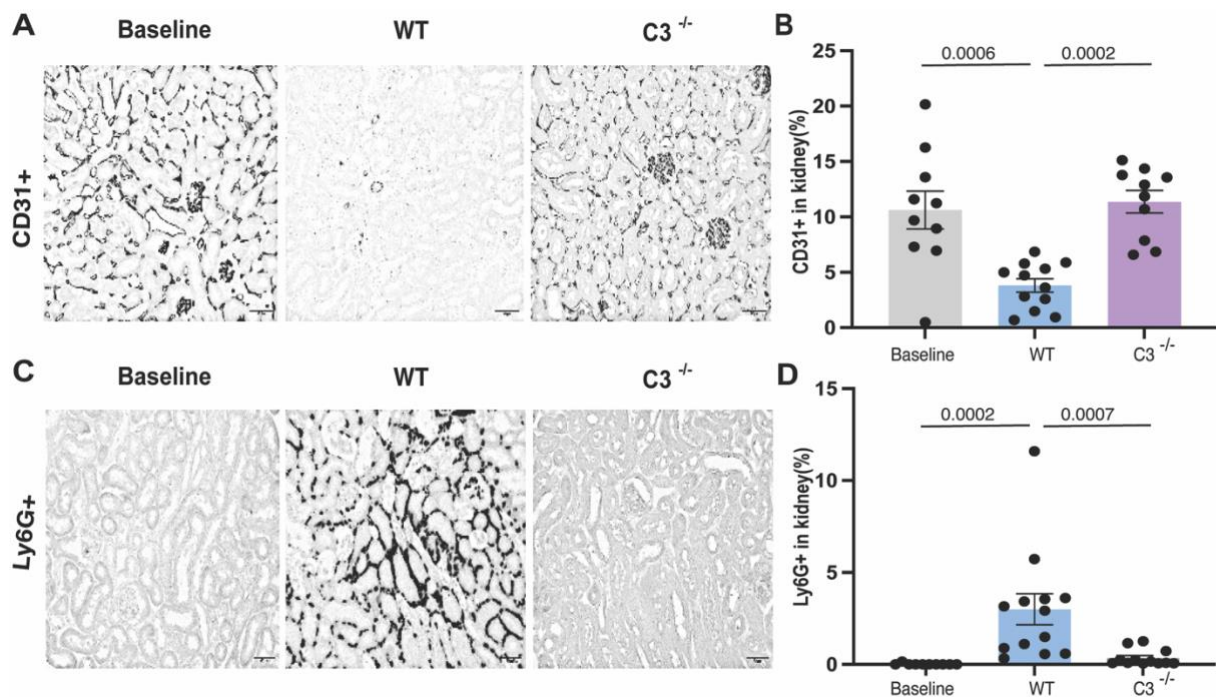


Figure 12: C3 deficiency protected from immune cell infiltration and endothelium injury in crystalline TMA. (A) Representative image of kidney CD31 positive staining, scale bar: 50 μ m. (B) Quantitative result of CD 31 positive area in baseline, wild-type mice and C3 knockout mice. (C) Representative image of kidney Ly6G positive staining in baseline, wild-type and C3 knockout mice, scale bar: 50 μ m. (D) Quantitative result of Ly6G positive area in baseline, wild-type mice and C3 knockout mice, all quantitative data are means \pm SEM and analyzed by one-way ANOVA.

Ly6G (Lymphocyte antigen 6 complex locus G6D) stands as a glycosylphosphatidylinositol (GPI)-linked differentiation antigen, exhibiting a molecular weight ranging between 21-25kD. Ly6G express primarily within myeloid-derived cells. Monocytes can transiently display the presence of Ly6G. Contrastingly, the expression of Ly6G in granulocytes and peripheral neutrophils manifest with a direct correlation to the cell's degree of differentiation and maturation. This distinguishing characteristic transforms Ly6G into a valuable marker for the identification of these specific cell populations. Beyond its role as a marker, Ly6G has also surfaced as an influential factor in antitumor response, further highlighting its significance in the field of immunology [131]. Therefore, I evaluated immune cell (neutrophils) infiltration and endothelial damage by employing Ly6G and CD31 immunohistochemistry. I found that wild-type mice had nearly 50 % of CD31 loss on the membrane of endothelial cells in contrast to the baseline, like GFR value as well as TTC staining, C3 deficiency displayed increased CD31 positive area (Figure 12A, B). In addition, similarly, kidney samples from deletion of C3 were infiltrated with fewer immune cells in the tubulointerstitial space of CC-perfused kidney

samples in comparison with wild-type mice (Figure 12C, D). Our findings indicated that C3, which is a pivotal fragment of the complement system, attracted neutrophils migration and induced the endothelial damage during CC-related thrombosis. Those findings imply that complement system-related components are a strong attractant for immune cell migration to damaged sites, reducing endothelial cell dysfunction, further causing kidney injury.

4.1.4 Kidney injury caused by cholesterol crystal-related thrombotic microangiopathy with C3-deficiency

To assess the extent of kidney tissue injury at the histochemical level, PAS staining was applied. This staining technique involves the evaluation of various tissue parameters, including the brush border, interstitial edema, tubular necrosis, tubular dilation, and lumen cast. Each parameter is scored on a scale ranging from 0 to 10, where a score of 0 signifies the absence of damage and a score of 10 signifies the most severe degree of tissue injury. Upon subjecting each kidney tissue section to PAS staining and recording the results. Immunostaining for PAS staining represents the unique characteristics of the kidney tissue in response to different conditions. In the case of CC-perfused wild-type mice, the staining revealed a worsened state, with evident tubular and glomerular disruptions. The brush border was significantly absent, rendering the normal tubular structure virtually invisible. Tubular necrosis became apparent through the disruption of the basement membrane, and there was an increase in tubular nuclear release (Figure 13A, B). Moreover, the aftermath of AKI manifested as the formation of cell debris within the tubules, and these casts were distinctly visualized under PAS staining when compared to the baseline conditions. In contrast, the C3 deficiency group presented a significantly different histological profile. Kidney tissues in this group exhibited reduced tissue necrosis, and there was a presence of the brush border. Tubular interstitial spaces appeared relatively normal, with minimal signs of swelling, and tubular dilation was notably less pronounced. My results demonstrated that deficiency of the complement system represented by deletion of C3 ameliorated kidney injury during CC thrombosis. These findings further highlighted the pivotal role of the complement system in the early progression of crystalline TMA. Through the assessment of PAS staining parameters, we gain valuable insights into the histological changes associated with kidney tissue injury and the potential therapeutic implications of complement system modulation in mitigating such damage.

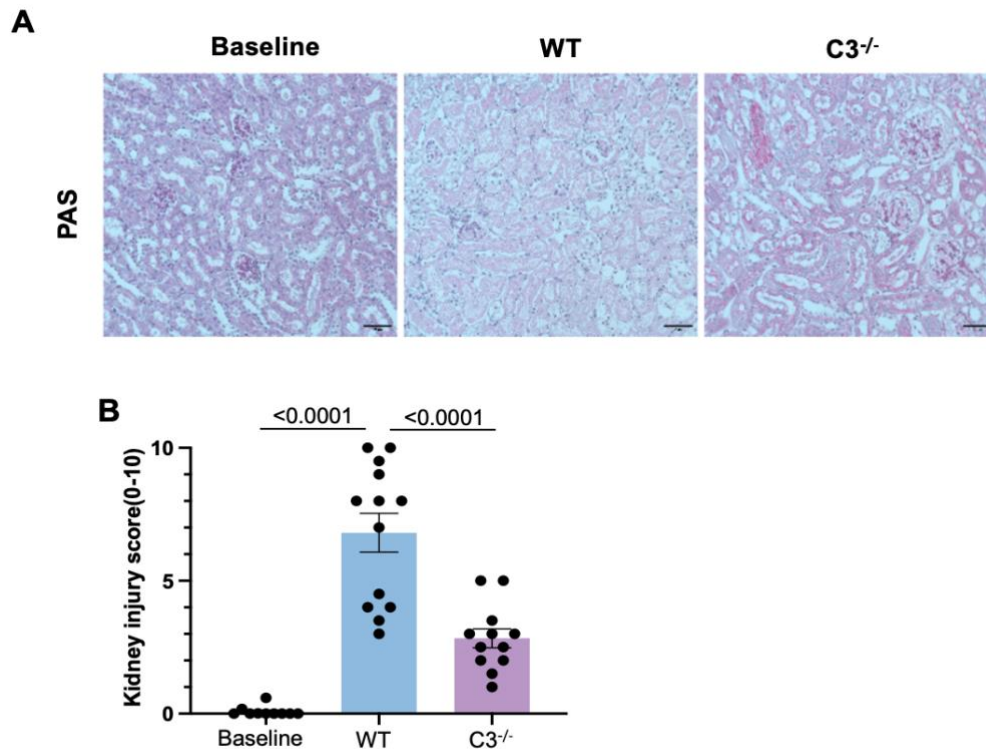


Figure 13: Kidney injury caused by CC-related TMA with C3 deficiency. (A) Representative image of PAS staining in baseline, wild-type mice and C3-deficiency mice; scale bar: 50 μ m. **(B)** Quantitative results of PAS staining score in baseline, wild-type mice and C3-deficiency mice, all quantitative data are means \pm SEM and analyzed by one-way ANOVA.

4.1.5 Thrombotic microangiopathy-related cell death in mice with C3-deficiency

To be supportive of the consequence from tissue damage undergoing PAS staining, quantitative TUNEL staining was employed to assess cell death throughout the duration of crystalline TMA induction. Cell death occurs after damage to kidney tissue, which is another marker to evaluate the extent of kidney tissue disruption. The TUNEL staining indicated an increasing TUNEL positive area of CC-perfused wild-type kidney, which was illustrated by green dye of TUNEL staining, while the C3 knockout mice displayed a relatively fewer cell death in contrast to the wild-type group (Figure 14A, B). For this reason, the complement system is taken part into the pathophysiological process of cell death under certain conditions. In summary, my findings demonstrated that activation of complement system after inflammation and tissue damage is involved in multifaceted pathogenesis during crystalline TMA, including improved kidney function indicated by GFR, less cell death revealed through

PAS staining and TUNEL staining, decreased neutrophil infiltration as well as ameliorated endothelial disruption.

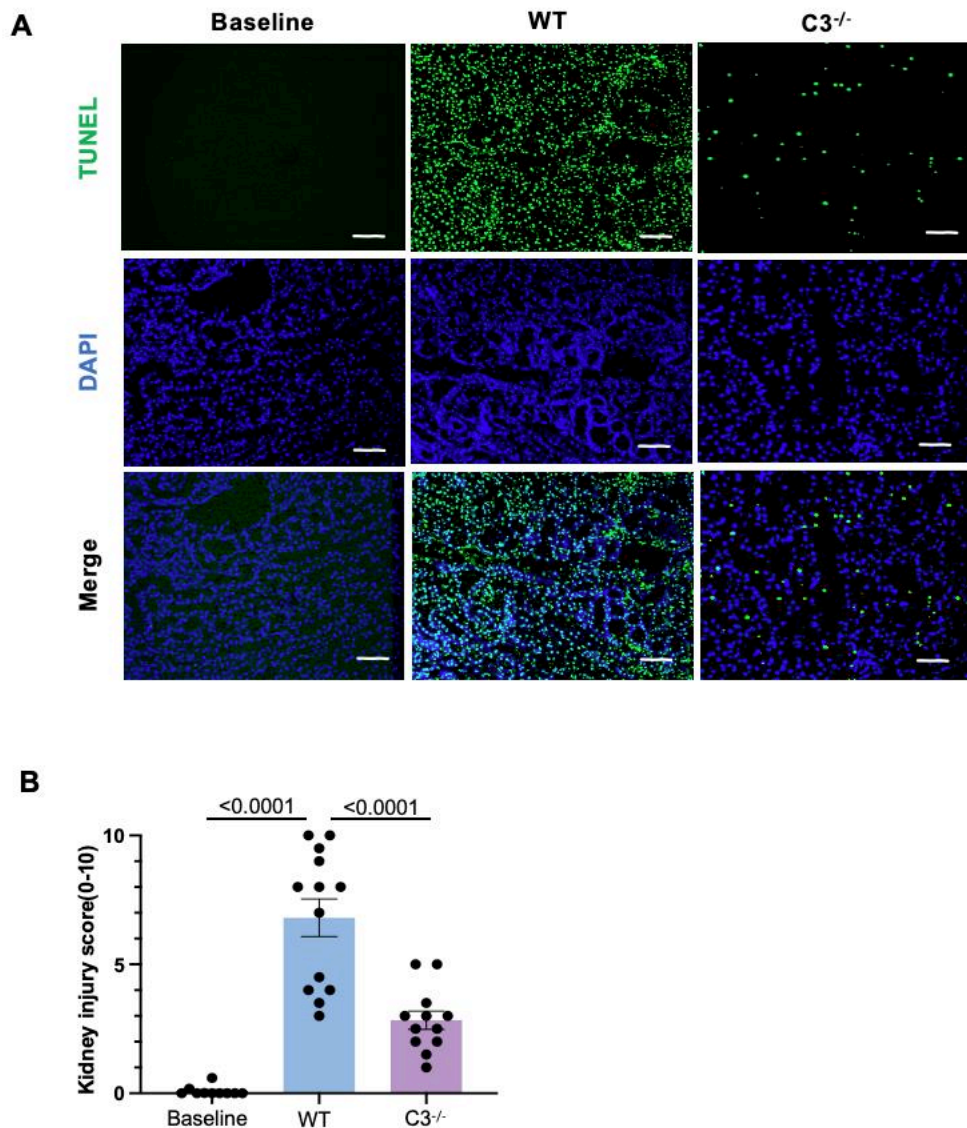


Figure 14: TMA-related cell death with C3 deficiency. (A) Representative image of TUNEL staining in baseline, wild-type mice and C3 knockout mice, scale bar: 50 μ m; **(B)** Quantitative results of TUNEL staining in baseline, wild-type mice and C3 ko mice, all quantitative data are means \pm SEM and analyzed by one-way ANOVA.

4.2 C5a/C5aR axis in crystalline thrombotic microangiopathy

4.2.1 C5a/C5aR axis improved kidney function and reduced infarct size in crystalline thrombotic microangiopathy

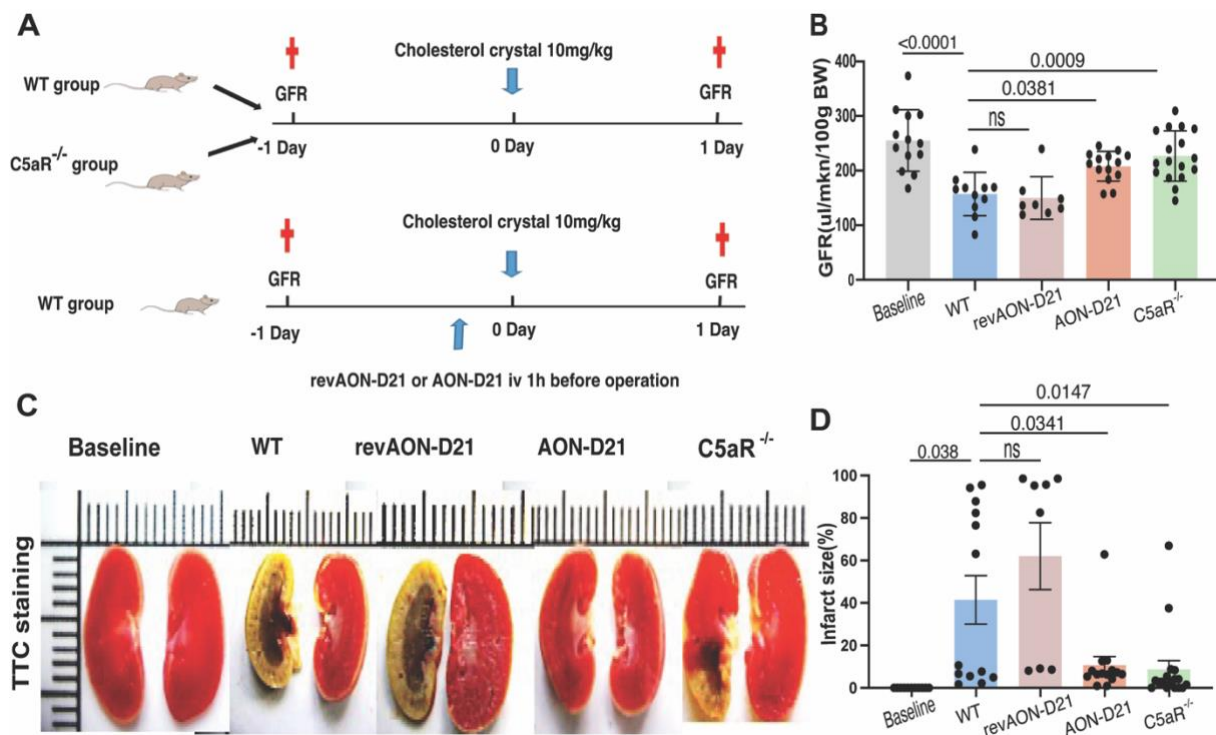


Figure 15: C5a/C5aR axis prevented the kidney from kidney failure and infarct size. (A) Schematic diagram of experimental design. **(B)** Quantitative of GFR measurement in baseline, wild-type mice, mice treated with revAON-D21 or AON-D21 and C5aR knockout mice. **(C)** Representative image of TTC staining in baseline, wild-type mice, mice treated with revAON-D21 or AON-D21 and C5aR knockout mice; **(D)** Quantitative of TTC staining in baseline, wild-type mice, mice treated with revAON-D21 or AON-D21 and C5aR knockout mice, all quantitative data are means \pm SEM and analyzed by one-way ANOVA.

AON-D21 (formerly NOX-D21) is a pegylated L-configured aptamer that binds and thereby neutralizes the complement component C5a from activating both C5 receptors. Wild-type mice received an intravenous injection of AON-21 1 hour before CC-driven TMA, and 1 hour before operation control mice were injected with reversed AON-D21 (revAON-D21) as shown in (Figure 15A), a control L-aptamer with the same nucleotide composition as AON-D21 that does not bind C5a [132]. To narrow down the exact mechanisms and directly assess the involvement of the C5a/C5aR axis, I performed CCE surgery on C5aR knockout mice as well. From the observations derived from GFR measurements in C5aR knockout mice, a notable revelation showed that the absence of the C5a receptor exerted a positive influence on kidney function, manifesting as a remarkable amelioration of kidney failure. This amelioration was further highlighted by a substantial elevation in GFR value, in contrast to the untreated wild-type group, as illustrated in Figure 15B.

Similarly, the preemptive treatment of the AON-21 group presented another intriguing aspect of this investigation. In the presence of C5a inhibition, the group exhibited a

significantly higher GFR value, showing the critical influence of C5a in the pathophysiological cascade. In contrast, the wild-type mice, left untreated or subjected to the administration of reAON-D21, displayed an almost 30 % reduction in their GFR values, further proving the significance of C5a. Moreover, the consequences of C5a receptor deletion revealed a reduction in the infarct size within the CC-perfused kidney, as illustrated in Figure 15C and D. This reduction contrasted with the untreated wild-type mice or those subjected to reAON-D21 administration. In sum, the abrogation of C5a receptor signaling paved the way for a more favorable outcome in terms of kidney injury. Intriguingly, the inhibitory impact of C5a was achieved by the injection of AON-D21, which notably reduced the infarct area, like the outcomes observed in C5aR knockout mice. This evidence highlighted the therapeutic promise of targeting the complement system, specifically the C5a/C5aR axis. Thus, it became clear that inhibiting C5a or blocking the C5a receptor represents a pivotal and effective strategy in regulating the pathophysiological progression of crystalline TMA.

4.2.2 The C5a/C5aR mediated cholesterol crystal embolism-related arterial occlusion

To better understand the characters of TMA arterial occlusion, α -SMA and fibrinogen co-staining were employed on kidney histological sections of baseline, wild-type mice with no treatment or revAON-D21 or AON-D21 injection as well as C5aR knockout mice. From the consequences derived from α -SMA and fibrinogen co-staining in C5aR knockout mice, a remarkable revelation displayed that the absence of C5aR lessen crystalline TMA as indicated by a robust reduction in arterial occlusion no matter interlobular or arcuate arteries classification (Figure 16A, B), wild-type mice as well as revAON-D21 mice exhibited roughly 30 % occluded arteries. However, mice treated with inhibitory C5a AON-D21 showed a notable 10 % arterial obstruction, which was like C5aR knockout mice. To explore the C5a involved role, the administration of inhibitory C5a AON-D21 significantly diminished the vessel obstruction in comparison to the untreated wild-type mice or those that were accepted to injection of control aptamer revAON-D21.

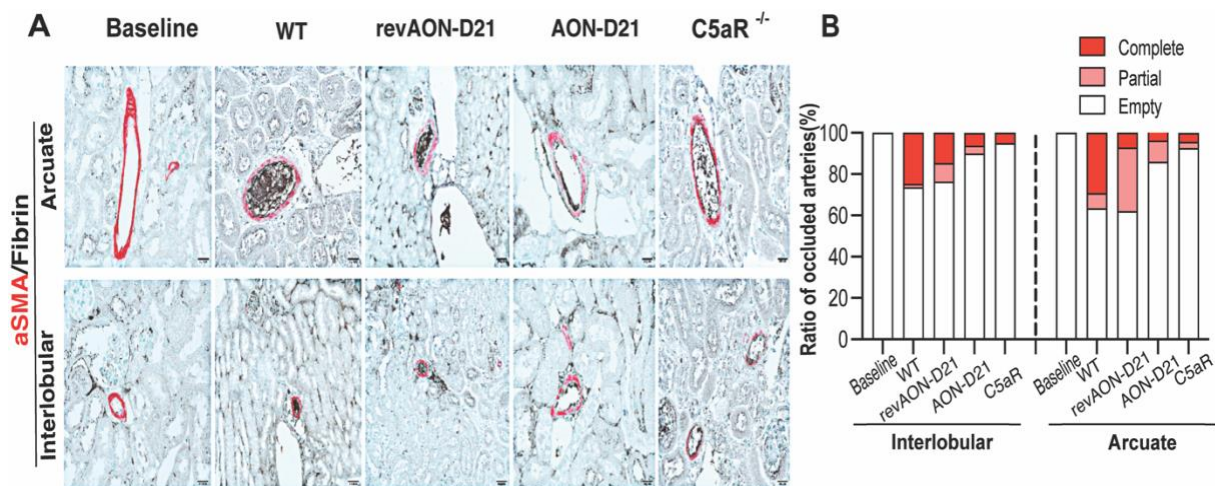


Figure 16: The C5a/C5aR reduced thrombus formation in crystalline TMA. (A) Representative image of interlobular and arcuate arterial occlusion crystalline thrombotic microangiopathy in baseline, wild-type mice, mice treated with revAON-D21 or AON-D21 and C5aR knockout mice, scale bar: 50 μ m. **(B)** Quantitative of Ratio of occluded interlobular and arcuate arteries in baseline, wild-type mice, mice treated with revAON-D21 or AON-D21 and C5aR knockout mice, all quantitative data are means \pm SEM and analyzed by one-way ANOVA.

Together, my findings demonstrate that the C5a/C5aR axis is sufficient to mitigate crystalline TMA by diminishing the vessel obstruction and reducing clot formation as illustrated by α -SMA and fibrinogen histological co-staining.

4.2.3 The C5a/C5aR mediated endothelial injury and immune cell infiltration

In the next step, I moved forward to investigate the role of the C5a/C5aR axis by the assessment of endothelial injury and neutrophil infiltration via histochemistry of CD31 and Ly6G staining. As endothelium contributes to the development of crystalline TMA, and immune cell infiltration as a key link of inflammation initiation, is a crucial way to be involved in a range of diseases. The absence of C5aR presented an impressive elevation of CD31 staining in comparison to untreated wild-type mice or mice subjected to administration of control aptamer revAON-D21, like the inhibition of C5a (Figure 17A, B). The blockage of C5a provided us another aspect of this process. The inhibition of C5a significantly protected endothelial cells from injury. To explore the crystalline TMA from another aspect of inflammatory-related neutrophil infiltration, Ly6G staining was employed in kidney sections of all groups, I observed that the deletion of the C5a receptor was sufficiently able to prevent neutrophils migrated to tissue injury sites,

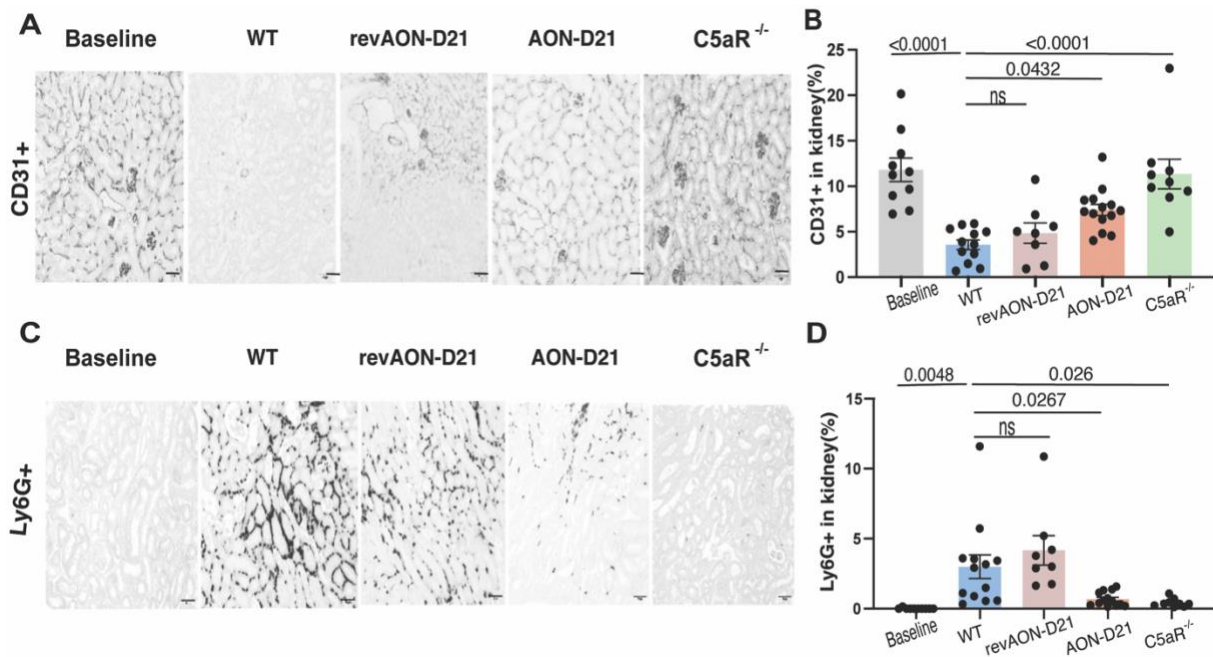


Figure 17: The C5a/C5aR mitigated TMA by diminishing endothelial injury and neutrophil migration. (A, C) Representative image of CD31 positive and Ly6G positive kidney section in baseline, wild-type mice, mice treated with revAON-D21 or AON-D21 and C5aR knockout mice; scale bar: 50 μ m. (B, D) Quantitative of CD31 positive and Ly6G positive area in baseline, wild-type mice, mice treated with revAON-D21 or AON-D21 and C5aR knockout mice, all quantitative data are means \pm SEM and analyzed by one-way ANOVA.

which was proved by a variety of elucidation that the C5a/C5aR axis is a strong attractant to immune cell migration from blood (Figure 17C, D). Therefore, the inhibitory C5a is enough to diminish neutrophil infiltration in the CC-perfused kidney section as we expected in contrast to the untreated wild-type group as well as mice subjected to administration of control aptamer revAON-D21.

In summary, the above findings demonstrate that the C5a/C5aR axis accelerates endothelial cell damage during the initiation of crystalline TMA. Besides, the C5a/C5aR attracts immune cells. Especially, neutrophils migrate to tissue injury sites from the blood and neutrophils further exacerbate the pathophysiological process of tissue inflammation.

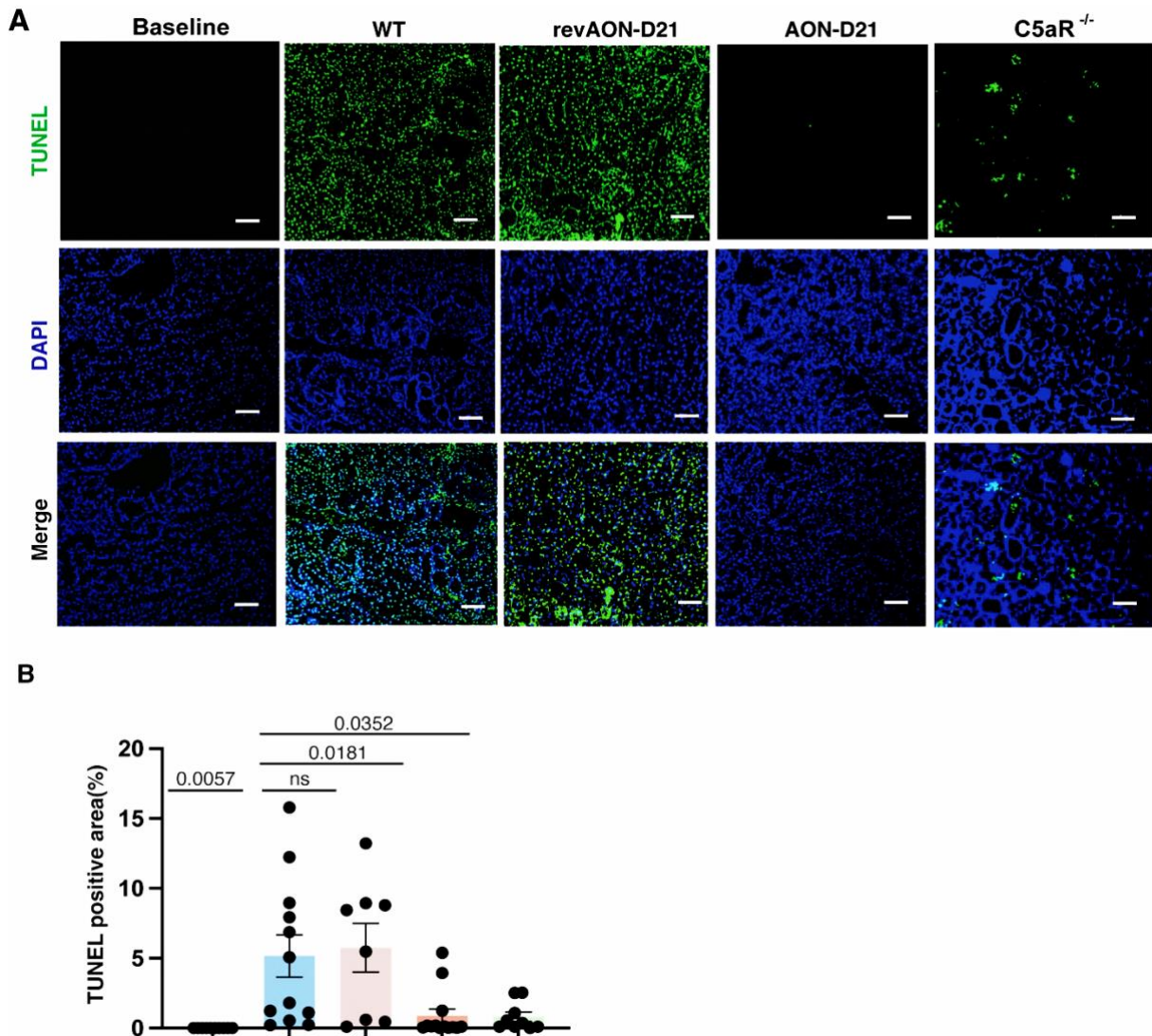


Figure 18: The C5a/C5aR diminished cell death in crystalline thrombotic microangiopathy. (A) Representative image of TUNNEL staining section in baseline, wild-type mice, mice treated with revAON-D21 or AON-D21 and C5aR knockout mice; scale bar: 20 μ m. **(B)** Quantitative of TUNEL staining in baseline, wild-type mice, mice treated with revAON-D21 or AON-D21 and C5aR knockout mice; all quantitative data are means \pm SEM and analyzed by one-way ANOVA.

4.2.4 C5a/C5aR diminished cell death in crystalline thrombotic microangiopathy

To characterize the impact of the C5a/C5aR on kidney injury, I performed TUNEL staining on CC-perfused kidney histochemical sections. From the observation I obtained from wild-type mice as well as revAON-D21 injection group by assessment of kidney cell death represented via TUNEL staining, without any interventions, the control group exhibited a strongly notable elevation of kidney cell death shown by green color. However, wild-type mice with preemptive administration of C5a inhibitor AON-D21 significantly reduced kidney cell death, which indicated that C5a was an important component in cell death pathogenesis. In addition, the

observation derived from the abrogation of the C5a receptor displayed that the C5a receptor contributed to the cell damage and death caused by CC-induced TMA (Figure 18A, B). Together, our observations demonstrate that the C5a/C5aR is sufficient to reduce cell injury and cell death during TMA induction, and consistently it further proves that the C5a/C5aR could be a potential target for TMA-associated diseases.

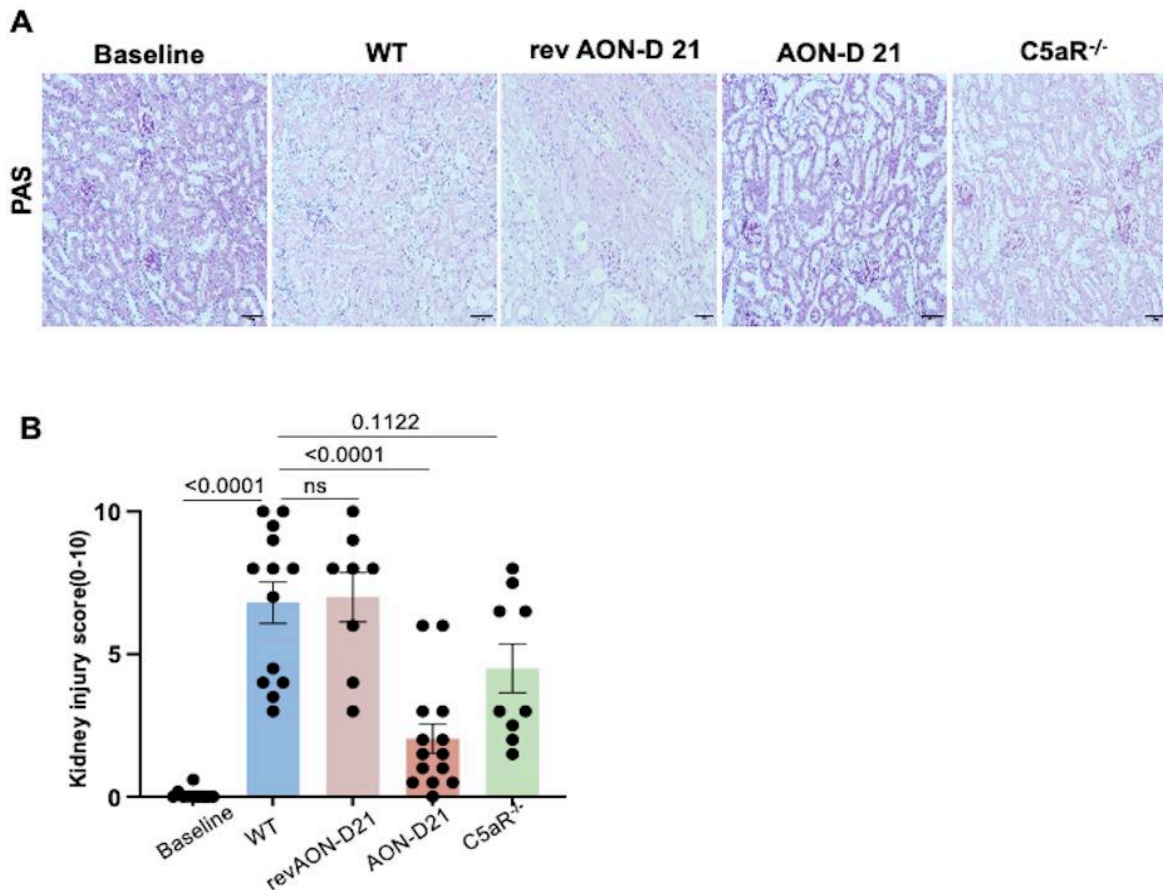


Figure 19: The C5a/C5aR mitigated kidney injury in crystalline TMA. (A) Representative images of PAS staining in baseline, wild-type mice, mice treated with revAON-D21 or AON-D21 and C5aR knockout mice, scale bar: 50um. **(B)** kidney injury of PAS-stained kidney section in baseline, wild-type mice, mice treated with revAON-D21 or AON-D21 and C5aR knockout mice, all quantitative data are means \pm SEM and analyzed by one-way ANOVA.

4.2.5 C5a/C5aR inhibition mitigated CCE-induced kidney injury

To verify the kidney injury extent during the CCE-driven TMA, PAS staining was employed in all treatment, C5aR knockout, and untreated groups. The inhibition of C5a as well as C5a receptor deletion attenuated kidney injury shown by less cell necrosis and tubular dilation and other parameters shown in Table 10. In contrast, wild-type and control aptamer groups had

higher and worse kidney tissue injury (Figure 19A, B). Therefore, PAS staining exhibited that the C5a/C5aR axis takes part in aggravating kidney damage in crystalline TMA.

4.3 C5a inhibition resolved established thrombotic microangiopathy

4.3.1 Early treatment of C5a inhibitor improved kidney function in established thrombotic microangiopathy

After having investigated the preemptive inhibition of the C5a/C5aR, I further evaluated the window-of-opportunity of the C5a inhibitor to address clinical scenario. Normal wild-type male mice at 6-8 weeks were subjected to inject AON-D21 3 hours, 6 hours, 9 hours, and 12 hours after TMA induction caused by CCE (Figure 20A, B), GFR was measured before surgery and 24 hours post-surgery. 24 hours after surgery kidneys were collected from all mice for the analysis. Kidney sections were cut into several pieces, one of which was stained for TTC. As a control, wild-type mice with no treatment accelerated kidney function shown by a nearly 40 % loss of GFR value. However, the administration of 5a inhibitory AON-D21 6 hours post-operation mitigated kidney function disruption via recovery of 20-30 % GFR loss, which was like treatment of C5a inhibitory AON-D21 12 hours in GFR monitor. The GFR result gives us a hint that ever 12 hours after crystalline TMA occurrence. Furthermore, as illustrated by (Figure 20C, D), the inhibitory C5a attenuated kidney infarct size at the early period of crystalline TMA induction and continued to functionate even at the later time point of 12 hours post operation.

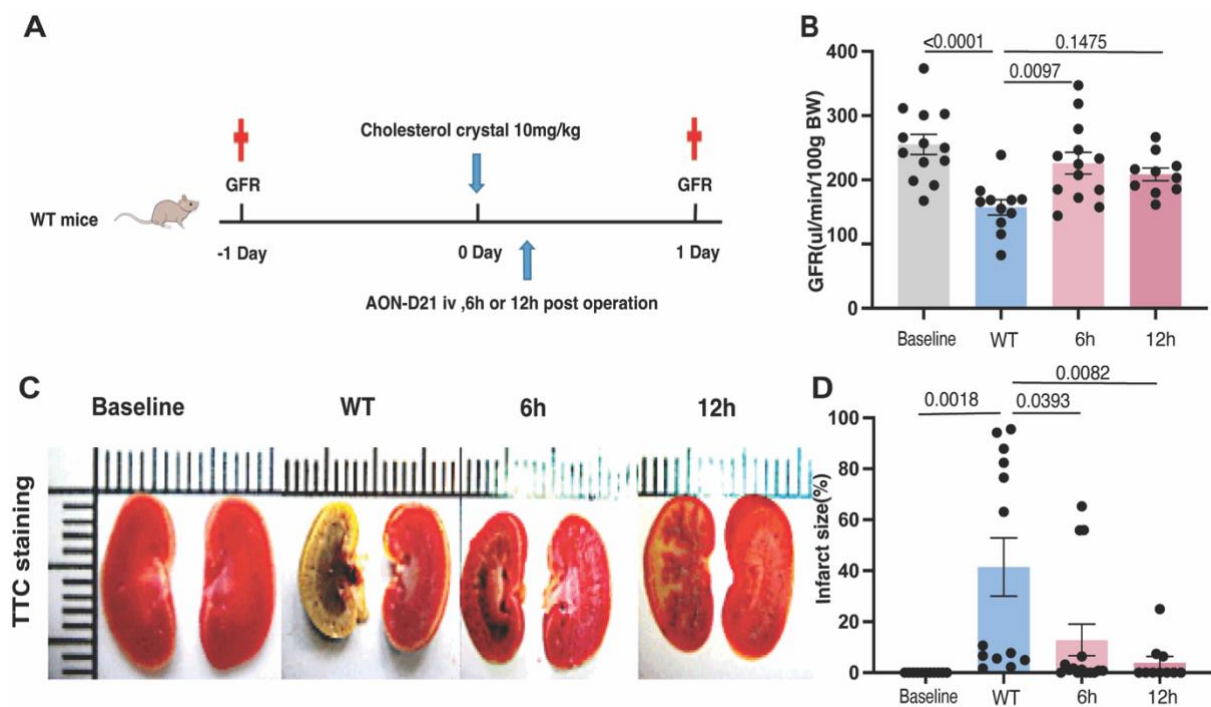


Figure 20: Treatment of C5a inhibitor improved kidney function in established TMA. (A) Schematic diagram of C5a inhibition window-of-opportunity therapy in established thrombotic microangiopathy. **(B)** GFR measurement of AON-D21 treatment 6 hours and 12 hours after TMA induction. **(C)**

Representative images of TTC stained kidney in baseline, wild-type ,6 hours and 12 hours post-operation. **(D)** Quantification of TTC stained kidney infarct size in baseline, wild-type ,6 hours and 12 hours post-operation, all quantitative data are means \pm SEM and analyzed by one-way ANOVA.

In sum, my results suggested that the strategy of AON-D21 treatment at the early stage of crystalline TMA progress was sufficient to counteract the kidney function disruption caused from TMA-driven kidney damage. In addition, blockage of C5a diminished the kidney tissue damage and the infarct size at 6 hours and 12 hours after CCE-induced TMA. Therefore, those findings demonstrate that at late time of crystalline TMA the administration of C5a inhibition could be effective for improving kidney function and reducing injury.

4.3.2 Administration of C5a inhibitor at early thrombotic microangiopathy alleviated thrombus formation

As we expected, α -SMA and fibrinogen co-staining revealed that inhibition of C5a prevents clot formation. Injection of AON-D21 6 hours after operation strongly reduced clot formation via only less than 10 % occluded arteries. However, wild-type mice with no treatment almost reached 30 % interlobular occluded arteries and nearly 40 % arcuate obstructed arteries as shown in Figure 21A and B. The consequence indicated that C5a presented in circulating blood is notably beneficial to thrombus formation under TMA condition. Therefore, aiming for C5a blockage is a potential approach to the TMA therapeutic strategy.

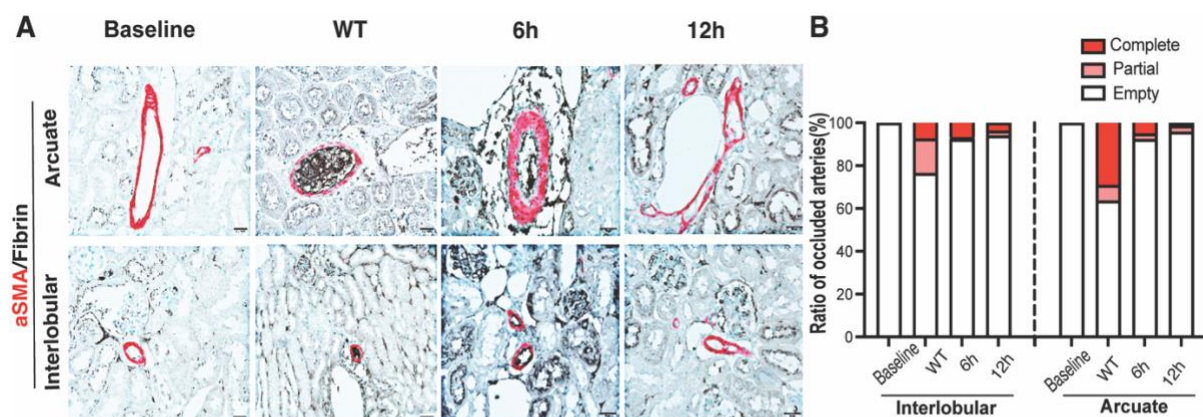


Figure 21: Administration of C5a inhibitor at early TMA alleviated thrombus formation. (A) Thrombus formation of AON-D21 treatment at early time of crystalline TMA induction, scale bar: 50um. **(B)** Quantification of ratio of occluded arteries, all quantitative data are means \pm SEM and analyzed by one-way ANOVA.

4.3.3 Early treatment of C5a inhibitor ameliorated endothelial injury and immune cell migration in established thrombotic microangiopathy

To test the impact of inhibitory C5a treatment at early time points under the duration of TMA-induction, the assessment of CD31 and Ly6G histochemical staining were analyzed by the means of quantification of CD31 and Ly6G positive areas in the whole kidney sections. In comparison to wild-type mice, which showed 50 % CD31 severe loss with the indication of elevated endothelial injury, treatment of C5a inhibitory AON-D21 displayed a noteworthy higher CD31 presence at 12 hours post CCE, which reached to the baseline level. Surprisingly, injecting C5a inhibitory AON-D21 at 6 hours after TMA induction showed no significant influence in the endothelial cell injury (Figure 22A, B). On the other hand, the therapy of inhibitory C5a AON-D21 had a strong influence on the immune cell migration, the treatment groups with injection of AON-D21 at 6 hours and 12 hours post TMA induction revealed a notable less neutrophils influx within kidney (Figure 22C, D).

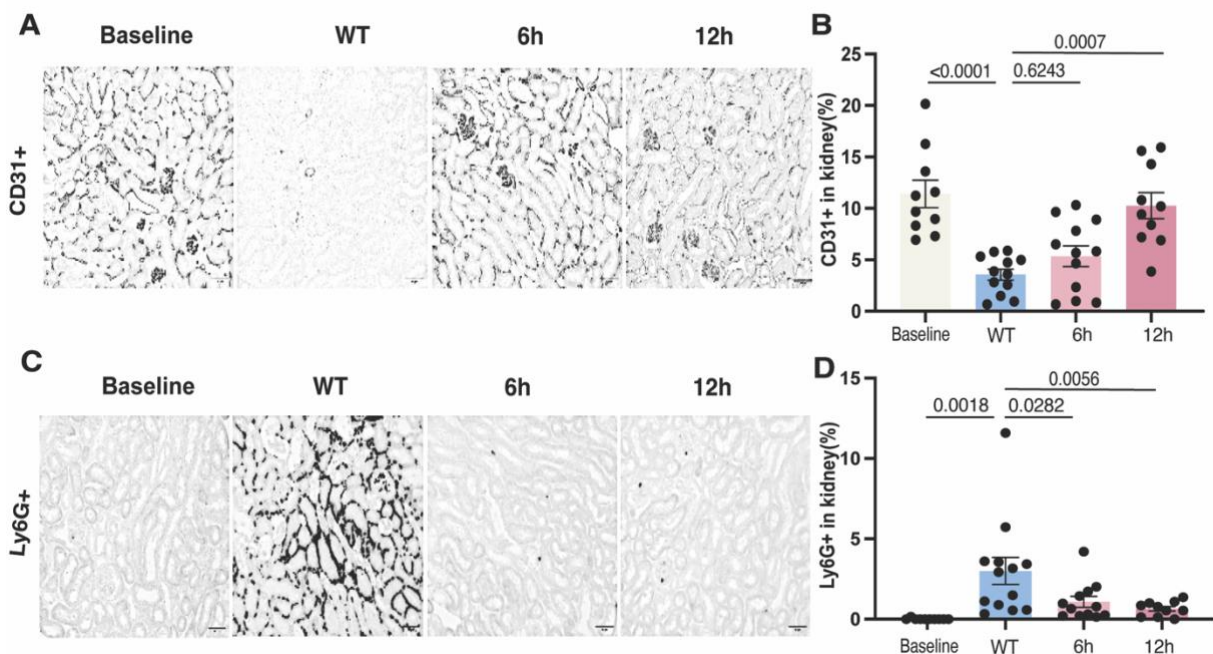


Figure 22: Early treatment of C5a inhibitor ameliorated endothelial injury and immune cell migration in established TMA. (A) Representative images of CD31 positive kidney sections with CC perfusion under AON-D treatment at 6 hours, and 12 hours post TMA induction; scale bar: 50 μ m. **(B)** Quantification of CD31 positive percentage in kidney sections at different time points. **(C)** Representative images of Ly6G positive kidney sections with CC perfusion under AON-D treatment at 6 hours, 12 hours post TMA induction; scale bar: 50 μ m. **(D)** Quantification of Ly6G CD31 positive

percentage in kidney sections at different time points, all quantitative data are means \pm SEM and analyzed by one-way ANOVA.

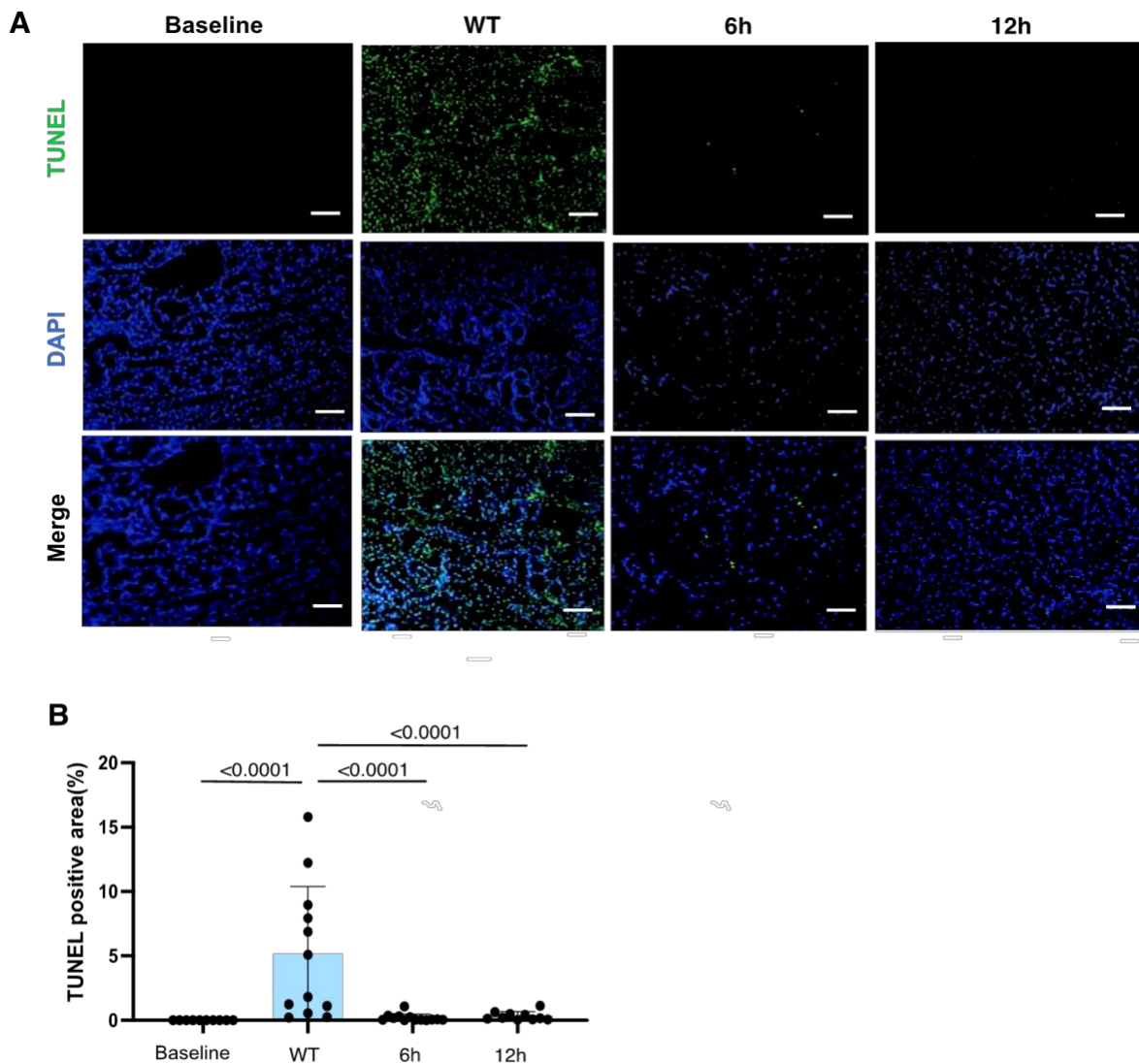


Figure 23: Early treatment of C5a inhibitor protected the kidney from cell death in established TMA. (A) TUNEL staining of CC-perfused kidney with the treatment of C5a inhibitory AON-D21 at 6 hours, 12 hours. **(B)** Quantification of TUNEL staining in CC perfused kidney, all quantitative data are means \pm SEM and analyzed by one-way ANOVA.

4.3.4 Early treatment of C5a inhibitor protected kidney from cell death in established thrombotic microangiopathy

Highly consistent with the above findings, injection of inhibitory C5a AON-D21 at 12 hours post TMA induction remarkably limited the spectrum of cell death during the kidney damage under the treatment at different time points. Shown via TUNEL staining (Figure 23A, B), both

two time points of AON-D21 administration remained more alive kidney residual cells in contrast to the untreated group . Taken together, TUNEL staining proves that even inhibiting C5a at a late time point such as 12 hours still provides a protective role in TMA-induced cell death.

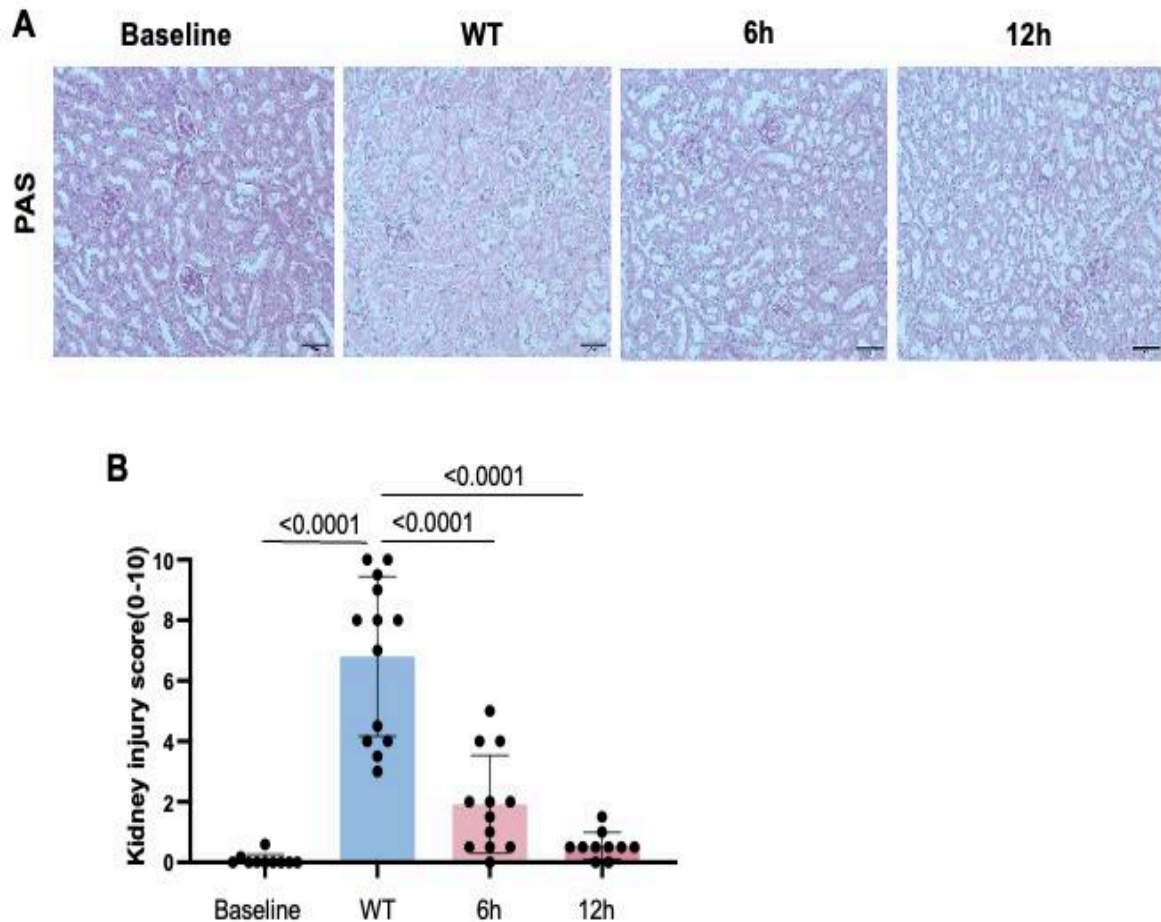


Figure 24: Kidney injury after treatment of C5a inhibitor in the crystalline TMA. (A) Representative of PAS staining shown with C5a inhibition treatment 6 hours and 12 hours after TMA induction, scale bar: 50 μ m. **(B)** Quantification of kidney injury after treatment of C5a inhibition; all quantitative data are means \pm SEM and analyzed by one-way ANOVA.

4.3.5 Role of C5a in kidney injury

To be in line with the consequence of cell death from TUNEL staining, I investigated PAS staining in kidney histochemical samples derived from the mice with AON-D21 therapy at different time points. As shown in Figure 25A and B, Ablation of C5a had a significant effect on the overall kidney injury. Inhibiting C5a 6 hours after CCE promoted normal kidney tissue ratio

by reducing kidney injury, similarly and intriguingly delayed treatment 12 hours post-TMA also remained more healthy tissue than early treatment 6 hours. Overall, C5a took part in an range of pathophysiological processes during TMA. Therefore, the approach of blocking C5a attributes to rescuing kidney from crystalline-induced kidney failure.

4.4 Mechanism-of-action of C5a inhibition

4.4.1 Role of C5a in endothelial cells injury caused by cholesterol crystals

To identify the mechanism of the C5a/C5aR axis on crystalline TMA, I assessed the impact of C5a inhibition on endothelial cells, neutrophils as well as platelets *in vitro*. To begin with the effect of C5a inhibition on endothelial cell injury, mouse glomerular endothelial cells (GenC) were used to measure injury severity by adding C5a protein and C5a inhibitor. The addition of CC into GenC damaged endothelial cells indicated by an increase of VCAM, ICAM as well as P-selectin (Figure 25A, B), which are the markers of the endothelial injury. While with the presence of C5a protein, the severity of endothelial injury was significantly raising 3-4 times in comparison to no treatment group. CXCL12 is a protein that mediates its effects through binding and activation of chemokine receptors CXCR4 expressed on the cell surface. Under activation of endothelial cells, CXCL12 is released from endothelial cells and attracts neutrophils migrating to the injury site.

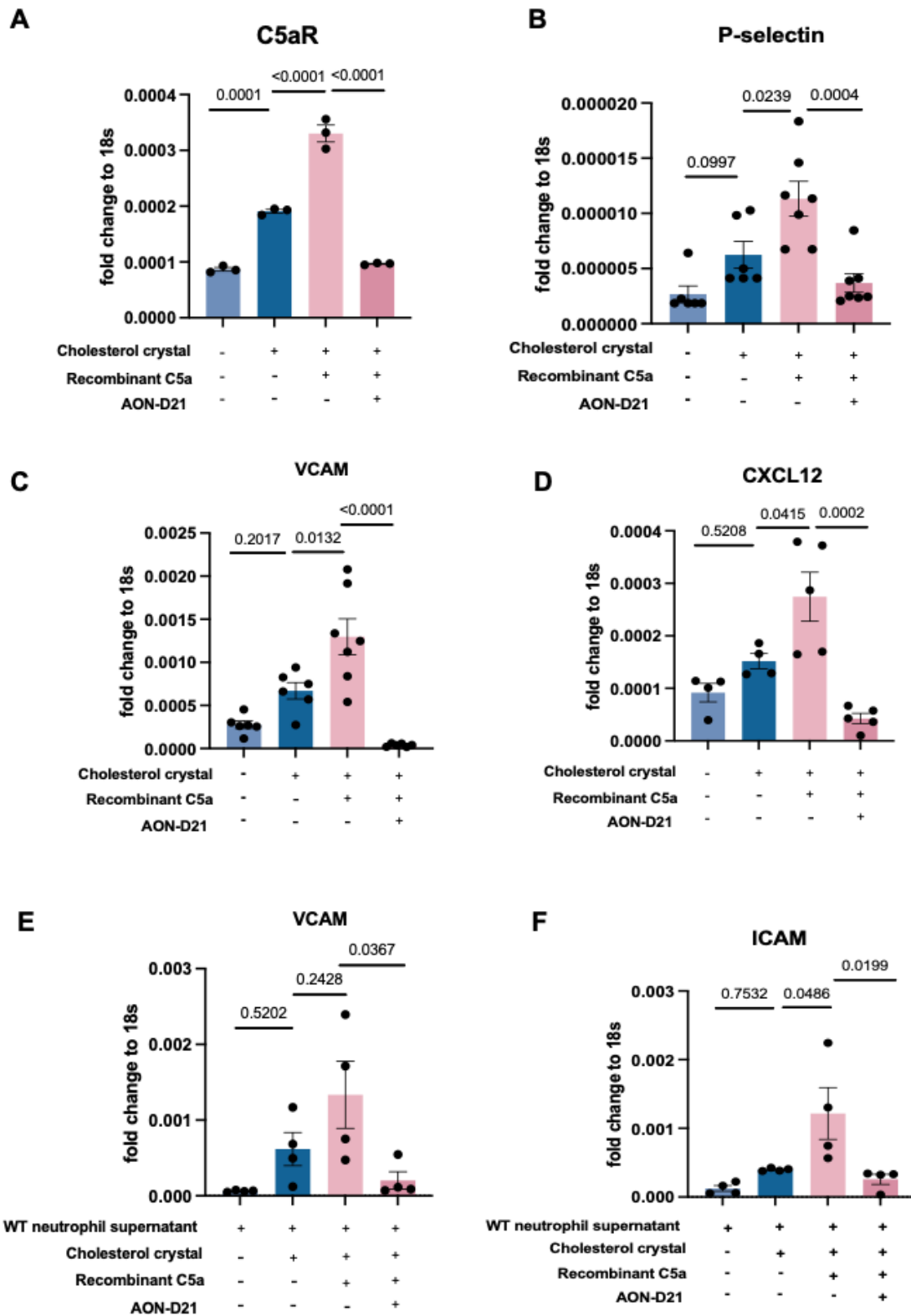


Figure 25: Endothelial cell injury in GenC. (A, B, C) Vcam, P-selectin, CXCL12 expression in mouse endothelial cells upon exposure to the treatment of CC, recombinant C5a protein, and C5a inhibitor. GenC after inhibition of C5a protein showed significantly less endothelial cells injury. (D, E) VCAM,

Results

ICAM expression level in mouse endothelial cells with treatment of CC, recombinant C5a protein C5a inhibitor under the presence of wild-type neutrophil supernatant. GenC after inhibition of C5a protein shows significantly less endothelial cell injury. **VCAM**: vascular cell adhesion molecule, **ICAM**: Intercellular adhesion molecule. All quantitative data are means \pm SEM and analyzed by using one-way ANOVA followed by Dunn post-test.

The expression of CXCL12 on endothelial cells increased after inculation with CC, even was higher with the presence of C5a protein. However, inhibition of C5a via AON-D21 noteworthyly reduced the level of the endothelial injury marker expression (Figure 25A, B, C). Under the presence of neutrophil supernatant, the results were consistant with our findings. Altogether, the presence of CC leads to severe damage on endothelial cells, while the blockage of C5a reverses this side effect caused by C5a protein and CC.

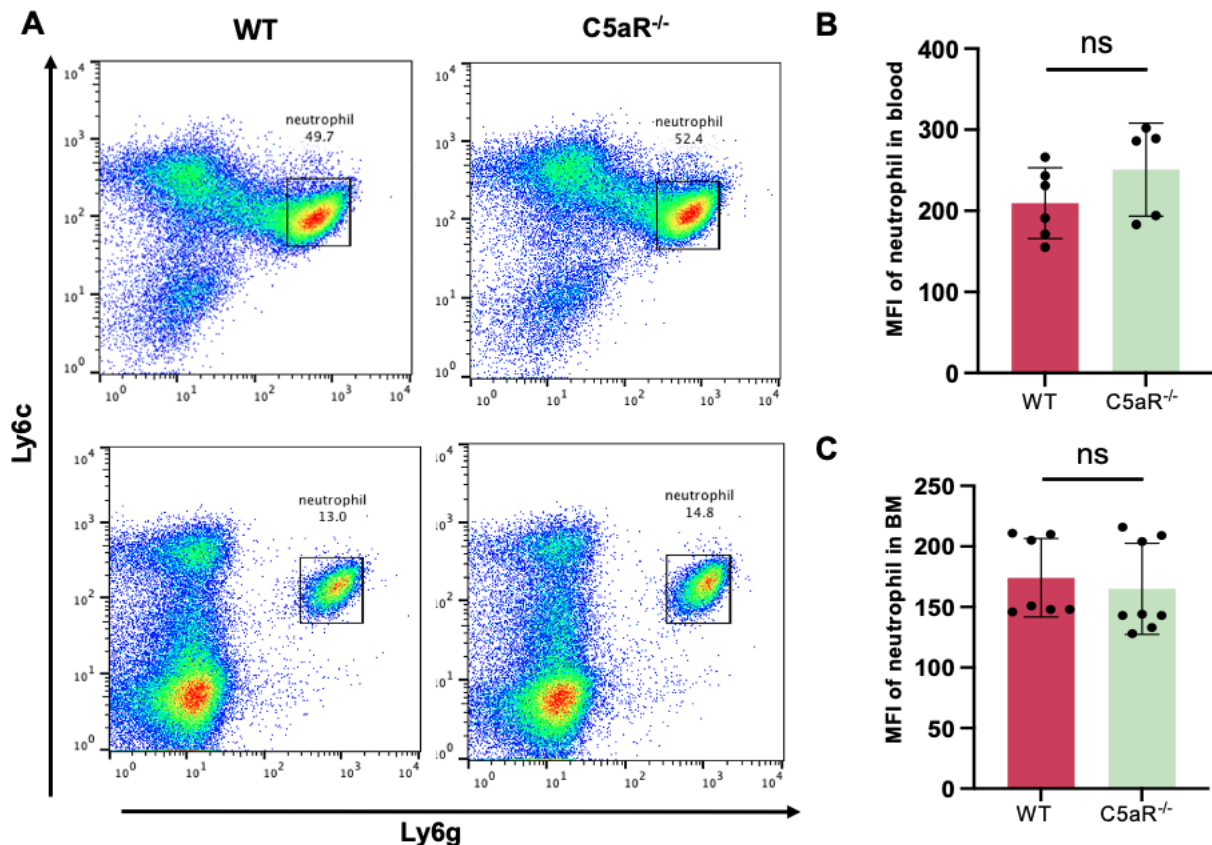


Figure 26: Neutrophil concentration in blood and bone marrow. (A) Flow cytometry showed the population of neutrophils in blood and bone marrow, neutrophils are both positive in Ly6c and Ly6g. **(B)** Neutrophil MFI of blood in C5aR knockout mice and wild-type mice. There is no significant difference in both groups. **(C)** Neutrophil MFI isolated from bone marrow of C5aR knockout mice and wild-type mice. All quantitative data are means \pm SEM and analyzed by one-way ANOVA.

4.4.2 Role of C5a in neutrophil migration initiated by cholesterol crystals

Neutrophils are front-line cells of the innate immune system. These effector leukocytes are armed with anti-microbial systems, which translate into a potent cytotoxicity. Accurate neutrophil recruitment plays a pivotal role in microbial defense, inflammation control, wound healing, and tissue repair [133].

To test the effect of the C5a/C5aR on neutrophil migration, at the beginning, collection of whole blood from wild-type mice and C5aR knockout mice was done and stained with CD45, Ly6G and LyC antibodies (Figure 26A). CD45 identifies immune cells, Ly6G is used to stain neutrophils in the blood, and Ly6C recognizes monocytes. After incubation with all the antibodies, blood samples from wild-type mice and C5aR knockout mice went through flow cytometry. The result showed that there is no significantly difference in wild-type mice and C5aR knockout mice on the number of neutrophils in blood (Figure 26B, C).

In the next step, I started to test neutrophil migration function by the mean of transwell migration assay. The transwell plate insert was coated with collagen overnight. 2×10^5 neutrophils were isolated from wild-type mice as well as C5aR knockout mice, then added neutrophils from different mice to the transwell upper insert. In the lower chamber, C5a protein/C5a inhibitory AON-D21 was added and incubated for 3 hours. Neutrophils were collected from the lower chamber and went through the flow cytometry.

Deletion of C5aR prevented neutrophils migration regardless of the C5a and C5a inhibitory AON-D21 addition. Neutrophils from wild-type mice exhibited a strong capacity of migration function under the presence of C5a. While after blockage of the C5a protein, wild-type neutrophils lose their quality of migration (27A, B, C). Altogether our findings suggest that C5a is a strong immune attractant to neutrophils. Inhibition of C5a attenuates neutrophil migration.

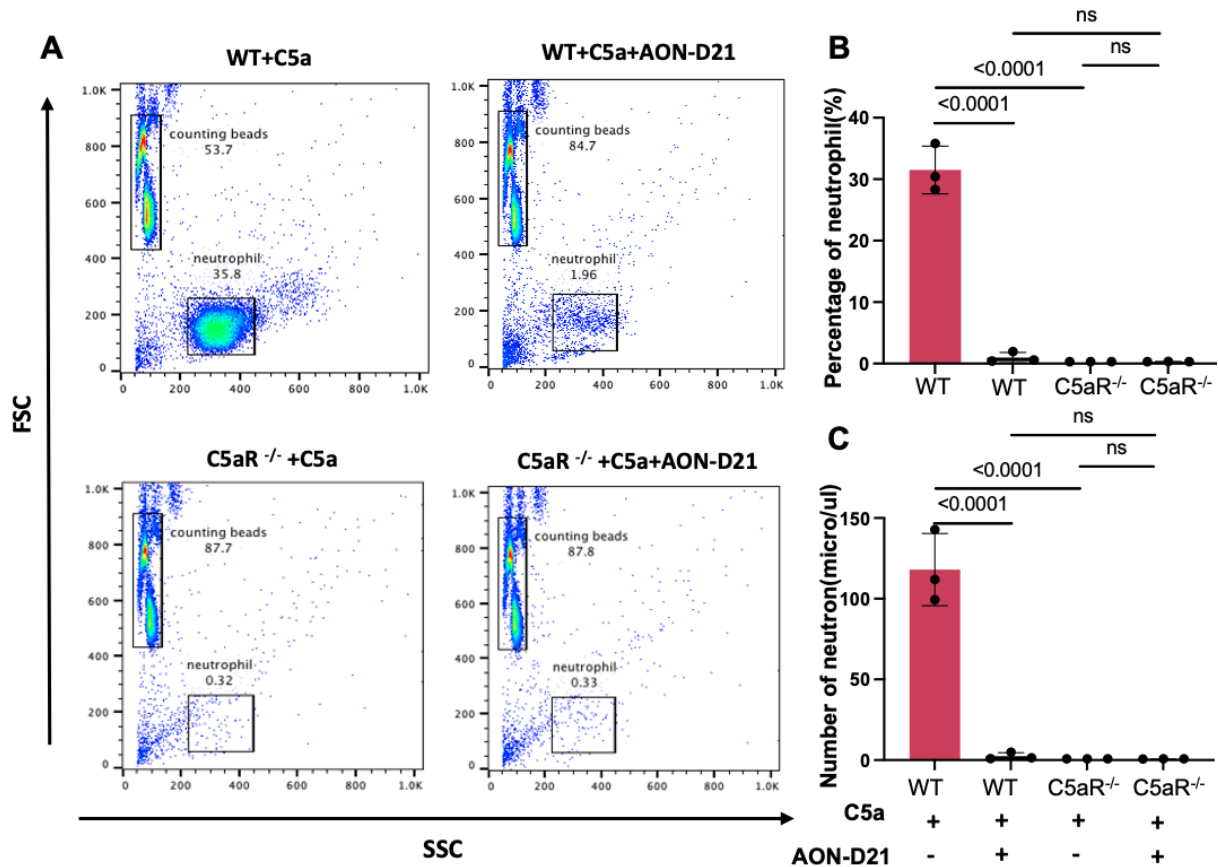


Figure 27: Neutrophil migration ex vivo. (A) Flow cytometry shows a population of migrated neutrophils under different treatments. (B). Percentage of migrated neutrophils in C5aR^{-/-} mice and wild-type mice under treatment of recombinant C5a and C5a-neutralizing L-aptamer, respectively. (C) Neutrophils isolated from C5aR^{-/-} mice and wild-type mice under the presence of recombinant C5a and C5a-neutralizing L-aptamer, respectively. C5aR^{-/-} and C5aR inhibitor treatment groups show less migrated neutrophil compared to wild-type group under chemoattractant C5a. All quantitative data are means ± SEM and analyzed by one-way ANOVA.

4.4.3 Role of C5a in platelet activation and platelet-interaction with neutrophils

In the intricate context of TMA, where the interplay between various cellular components participates in the course of the disease, platelets act as key players. They serve not only as thrombogenic elements but also provide a critical surface for the adhesion of various circulating cells, including neutrophils. Thus, I carried on the influence of C5aR in thrombus formation on a collagen-coated surface within a flow chamber. Under the conditions characterized by a shear rate of 1000 s⁻¹, I observed a significant impairment in platelets adhesion and a significant reduction in thrombus formation on the collagen matrix in samples from C5aR-deficient mice. In contrast to the outcomes observed in wild-type samples,

documented in Figure 28A and C. This evidence underscores the potential anti-thrombotic efficacy of inhibiting C5aR function, mitigating the thrombotic aspects of TMA.

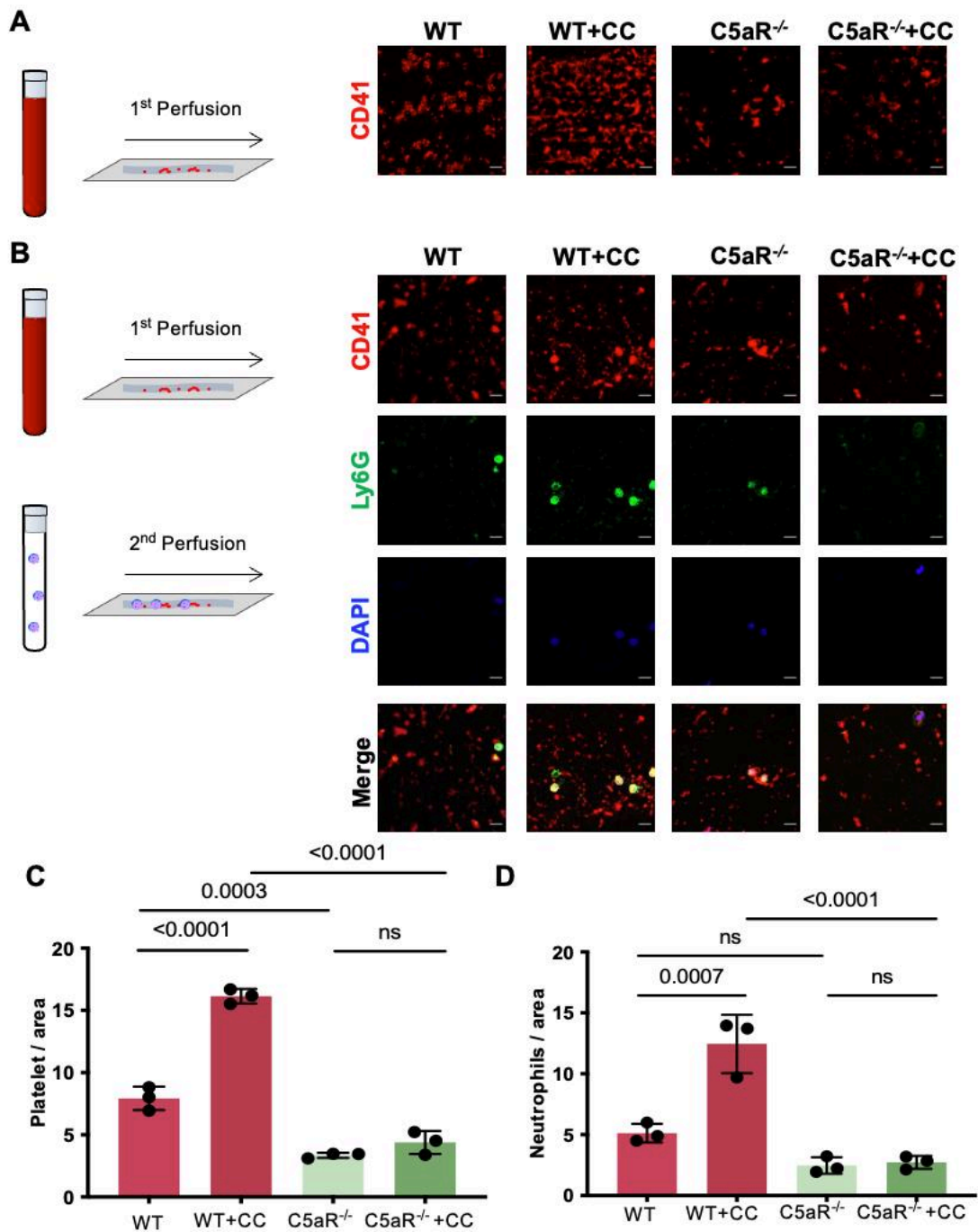


Figure 28: C5aR deficiency inhibited CC-induced thrombus growth on collagen and prevents the adhesion of neutrophils to the thrombogenic surface. (A) In a one-step flow chamber assay, platelet-rich thrombi were formed by perfusing heparinized whole blood from wild-type or C5aR knockout mice at $1000s^{-1}$ over a collagen-coated surface in the presence or absence of CC. **(B)** In a second-step flow chamber assay, mouse bone marrow neutrophils were perfused through the chamber at $500s^{-1}$. Platelets and neutrophils were stained an anti-CD41 (red) and anti-Ly6G (green) antibodies. Nuclei were stained with DAPI (blue). **(C, D)** Quantification of the area fraction of fluorescent signals

corresponding to the number of adherent platelets or neutrophils. Scale bar: 20 μ m. All quantitative data are means \pm SEM and analyzed by one-way ANOVA.

Subsequently, I assessed the recruitment of neutrophils to previously formed thrombi under flow conditions. I observed that mouse neutrophils perfused through the flow chamber system adhered to wild-type thrombi, whereas the attachment of neutrophils to C5aR^{-/-} thrombi was strongly inhibited (Figure 28B, D), indicating that targeting C5aR during TMA reduced thrombus growth and prevented neutrophil adhesion to the formed thrombi. Together, these findings indicated that blockade of the C5a-C5aR axis effectively reduced the critical steps of TMA formation, including the adhesion of platelets, thrombus growth and migration and recruitment of neutrophils to the thrombogenic kidney injury sites. In sum, my investigation into the role of C5aR in TMA illuminated various aspects of its pathogenesis. From neutrophil migration to platelet-mediated thrombosis and neutrophils adhesion. The evidence consistently points to the potential therapeutic efficacy of C5aR inhibition in the pathophysiology of crystalline TMA.

5. Discussion

We had hypothesized that using a reproducible model of crystalline TMA would be helpful in dissecting the pathophysiological process underlying CC-driven arterial obstruction, kidney failure tissue damage and cell death. The recently established model of crystalline TMA involves injecting CC into left kidney arteries of mice to mimic human CCE and focal TMA. During the acute stage injection results in several microvascular obstructions caused by ischemic infarction like the immunopathology of human TMA-related kidney diseases. This model provides us a novel approach to unraveling unknown pathomechanisms of vascular-related manifestations. In addition, this novel model also allows us to investigate gene-deficient mice as an experimental tool to unfold molecular pathomechanisms of certain gene implication in arterial thrombotic diseases. Therefore, in my experiments, C5aR-deficiency, C3-deficiency and a C5a inhibitor are used to study this CCE model to explore the implication of the C5a/C5aR on the crystalline TMA to provide a potential therapeutic guide to thrombosis diseases.

5.1 Ablation of the complement system attenuates kidney thrombotic microangiopathy and its consequences

Previous studies have reported that complement not only plays its potent effector role in antimicrobial defense but also probably directly forms on endogenous and exogenous surfaces to confer broader immunosurveillance [134] and activate cell lysis, phagocytosis, and downstream immune responses. Kidney TMA is acquired by either genetic mutations or antibodies against complement regulators [135]. Nearly 40-60 % of aHUS patients carry genetic mutations in genes such as factor H, factor I, membrane cofactor protein, C3 convertase and so on. Those genes are identified as complement regulatory proteins [136]. Overactivation of the complement system caused by genetic factors leads to endothelial damages, interaction with inflammation by recruiting plenty of immune cells, deposition of immune complexes as well as a reduction in the capacity of host defense.

In the CCE model, CC injection caused a sudden drop of GFR on average by about 40 % within the 24 hours after CC injection, i.e., acute kidney injury. However, deletion of the complement system entirely reverses the loss of GFR shown in wild-type mice, which tells us that the complement system contributes to ameliorate either the formation of clots or damage of

kidney residual tissues or both during kidney thrombotic microangiopathy. Our results suggest that in the acute phase of CCE, the complement system is a positive effector in accelerating kidney tubular and glomerular collapse. Kidney necrosis was associated with acute necroinflammation as indicated by the presence of neutrophils, cell death and kidney injury all around and inside the ischemic necrosis. Immunostaining outcomes reveal occlusive TMA in SMA-positive arcuate and interlobular arterial vessels with fibrinogen-positive clots surrounding CC clefts and loss of CD31+ endothelial cells. The cause of tissue infarction is diminished by abrogation of C3, which indicates that the complement system contributes to accelerate the kidney function disruption and cell death by the means of intervention of endothelium and clot formation as well as neutrophil infiltration. Therefore, the ablation of C3, a key and central element of all three complement activation pathways, results in a pivotal improvement of the complement system impact on kidney diseases. Genetic deficiency of C3 entirely prevented TMA and any of the consequences upon injection of the identical amount of CC into the kidney artery.

These data are consistent with the known role of the complement system in immunothrombosis, including TMA triggered by other mechanisms, such as COVID-19 [137]. COVID-19 is a new disease caused by severe acute respiratory syndrome coronavirus, which is associated with a hypercoagulable state characterized by increasing D-dimer and fibrin degradation products. In addition, COVID-19 has been shown an increased rate of thrombotic complications and overreaction of the complement system [138]. In immunothrombosis, complement can be initiated by chondroitin sulfate A, which is released from platelet α -granules and mediates the binding of complement fragments to platelets. Meanwhile, platelet activation triggers the activation of FXI and FXII within the coagulation system [139]. Besides the proteases MASP-1 and MASP2 of the activated complement lectin pathway are capable of cleaving the coagulation components such as pro-thrombin, fibrinogen, factor XIII, and thrombin-activatable fibrinolysis inhibitor in the context of thromboinflammation [140].

Thus, our results are consistent with recent studies indicating the vital role of the complement system in non-crystalline forms of TMA which provides the rationale for targeting C5, a downstream element of C3 activation fueling both into the C5a/C5aR-mediated immune cell recruitment and activation of immune cells or formation of the membrane attack complex C5b-9 [141].

5.2 Targeting the C5a/C5aR axis reduces kidney damage during crystalline thrombotic microangiopathy

Because C3 convertase is a central effector molecule of the entire complement system, genetic C3 deficiency is rare and leads to recurrent pyogenic infections, mainly caused by *Streptococcus pneumoniae* and *Neisseria meningitidis* [142]. C3-deficient patients were shown to develop immune complex(IC)-related diseases for instance systemic lupus erythematosus(SLE)-like disruption and kidney disease. C3 deficiency is also linked to impaired dendritic cell differentiation, B-cell response as well as T cell development in humans [143]. However, our results show that blockage of the complement system could be a potential approach for TMA. Therefore, the C5a/C5aR axis comes to our view with the benefit of no effects on complement main components.

I induced the same CC-TMA in mice with genetic deficiency of the C5aR and obtained similar results as with C3-deficiency in terms of AKI, diminished intravascular TMA arterial obstruction lesions, low ischemic necrosis, reduced CD31 loss in the microvasculature, small neutrophil infiltration in kidney, all those consequences strongly provide a hint that C5aR is dominant effector receptor in the pathomechanisms of CC-induced TMA. C5aR1/CD88 shows a high affinity binding transmembrane receptor to C5a, and C5aR1 is expressed by an extensive variety of cells types throughout human body, and mainly on immune cells such as granulocytes, macrophages, monocytes, and DCs [144], CD88 activation results in increased intracellular calcium levels and further activation of intracellular signaling pathways in the company of a series of functional response like recruitment and activation immune cells, generation of cytokines and chemokines, and release of granule-based enzymes [145].

Next, I evaluated the efficacy of AON-D21, an L-configured mixed RNA/DNA aptamer that binds and neutralizes murine C5a with favorable *in vivo* pharmacokinetics and pharmacodynamics regarding our study design [146, 147, 148]. Compared to the inactive control L-aptamer revAON-D21 consisting of the inverse sequence, the active inhibitor AON-D21 significantly improved GFR, abrogated kidney infarction, reduced intravascular TMA lesions and suppressed neutrophil influx in the treated mice. However, the effect on the preservation of CD31+ endothelial cells was less prominent.

Thus, in my studies, the C5a/C5aR axis seems to be the major effector element of complement activation in crystalline TMA, which is consistent with data obtained from mouse

models of anti-neutrophil cytoplasmic antibody (ANCA) vasculitis [149, 150], an autoimmune form of microvascular injury associated with complement-driven tissue necrosis [151]. In human biopsy, C5aR and soluble C5b-9 levels were significantly higher in patients with kidney microthrombosis and microvascular thrombosis [152]. C5a-C5aR interaction is a crucial step for the activation of coagulation and TMA [153]. In addition, the C5a/C5aR interaction contributes to the IR induced AKI by regulating progranulin expression [154].

5.3 Mechanism-of-action of C5a inhibition

TMA is comprised of a range of different disorders that share a common underlying mechanism, i.e., endothelial injury. These disruptions probably show different mechanisms of endothelial damage depending on diverse pathological triggers [155]. An increasing amount of evidence exhibits the role of complement in mediating endothelial damage and TMA [156, 157]. In addition, C5a activation on human vascular endothelial cells also affects the migration and activation of B-cells and polarization of T-cells [158]. For that reason, I assessed the impact of C5a inhibition on endothelial cells. The addition of C5a itself amplified CC-induced endothelial cell activation indicated by VCAM and P-selectin expression. As expected, I observed that the pharmacologic neutralization of C5a blockage reduced endothelial cell activation compared to the other experimental groups. Our findings show that complement activation contributes to endothelial damage, the underlying mechanism might be that harmful factors such as infections, inflammation or AKI lead to direct damage on the endothelial cells. On the other hand, the complement system is initiated by TMA-induced thrombosis, C5a produced from the complement system binds with its receptor C5aR expressed on the surface of neutrophils and endothelial cells, which result in the release of ROS from neutrophils and cytokines such as P-selectin and NFkB from endothelial cells, further enhance endothelial injury, leading to the platelets aggregation and microthrombi formation illustrated in Figure 29.

Most complement components are present in the fluid phase and complement-related receptors are expressed prominently on the surface of immune cells. Therefore, I analysed single cell RNA sequencing data sets for the cell type-specific expression patterns during AKI. Single cell RNA-sequencing analysis showed that complement factor transcripts are mostly absent in kidney parenchymal cells. C2 and C3 are mainly present in proximal tubular cells in an inactive complement molecules form. But the C5aR is expressed by immune cells infiltrating

the ischemic kidney and also in circulating platelets. From the idea of , I assessed Single cell RNA-sequencing analysis the functions of neutrophils as well as platelets *in vitro*, which are key components of thrombi formation. I evaluated the migratory capacity of neutrophils isolated from C5aR-deficient mice and wild-type mice and found that C5aR deficiency abrogated neutrophils migration towards recombinant C5a and the inhibition of C5a in wild-type mice displayed similar results, those results indicated that C5a is a strong attractant for neutrophils migration to the injury site, blockage of C5a or deletion of C5a receptor on neutrophils surface, neutrophils fail to recruit on kidney injury areas. Those results are supportive of the current knowledge that the C5a-C5aR interaction plays a crucial role in neutrophils functions. Poorly controlled neutrophils serine protease induced by neutrophil dysfunction inactivates C5a receptor [159].

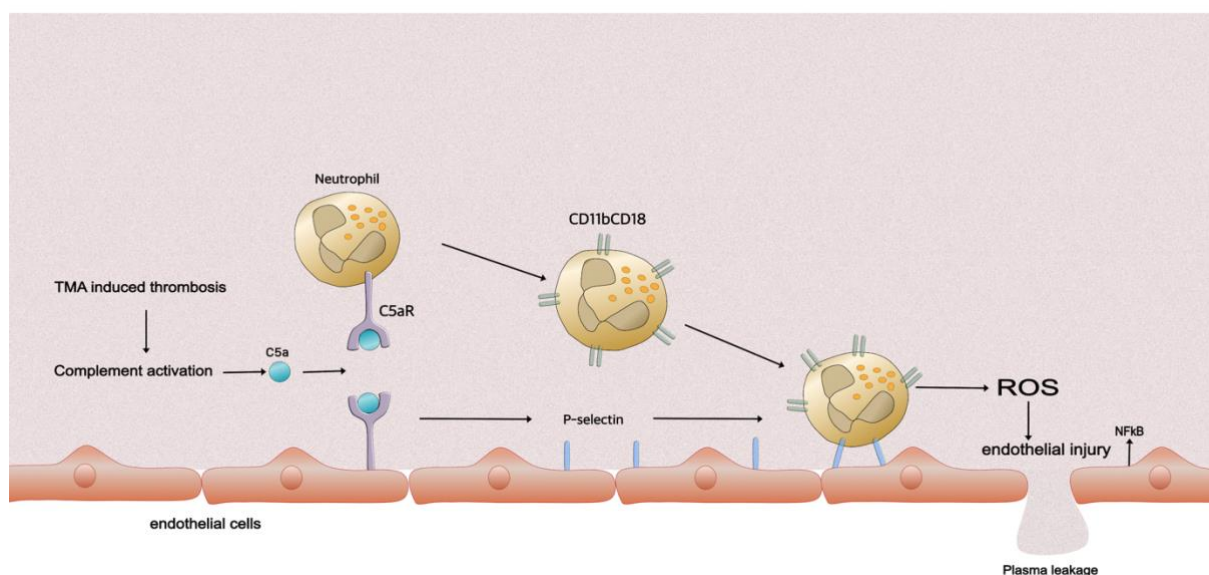


Figure 29: The role of complement activation in endothelial injury under TMA. Formation of TMA-induced thrombosis activates the complement system, C5a cleaved from C5 binds with C5a receptor expressed on neutrophil and endothelial cells, which leads to the release of ROS from neutrophil and P-selectin, NFκB from endothelial cells, with the presence of cytokines and ROS, endothelial injury occurs, resulting in the increase of endothelial permeability and plasma leakage, resulting in the downstream reactions. TMA: thrombotic microangiopathy; C5a: complement factor 5a; C5aR: complement factor 5a receptor; ROS: reactive oxygen species; NFκB: nuclear factor kappa-light-chain-enhancer of activated B cells; CD11b: integrin alpha M; CD18: integrin beta-2.

In addition, C5a is capable to induce neutrophils extracellular traps by myeloid-derived suppressor cells to promote metastasis [160]. Together, those findings suggested that except for the impact of the C5/C5aR axis on endothelial cells, abrogation of neutrophils migration

function could be another underlying mechanism that leads to ameliorated kidney injury during CC driven TMA.

Even more than neutrophils, platelets are key components of TMA lesions, thereby providing a thrombogenic surface for various circulating cells, including neutrophils. In addition, it has been proved that the C5a/C5aR is able to mediate platelet hyperactivation under the TMA disorders like COVID-19 [161]. In ischemic organ, platelets can modulate angiogenesis, the complement C5a and its C5a receptor expressed on the membrane of platelets regulate revascularization via platelets [162]. Besides, C5a shows a capacity for platelet aggregation under platelet-rich plasma and suspensions [163]. Therefore, in light of our extensive research, I undertake a comprehensive investigation into the pivotal role played by C5aR in thrombus formation on collagen-coated surfaces within a controlled flow chamber setting. My objective is to figure out the intricate mechanisms governing this physiological process, and the implications of C5aR in this context. I found that in blood samples derived from C5aR knockout mice, I observed a significant impairment in platelets adhesion and a notable reduction in thrombus formation when compared to wild-type counterparts. These findings provide a notable evidence in support for the notion that inhibiting the function of C5aR holds great promise for its anti-thrombotic potential. This observation has far-reaching implications for our understanding of thrombotic processes and presents a promising way for the development of novel therapeutic strategies to thrombotic disorders. Building upon these outcomes, I further evaluated the dynamics mechanism of thrombus formation. Specifically, I examined the recruitment of neutrophils to thrombi that had already formed in a dynamic flow environment. My results reveal a fascinating difference in behavior between wild-type and C5aR deficiency thrombi. When mouse neutrophils were perfused through our experimental system, they exhibited a robust attachment to wild-type thrombi, indicating the impact of neutrophils to adhere under these conditions. However, the most intriguing finding is the diminished attachment of neutrophils to C5aR deficiency thrombi. This marked reduction in neutrophil adhesion to the C5aR deficiency thrombi suggests a promising therapeutic approach. The above consequences are in accordance with the impact of the C5a/C5aR interaction on platelets. The C5a/C5aR interaction are key drivers of circulating platelets aggregation in both a HUS and COVID-19 conditions [164]. My findings are supportive to the role of C5a/C5aR on the platelets functions during a range of thrombotic diseases. Together, these findings indicated that blockade of the C5a-C5aR axis effectively reduced the

critical steps of TMA formation, including the adhesion of platelets, thrombus growth, and migration and recruitment of neutrophils to the thrombogenic kidney injury sites, as illustrated in Figure 31.

5.4 Delayed therapy of C5a inhibition still alleviates kidney injury

TMA starts as early as 2 hours after CC injection with first complete vascular occlusions at 6 hours and a plateau starting from 12 hours after CC injection. We therefore, tested the window-of-opportunity for C5a blockade with AON-D21 by administering the first dose either 6 or 12 hours after CC injection. Even the 12 hours delayed initiation of AON-D21 therapy significantly attenuated GFR drop from baseline and similar results were obtained for C5a inhibition started 6h after CC injection.

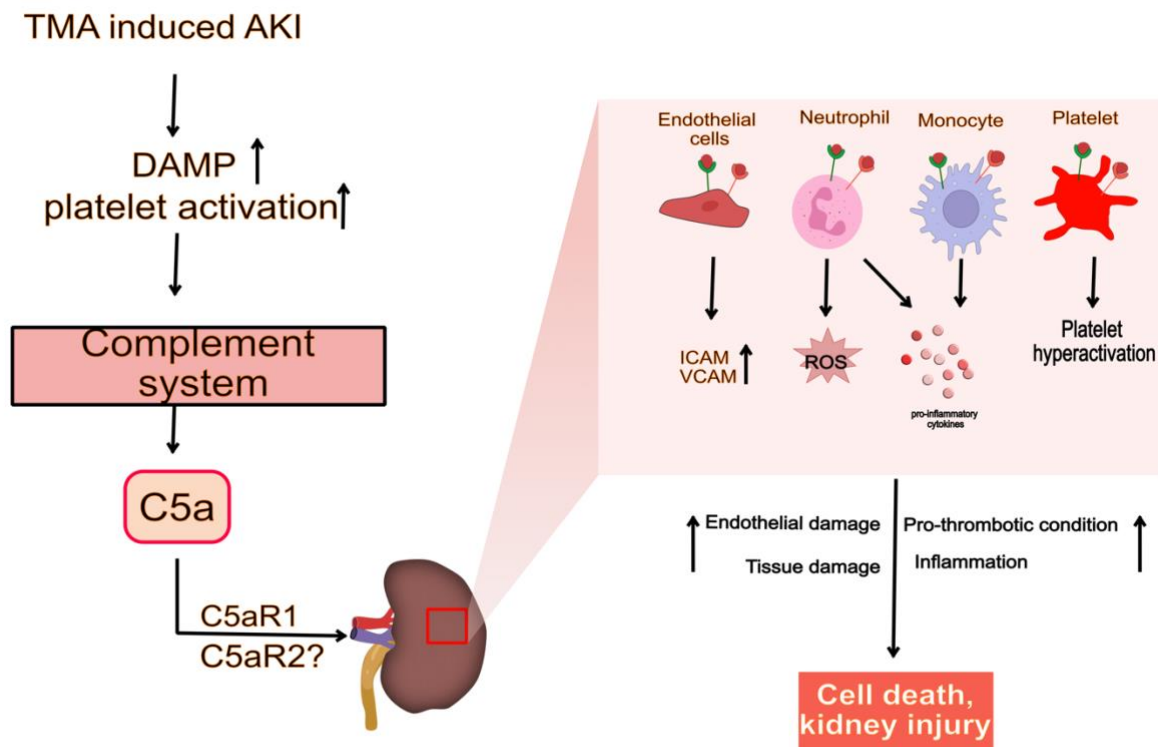


Figure 30: Mechanism of the C5a-C5aR axis effect on crystalline TMA. CCs obstruct kidney arteries, subsequently, platelet activation is elevated and coagulation is initiated, which switches on the complement system, C5a, as a complement component, combines with its receptors (C5a receptor 1, C5a receptor 2) expression on variable cell types such as endothelial cells, monocytes, neutrophils as well as platelets, cause a series pro-inflammatory processes, cell death and kidney injury. TMA: thrombotic microangiopathy; AKI: acute kidney injury; C5a: complement factor 5a; C5aR1: complement factor 5a receptor 1; C5aR2: complement factor

5a receptor 2; ICAM: intercellular adhesion molecule 1; VCAM: vascular cell adhesion protein 1; ROS: reactive oxygen species.

Infarct size was significantly reduced in both delayed treatment groups, and these treatment groups also showed a potent attenuation of intravascular TMA lesions. Furthermore, C5a inhibition starting at 12 hours after CC injection significantly prevented the loss of CD31+ endothelial cells and the influx of neutrophils, reduced kidney injury and ischemic necrosis. The above observations are consistent with our findings on the implication of C5a/C5aR strength on crystalline TMA. In addition, delayed treatment of C5a was still capable to reverse the damage caused by crystalline TMA regardless of GFR results. We conclude that C5a inhibition with AON-D21 is sufficient to attenuate even established TMA probably by shifting the balance between complement-driven prothrombotic activity and intrinsic fibrinolytic activity to the latter [165].

However, there are some limitations to the present experiments:

1. In my model, the efficiency of administration of C5a inhibitor or C5aR knockout mice was assessed only 24h after CCE induction. However, CCE-induced TMA is not just an acute disorder, further transition impact from acute kidney injury to chronic disease for long-term C5a inhibitor treatment remains still unknown.
2. CCE-driven TMA is performed on young, healthy, and male mice. While CCE occurs mostly in the condition of atherosclerosis, which happens mostly in the elderly.
3. The intervention with a C5a inhibitor *in vivo* was only at a single dose throughout the studies. There might be possibilities that the C5a inhibitor blocks C5a completely or an insufficient manner. We cannot exclude that higher doses of C5a inhibition could be more protective.
4. Only a single animal model and mouse cell lines were involved in my experiments, to better validate the impact of C5a/C5aR on CC-driven TMA, human tissue as well as human cell lines could be used.
5. CCs are the only reagent I used to induce TMA. However, this cannot fully mimic human TMA characteristics, even the kidney is the most common damaged organ in TMA.
6. TMA is associated with hemolysis and thrombocytopenia, which were not assessed here. The way the model was designed, we could induce only a focal TMA, which lacks some characteristics of diffuse TMA.

Thrombosis formation

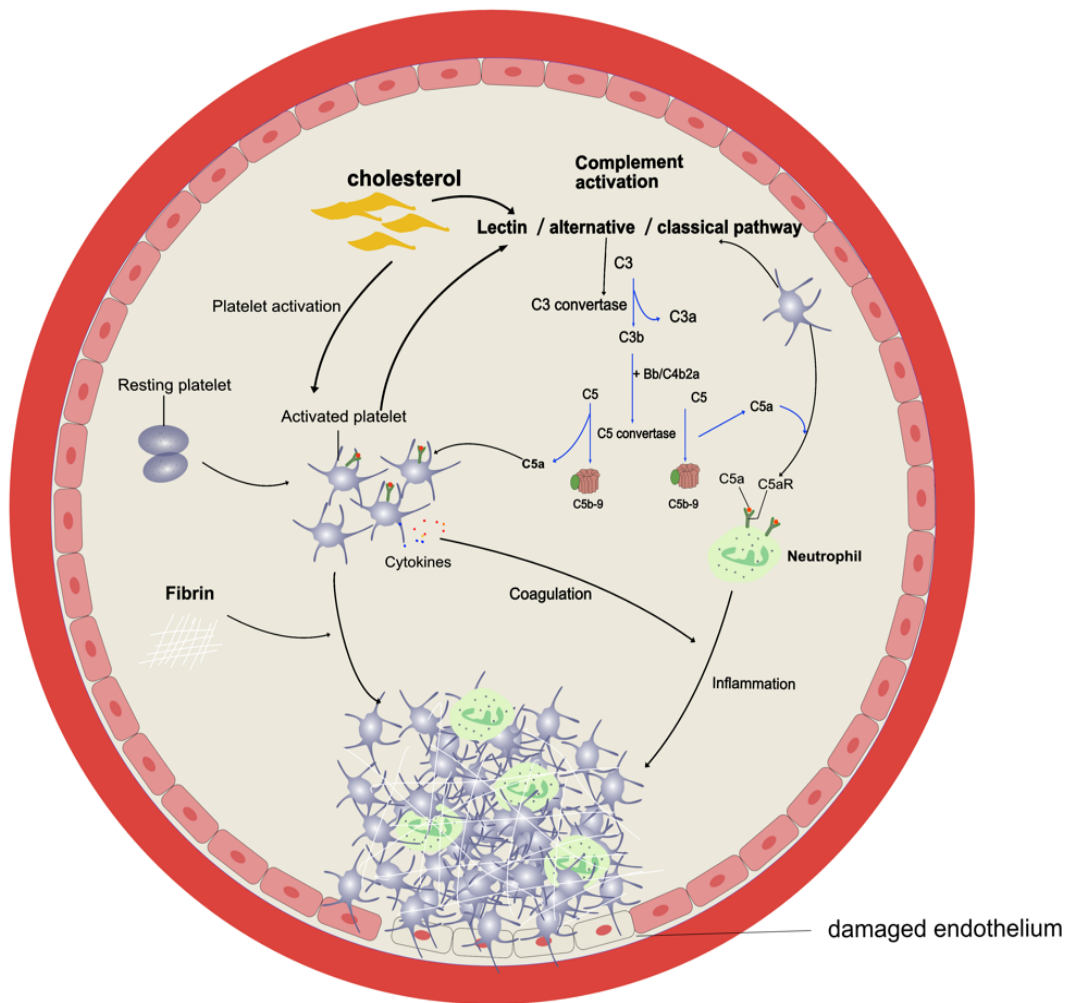


Figure 31: Schematic graphic of C5a-C5aR axis in crystalline TMA. CC blocks mice kidney arteries, and low oxygen and nutrients induce damaged endothelium, the coagulation system is activated by active platelet via CC. Meanwhile, the complement system is initiated by interplay from coagulation system, further attracting neutrophils from blood to the injured endothelial sites. The interaction between the complement system, the coagulation system, and inflammation is amplified by the constant activation of CCE. C5: complement factor 5; C5a: complement factor 5a; C3: complement factor 3; C3a: complement factor 3a; C3b: complement factor 3b; C5: complement factor 5; C5aR: complement factor 5 receptor.

In summary, TMA is a medical term used to describe a group of rare and serious disorders characterized by the formation of blood clots in small vessels, specifically the arterioles and capillaries. Those clots can disrupt the normal flow of blood and damage organs throughout the body, resulting in a range of health problems. The mechanisms of TMA can be distinct depending on the different types of TMA, such as hemolytic uremia syndrome or thrombotic thrombocytopenic purpura, including the coagulation activation, accumulation of neutrophil

as well as endothelium damage (Figure 31). Nowadays, increasing evidence indicates that the complement system plays an integral role as a central pathogenic driver in a series of pathophysiologic processes such as inducing endothelial damage, enhancing inflammation by attracting immune cells, and contributing to thrombosis formation. Our findings provide a novel insight that selective blockade of the C5a/C5aR is sufficient to alleviate crystalline TMA and might have a similar impact on human disease, potentially at a better safety profile in comparison to C5 inhibition, demonstrated in Figure 32.

Thrombosis formation under intervention

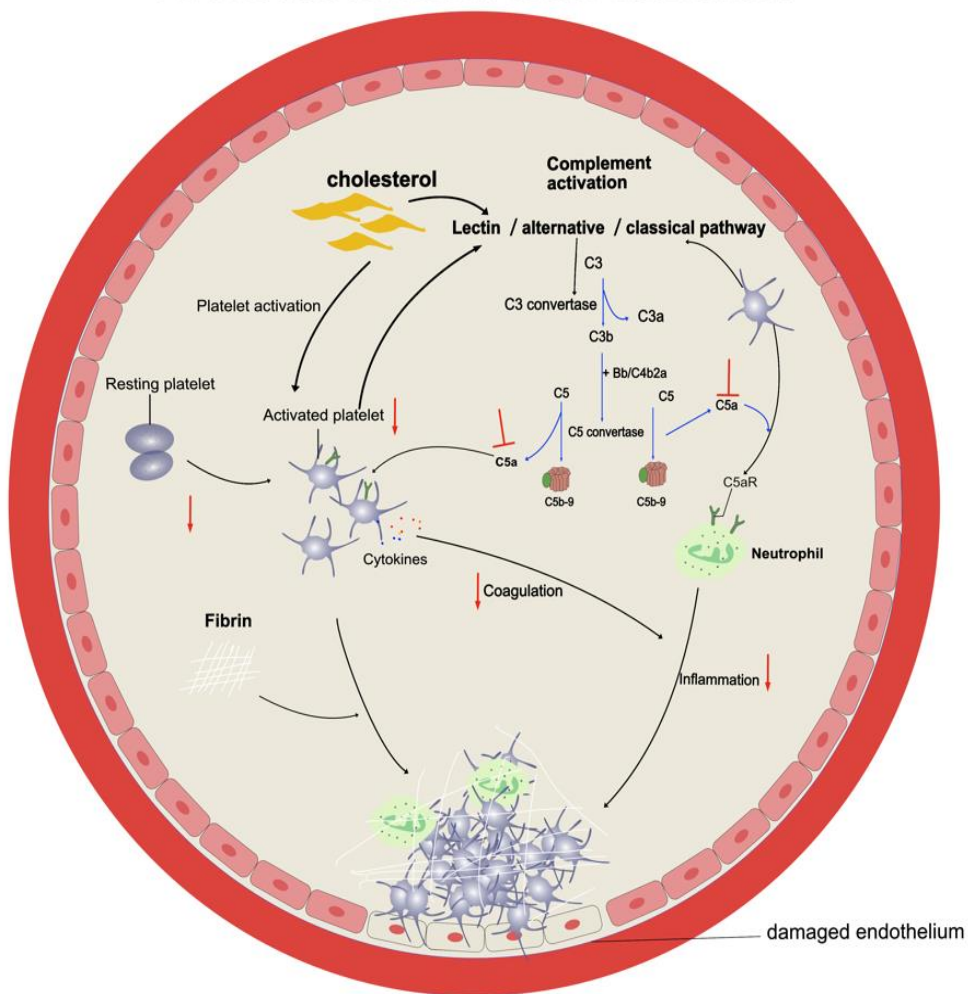


Figure 32: Schematic graphic of C5a-C5aR blockage in crystalline TMA. CC blocks mice kidney arteries, low oxygen, and nutrients induce damaged endothelium. By intervention of C5a inhibition or C5aR deletion, coagulation diminishes via low platelet activation, accordingly with reducing the interaction of platelets and neutrophils. C5a is a strong attractant of neutrophils, inhibition of the C5a-C5aR axis decreases neutrophil accumulation, further reducing the interplay between the complement system, the coagulation system and inflammation is amplified by constant activation of CCE. C5: complement factor 5; C5a:

complement factor 5a; C3: complement factor 3; C3a: complement factor 3a; C3b: complement factor 3b; C5: complement factor 5; C5aR: complement factor 5 receptor.

Future expectation

The C5aR/C5a axis in chronic kidney disease. Chronic kidney disease is a public health problem worldwide, with an increasing incidence and prevalence. Disease progression to kidney failure generates to dramatic increases in morbidity and mortality, and it is linked to progressive glomerulosclerosis, tubulointerstitial and vascular fibrosis [166]. Activation of the complement system is associated with a range of kidney diseases, such as aHUS. I found that C5a inhibition/C5aR deficiency attenuates endothelial dysfunction in acute kidney injury, which also occurs in chronic kidney injury [167]. Increasing evidence indicates the role of the C5a/C5aR in inflammatory diseases, including acute kidney injury. However, its role in chronic diseases is less reported. Therefore, it would be interesting to know whether the C5a/C5aR axis is a critical factor in chronic kidney disease and transition from AKI to CKD.

Role of the C5a/C5aR in dendritic cells. DCs are main inducers of the adaptive immunity and regulate the local inflammation reaction through the human body. DCs comprise the most abundant immune cells within the intrarenal immune system, collaborating with macrophages. In AKI, DCs are anti-inflammatory and restrict the kidney damage caused by immunity [168]. During CKD, DCs show functional changes and might contribute to progression of kidney diseases. C5aR also express on the surface of DCs, the crosstalk of C5aR and toll-like receptor 4 induces DCs functional changes [169]. Hence, it would be intriguing to unravel the role of the C5a/C5aR on dendritic cells differentiation and phagocytosis on the premise of AKI and CKD.

Finally, in this study, I demonstrate the role of the C5a/C5aR on neutrophil migration, to understand the molecular mechanism under this phenomenon, neutrophil phagocytosis and other neutrophil molecular related studies can be explored (Figure 33), meanwhile it would be necessary to test the effect of the C5a/C5aR on other immune cells functions.

6. Summary

Thrombotic microangiopathies (TMA) are rare but severe small vessel injuries commonly affecting the kidney. Therapy with C5 inhibitors is effective but can be associated with severe infectious complications due to blockage of the entire terminal complement pathway. C5aR blockade in systemic vasculitis has been shown to be efficacious while avoiding infectious complications seen with C5 antagonists in thrombotic microangiopathy. We therefore speculated that the more selective blockage of the C5a/C5aR blockade would be also sufficient to control TMA. Cholesterol microcrystal injection into the left kidney artery of wild-type mice initiated diffuse TMA within a few hours followed by a sudden drop of GFR and ischemic kidney necrosis after 24 hours. Genetic deficiency of C3 convertase or of C5aR prevented TMA, GFR decline, and ischemic necrosis at 24 hours to the same extent as did preemptive treatment with a C5a antagonist. C5a blockade initiated up to 12h after crystal injection resolved TMA and prevented all associated consequences. Using a novel model of crystalline TMA, we demonstrate that selective C5a inhibition (or absence of C5aR) is potent in preventing and resolving TMA lesions. A more selective therapeutic approach might have a more favorable safety profile. Thus, selective blockade of the C5a/C5aR is sufficient to attenuate established TMA and might do so in humans, potentially at a better safety profile compared to C5 inhibition.

7. References

- [1] S. Paul, E. Lalthavel Hmar, and H. Kr Sharma, "Strengthening immunity with immunostimulants: a review," 2020. [Online]. Available: <https://www.researchgate.net/publication/342663166>
- [2] W. de Melo Cruvinel *et al.*, "Immune system-Part I Fundamentals of innate immunity with emphasis on molecular and cellular mechanisms of inflammatory response," 2010.
- [3] D. D. Chaplin, "Overview of the immune response," *J Allergy Clin Immunol*, vol. 125, no. 2 Suppl 2, Feb. 2010, doi: 10.1016/J.JACI.2009.12.980.
- [4] D. E. Place and T. D. Kanneganti, "The innate immune system and cell death in autoinflammatory and autoimmune disease," *Curr Opin Immunol*, vol. 67, pp. 95–105, Dec. 2020, doi: 10.1016/J.COI.2020.10.013.
- [5] S. Bekkering, J. Dominguez-Andres, L. A. B. Joosten, N. P. Riksen, and M. G. Netea, "Trained Immunity: Reprogramming Innate Immunity in Health and Disease," *Annu Rev Immunol*, vol. 39, pp. 667–693, Apr. 2021, doi: 10.1146/ANNUREV-IMMUNOL-102119-073855.
- [6] M. G. Netea, J. Quintin, and J. W. M. Van Der Meer, "Trained immunity: A memory for innate host defense," *Cell Host and Microbe*, vol. 9, no. 5. pp. 355–361, May 19, 2011. doi: 10.1016/j.chom.2011.04.006.
- [7] N. S. Merle, S. E. Church, V. Fremeaux-Bacchi, and L. T. Roumenina, "Complement system part I - molecular mechanisms of activation and regulation," *Frontiers in Immunology*, vol. 6, no. JUN. Frontiers Research Foundation, 2015. doi: 10.3389/fimmu.2015.00262.
- [8] D. Elieh Ali Komi, F. Shafaghat, P. T. Kovanen, and S. Meri, "Mast cells and complement system: Ancient interactions between components of innate immunity," *Allergy*, vol. 75, no. 11, pp. 2818–2828, Nov. 2020, doi: 10.1111/ALL.14413.
- [9] A. Java *et al.*, "The complement system in COVID-19: Friend and foe?," *JCI Insight*, vol. 5, no. 15, Aug. 2020, doi: 10.1172/jci.insight.140711.
- [10] E. Rawish, M. Sauter, R. Sauter, H. Nording, and H. F. Langer, "Complement, inflammation and thrombosis," *Br J Pharmacol*, vol. 178, no. 14, pp. 2892–2904, Jul. 2021, doi: 10.1111/BPH.15476.

-
- [11] J. T. Merrill, D. Erkan, J. Winakur, and J. A. James, "Emerging evidence of a COVID-19 thrombotic syndrome has treatment implications," *Nature Reviews Rheumatology*, vol. 16, no. 10. Nature Research, pp. 581–589, Oct. 01, 2020. doi: 10.1038/s41584-020-0474-5.
- [12] B. G. Pires and R. T. Calado, "Hyper-inflammation and complement in COVID-19," *Am J Hematol*, vol. 98 Suppl 4, no. S4, pp. S74–S81, May 2023, doi: 10.1002/AJH.26746.
- [13] V. Murugaiah, P. M. Varghese, N. Beirag, S. Decordova, R. B. Sim, and U. Kishore, "Complement proteins as soluble pattern recognition receptors for pathogenic viruses," *Viruses*, vol. 13, no. 5. MDPI AG, May 01, 2021. doi: 10.3390/v13050824.
- [14] M. Noris and G. Remuzzi, "Overview of complement activation and regulation," *Semin Nephrol*, vol. 33, no. 6, pp. 479–492, Nov. 2013, doi: 10.1016/J.SEMNEPHROL.2013.08.001.
- [15] P. Bus *et al.*, "Complement Activation in Patients With Diabetic Nephropathy," *Kidney Int Rep*, vol. 3, no. 2, pp. 302–313, Mar. 2018, doi: 10.1016/j.ekir.2017.10.005.
- [16] Y. Jiao *et al.*, "Activation of complement C1q and C3 in glomeruli might accelerate the progression of diabetic nephropathy: Evidence from transcriptomic data and renal histopathology," *J Diabetes Investig*, vol. 13, no. 5, pp. 839–849, May 2022, doi: 10.1111/JDI.13739.
- [17] M. K. Pangburn, "Initiation of the alternative pathway of complement and the history of 'tickover,'" *Immunol Rev*, vol. 313, no. 1, pp. 64–70, Jan. 2023, doi: 10.1111/IMR.13130.
- [18] A. F. Esser, "The membrane attack complex of complement. Assembly, structure and cytotoxic activity."
- [19] M. A. Hadders *et al.*, "Assembly and regulation of the membrane attack complex based on structures of C5b6 and sC5b9," *Cell Rep*, vol. 1, no. 3, pp. 200–207, Mar. 2012, doi: 10.1016/J.CELREP.2012.02.003.
- [20] A. Zarantonello, M. Revel, A. Grunenwald, and L. T. Roumenina, "C3-dependent effector functions of complement," *Immunological Reviews*, vol. 313, no. 1. John Wiley and Sons Inc, pp. 120–138, Jan. 01, 2023. doi: 10.1111/imr.13147.
- [21] B. V. Geisbrecht, J. D. Lambris, and P. Gros, "Complement component C3: A structural perspective and potential therapeutic implications," *Semin Immunol*, vol. 59, p. 101627, Jan. 2022, doi: 10.1016/J.SMIM.2022.101627.

- [22] M. Elvington, M. K. Liszewski, P. Bertram, H. S. Kulkarni, and J. P. Atkinson, "A C3(H2O) recycling pathway is a component of the intracellular complement system," *J Clin Invest*, vol. 127, no. 3, pp. 970–981, Mar. 2017, doi: 10.1172/JCI89412.
- [23] J. Friščić *et al.*, "The complement system drives local inflammatory tissue priming by metabolic reprogramming of synovial fibroblasts," *Immunity*, vol. 54, no. 5, pp. 1002–1021.e10, May 2021, doi: 10.1016/J.IMMUNI.2021.03.003/ATTACHMENT/EC580048-4927-4D70-8895-5775016AC913/MMC6.DOCX.
- [24] B. C. King *et al.*, "Complement Component C3 Is Highly Expressed in Human Pancreatic Islets and Prevents β Cell Death via ATG16L1 Interaction and Autophagy Regulation," *Cell Metab*, vol. 29, no. 1, pp. 202–210.e6, Jan. 2019, doi: 10.1016/j.cmet.2018.09.009.
- [25] M. Kremlitzka *et al.*, "Alternative translation and retrotranslocation of cytosolic C3 that detects cytoinvasive bacteria," *Cellular and Molecular Life Sciences*, vol. 79, no. 6, pp. 1–17, Jun. 2022, doi: 10.1007/S00018-022-04308-Z/FIGURES/8.
- [26] A. K. Davis, N. Bingham, and J. Szer, "Normalisation of haemoglobin and control of breakthrough haemolysis with increased frequency pegcetacoplan dosing in treated paroxysmal nocturnal haemoglobinuria," *EJHaem*, vol. 4, no. 3, May 2023, doi: 10.1002/JHA2.714.
- [27] N. M and R. G, "C3G and Ig-MPGN - treatment standard," *Nephrol Dial Transplant*, vol. 16, no. 3, pp. 518–524, 2023, doi: 10.1093/NDT/GFAD182.
- [28] B. Prat-Luri *et al.*, "The C5a-C5aR1 complement axis is essential for neutrophil recruitment to draining lymph nodes via high endothelial venules in cutaneous leishmaniasis," *Cell Rep*, vol. 39, no. 5, May 2022, doi: 10.1016/J.CELREP.2022.110777.
- [29] J. V. Desai *et al.*, "C5a-licensed phagocytes drive sterilizing immunity during systemic fungal infection," *Cell*, vol. 186, no. 13, pp. 2802–2822.e22, Jun. 2023, doi: 10.1016/J.CELL.2023.04.031.
- [30] Y. Laumonier, R. Ü. Korkmaz, A. A. Nowacka, and J. Köhl, "Complement-mediated immune mechanisms in allergy," *Eur J Immunol*, Jul. 2023, doi: 10.1002/EJI.202249979.
- [31] Y. Wang *et al.*, "Revealing the signaling of complement receptors C3aR and C5aR1 by anaphylatoxins," *Nature Chemical Biology* 2023, pp. 1–10, May 2023, doi: 10.1038/s41589-023-01339-w.
- [32] H. Velazquez-Soto, S. Groman-Lupa, M. Cruz-Aguilar, A. L. Salazar, J. C. Zenteno, and M. C. Jimenez-Martinez, "Exogenous CFH Modulates Levels of Pro-Inflammatory Mediators

- to Prevent Oxidative Damage of Retinal Pigment Epithelial Cells with the At-Risk CFH Y402H Variant,” *Antioxidants (Basel)*, vol. 12, no. 8, p. 1540, Jul. 2023, doi: 10.3390/ANTIOX12081540.
- [33] J. Li *et al.*, “Complement factor H inhibits endothelial cell migration through suppression of STAT3 signaling,” *Exp Ther Med*, vol. 26, no. 2, p. 408, Jul. 2023, doi: 10.3892/ETM.2023.12107.
- [34] M. S. Meuleman *et al.*, “Rare Variants in Complement Gene in C3 Glomerulopathy and Immunoglobulin-Mediated Membranoproliferative Glomerulonephritis,” *Clin J Am Soc Nephrol*, Aug. 2023, doi: 10.2215/CJN.0000000000000252.
- [35] J. N. George and C. M. Nester, “Syndromes of thrombotic microangiopathy,” *N Engl J Med*, vol. 371, no. 7, pp. 654–666, Aug. 2014, doi: 10.1056/NEJMRA1312353.
- [36] P. Coppo, “[Secondary thrombotic microangiopathies],” *Rev Med Interne*, vol. 38, no. 11, pp. 731–736, Nov. 2017, doi: 10.1016/J.REVMED.2017.06.025.
- [37] J. Oel and L. M. Oake, “T HROMBOTIC M ICROANGIOPATHIES,” 2002. [Online]. Available: www.nejm.org
- [38] “moake1982”.
- [39] D. S. Genest, C. J. Patriquin, C. Licht, R. John, and H. N. Reich, “Renal Thrombotic Microangiopathy: A Review,” *Am J Kidney Dis*, vol. 81, no. 5, pp. 591–605, May 2023, doi: 10.1053/J.AJKD.2022.10.014.
- [40] R. Raina *et al.*, “Atypical Hemolytic-Uremic Syndrome: An Update on Pathophysiology, Diagnosis, and Treatment,” *Therapeutic Apheresis and Dialysis*, vol. 23, no. 1, pp. 4–21, Feb. 2019, doi: 10.1111/1744-9987.12763.
- [41] M. N. Yenerel, “Atypical Hemolytic Uremic Syndrome: Differential Diagnosis from TTP/HUS and Management,” *Turk J Haematol*, vol. 31, no. 3, pp. 216–225, 2014, doi: 10.4274/TJH.2013.0374.
- [42] M. Noris, F. Mescia, and G. Remuzzi, “STEC-HUS, atypical HUS and TTP are all diseases of complement activation,” *Nat Rev Nephrol*, vol. 8, no. 11, pp. 622–633, Nov. 2012, doi: 10.1038/NRNEPH.2012.195.
- [43] Y. Yoshida, H. Kato, Y. Ikeda, and M. Nangaku, “Pathogenesis of Atypical Hemolytic Uremic Syndrome,” *J Atheroscler Thromb*, vol. 26, no. 2, pp. 99–110, 2019, doi: 10.5551/JAT.RV17026.

- [44] J. Leon *et al.*, “Complement-driven hemolytic uremic syndrome,” *Am J Hematol*, vol. 98, no. S4, pp. S44–S56, May 2023, doi: 10.1002/AJH.26854.
- [45] R. Piras *et al.*, “Molecular Studies and an ex vivo Complement Assay on Endothelium Highlight the Genetic Complexity of Atypical Hemolytic Uremic Syndrome: The Case of a Pedigree With a Null CD46 Variant,” *Front Med (Lausanne)*, vol. 7, p. 579418, Nov. 2020, doi: 10.3389/fmed.2020.579418.
- [46] E. F. Chief, M. D. Mammen, K. Guest Editors, M. D. Kentouche, J. Misselwitz, and P. F. Zipfel, “Epidemiology, Clinical Presentation, and Pathophysiology of Atypical and Recurrent Hemolytic Uremic Syndrome,” 2006.
- [47] F. Fakhouri, N. Schwotzer, and V. Frémeaux-Bacchi, “How I diagnose and treat atypical hemolytic uremic syndrome,” *Blood*, vol. 141, no. 9, pp. 984–995, Mar. 2023, doi: 10.1182/BLOOD.2022017860.
- [48] M. Noris *et al.*, “Relative role of genetic complement abnormalities in sporadic and familial aHUS and their impact on clinical phenotype,” *Clin J Am Soc Nephrol*, vol. 5, no. 10, pp. 1844–1859, Oct. 2010, doi: 10.2215/CJN.02210310.
- [49] V. Fremeaux-Bacchi *et al.*, “Genetics and outcome of atypical hemolytic uremic syndrome: a nationwide French series comparing children and adults,” *Clin J Am Soc Nephrol*, vol. 8, no. 4, pp. 554–562, Apr. 2013, doi: 10.2215/CJN.04760512.
- [50] K. L. Wijnsma, C. Duineveld, J. F. M. Wetzels, and N. C. A. J. van de Kar, “Eculizumab in atypical hemolytic uremic syndrome: strategies toward restrictive use,” *Pediatr Nephrol*, vol. 34, no. 11, pp. 2261–2277, Nov. 2019, doi: 10.1007/S00467-018-4091-3.
- [51] C. M. Legendre *et al.*, “Terminal complement inhibitor eculizumab in atypical hemolytic-uremic syndrome,” *N Engl J Med*, vol. 368, no. 23, pp. 2169–2181, Jun. 2013, doi: 10.1056/NEJMOA1208981.
- [52] M. Okumi and K. Tanabe, “Prevention and treatment of atypical haemolytic uremic syndrome after kidney transplantation,” *Nephrology (Carlton)*, vol. 21 Suppl 1, pp. 9–13, Jul. 2016, doi: 10.1111/NEP.12776.
- [53] C. C. González, V. López-Jiménez, T. Vázquez-Sánchez, E. Vázquez-Sánchez, M. Cabello, and D. Hernández-Marrero, “Efficacy and Safety of Eculizumab in Kidney Transplant Patients With Primary Atypical Hemolytic-Uremic Syndrome,” *Transplant Proc*, vol. 54, no. 1, pp. 25–26, Jan. 2022, doi: 10.1016/J.TRANSROCEED.2021.09.063.

- [54] N. Ito *et al.*, “Efficacy and safety of eculizumab in childhood atypical hemolytic uremic syndrome in Japan,” *Clin Exp Nephrol*, vol. 20, no. 2, pp. 265–272, Apr. 2016, doi: 10.1007/S10157-015-1142-Y.
- [55] K. McKeage, “Ravulizumab: First Global Approval,” *Drugs*, vol. 79, no. 3, pp. 347–352, Feb. 2019, doi: 10.1007/S40265-019-01068-2.
- [56] Y. Y. Syed, “Ravulizumab: A Review in Atypical Haemolytic Uraemic Syndrome,” *Drugs*, vol. 81, no. 5, pp. 587–594, Apr. 2021, doi: 10.1007/S40265-021-01481-6.
- [57] K. Tanaka *et al.*, “The long-acting C5 inhibitor, ravulizumab, is efficacious and safe in pediatric patients with atypical hemolytic uremic syndrome previously treated with eculizumab,” *Pediatr Nephrol*, vol. 36, no. 4, pp. 889–898, Apr. 2021, doi: 10.1007/S00467-020-04774-2.
- [58] Y. Ueda *et al.*, “Blocking Properdin Prevents Complement-Mediated Hemolytic Uremic Syndrome and Systemic Thrombophilia,” *J Am Soc Nephrol*, vol. 29, no. 7, pp. 1928–1937, Jul. 2018, doi: 10.1681/ASN.2017121244.
- [59] C. Q. Schmidt and R. J. H. Smith, “Protein therapeutics and their lessons: Expect the unexpected when inhibiting the multi-protein cascade of the complement system,” *Immunol Rev*, vol. 313, no. 1, pp. 376–401, Jan. 2023, doi: 10.1111/IMR.13164.
- [60] R. P. Rother, S. A. Rollins, C. F. Mojcik, R. A. Brodsky, and L. Bell, “Discovery and development of the complement inhibitor eculizumab for the treatment of paroxysmal nocturnal hemoglobinuria,” *Nature Biotechnology 2007 25:11*, vol. 25, no. 11, pp. 1256–1264, Nov. 2007, doi: 10.1038/nbt1344.
- [61] A. M. Risitano *et al.*, “Anti-complement Treatment for Paroxysmal Nocturnal Hemoglobinuria: Time for Proximal Complement Inhibition? A Position Paper From the SAAWP of the EBMT,” *Front Immunol*, vol. 10, no. JUN, 2019, doi: 10.3389/FIMMU.2019.01157.
- [62] W. Hayes, S. Tschumi, S. C. Ling, J. Feber, M. Kirschfink, and C. Licht, “Eculizumab hepatotoxicity in pediatric aHUS,” *Pediatr Nephrol*, vol. 30, no. 5, pp. 775–781, May 2015, doi: 10.1007/S00467-014-2990-5.
- [63] R. K. Dhanoa *et al.*, “Eculizumab’s Unintentional Mayhem: A Systematic Review,” *Cureus*, vol. 14, no. 6, Jun. 2022, doi: 10.7759/CUREUS.25640.
- [64] J. A. Kellum *et al.*, “Kidney disease: Improving global outcomes (KDIGO) acute kidney injury work group. KDIGO clinical practice guideline for acute kidney injury,” *Kidney*

- International Supplements*, vol. 2, no. 1. Nature Publishing Group, pp. 1–138, 2012. doi: 10.1038/kisup.2012.1.
- [65] J. A. Kellum, P. Romagnani, G. Ashuntantang, C. Ronco, A. Zarbock, and H. J. Anders, “Acute kidney injury,” *Nat Rev Dis Primers*, vol. 7, no. 1, Dec. 2021, doi: 10.1038/S41572-021-00284-Z.
- [66] M. Al-Jaghbeer, D. Dealmeida, A. Bilderback, R. Ambrosino, and J. A. Kellum, “Clinical Decision Support for In-Hospital AKI,” *J Am Soc Nephrol*, vol. 29, no. 2, pp. 654–660, Feb. 2018, doi: 10.1681/ASN.2017070765.
- [67] E. A. J. Hoste *et al.*, “Epidemiology of acute kidney injury in critically ill patients: the multinational AKI-EPI study,” *Intensive Care Med*, vol. 41, no. 8, pp. 1411–1423, Aug. 2015, doi: 10.1007/S00134-015-3934-7.
- [68] S. Peerapornratana, C. L. Manrique-Caballero, H. Gómez, and J. A. Kellum, “Acute kidney injury from sepsis: current concepts, epidemiology, pathophysiology, prevention and treatment,” *Kidney Int*, vol. 96, no. 5, pp. 1083–1099, Nov. 2019, doi: 10.1016/J.KINT.2019.05.026.
- [69] Y. Wang and R. Bellomo, “Cardiac surgery-associated acute kidney injury: risk factors, pathophysiology and treatment,” *Nat Rev Nephrol*, vol. 13, no. 11, pp. 697–711, Nov. 2017, doi: 10.1038/NRNEPH.2017.119.
- [70] A. A. Sharfuddin and B. A. Molitoris, “Pathophysiology of ischemic acute kidney injury,” *Nat Rev Nephrol*, vol. 7, no. 4, pp. 189–200, Apr. 2011, doi: 10.1038/NRNEPH.2011.16.
- [71] S. L. Kane-Gill and S. L. Goldstein, “Drug-Induced Acute Kidney Injury: A Focus on Risk Assessment for Prevention,” *Crit Care Clin*, vol. 31, no. 4, pp. 675–684, Oct. 2015, doi: 10.1016/J.CCC.2015.06.005.
- [72] R. L. Mehta *et al.*, “Sepsis as a cause and consequence of acute kidney injury: Program to Improve Care in Acute Renal Disease,” *Intensive Care Med*, vol. 37, no. 2, pp. 241–248, Feb. 2011, doi: 10.1007/S00134-010-2089-9.
- [73] S. Peerapornratana, C. L. Manrique-Caballero, H. Gómez, and J. A. Kellum, “Acute kidney injury from sepsis: current concepts, epidemiology, pathophysiology, prevention and treatment,” *Kidney Int*, vol. 96, no. 5, p. 1083, Nov. 2019, doi: 10.1016/J.KINT.2019.05.026.

- [74] A. Zarbock *et al.*, “Sepsis-associated acute kidney injury: consensus report of the 28th Acute Disease Quality Initiative workgroup,” *Nat Rev Nephrol*, vol. 19, no. 6, pp. 401–417, Jun. 2023, doi: 10.1038/S41581-023-00683-3.
- [75] S. M. Bagshaw, C. George, and R. Bellomo, “Early acute kidney injury and sepsis: a multicentre evaluation,” *Crit Care*, vol. 12, no. 2, p. R47, Apr. 2008, doi: 10.1186/CC6863.
- [76] Y. Wang and R. Bellomo, “Cardiac surgery-associated acute kidney injury: risk factors, pathophysiology and treatment,” *Nat Rev Nephrol*, vol. 13, no. 11, pp. 697–711, Nov. 2017, doi: 10.1038/NRNEPH.2017.119.
- [77] C. Xiong *et al.*, “Early Postoperative Acetaminophen Administration and Severe Acute Kidney Injury After Cardiac Surgery,” *Am J Kidney Dis*, vol. 81, no. 6, pp. 675–683.e1, Jun. 2023, doi: 10.1053/J.AJKD.2022.11.009.
- [78] A. A. Sharfuddin and B. A. Molitoris, “Pathophysiology of ischemic acute kidney injury,” *Nat Rev Nephrol*, vol. 7, no. 4, pp. 189–200, Apr. 2011, doi: 10.1038/NRNEPH.2011.16.
- [79] J. V. Bonventre and L. Yang, “Cellular pathophysiology of ischemic acute kidney injury,” *J Clin Invest*, vol. 121, no. 11, pp. 4210–4221, Nov. 2011, doi: 10.1172/JCI45161.
- [80] D. P. Basile, “The endothelial cell in ischemic acute kidney injury: implications for acute and chronic function,” *Kidney Int*, vol. 72, no. 2, pp. 151–156, Jul. 2007, doi: 10.1038/SJ.KI.5002312.
- [81] J. V. Bonventre and J. M. Weinberg, “Recent advances in the pathophysiology of ischemic acute renal failure,” *J Am Soc Nephrol*, vol. 14, no. 8, pp. 2199–2210, Aug. 2003, doi: 10.1097/01.ASN.0000079785.13922.F6.
- [82] P. Devarajan, “Update on mechanisms of ischemic acute kidney injury,” *J Am Soc Nephrol*, vol. 17, no. 6, pp. 1503–1520, Jun. 2006, doi: 10.1681/ASN.2006010017.
- [83] S. Godo and H. Shimokawa, “Endothelial Functions,” *Arterioscler Thromb Vasc Biol*, vol. 37, no. 9, pp. e108–e114, Sep. 2017, doi: 10.1161/ATVBAHA.117.309813.
- [84] N. Jourde-Chiche *et al.*, “Endothelium structure and function in kidney health and disease,” *Nature Reviews Nephrology* 2018 15:2, vol. 15, no. 2, pp. 87–108, Jan. 2019, doi: 10.1038/s41581-018-0098-z.
- [85] K. Zhang *et al.*, “Renal Endothelial Cell-Targeted Extracellular Vesicles Protect the Kidney from Ischemic Injury,” *Adv Sci (Weinh)*, vol. 10, no. 3, Jan. 2023, doi: 10.1002/ADVS.202204626.

- [86] T. Chiba *et al.*, "Endothelial-Derived miR-17~92 Promotes Angiogenesis to Protect against Renal Ischemia-Reperfusion Injury," *J Am Soc Nephrol*, vol. 32, no. 3, pp. 553–562, Mar. 2021, doi: 10.1681/ASN.2020050717.
- [87] A. G. Basnakian, G. P. Kaushal, and S. V. Shah, "Apoptotic pathways of oxidative damage to renal tubular epithelial cells," *Antioxid Redox Signal*, vol. 4, no. 6, pp. 915–924, 2002, doi: 10.1089/152308602762197452.
- [88] B. C. Liu, T. T. Tang, L. L. Lv, and H. Y. Lan, "Renal tubule injury: a driving force toward chronic kidney disease," *Kidney Int*, vol. 93, no. 3, pp. 568–579, Mar. 2018, doi: 10.1016/J.KINT.2017.09.033.
- [89] Z. Li, S. Lu, and X. Li, "The role of metabolic reprogramming in tubular epithelial cells during the progression of acute kidney injury," *Cell Mol Life Sci*, vol. 78, no. 15, pp. 5731–5741, Aug. 2021, doi: 10.1007/S00018-021-03892-W.
- [90] P. X. Liew and P. Kubes, "The Neutrophil's Role During Health and Disease," *Physiol Rev*, vol. 99, no. 2, pp. 1223–1248, Apr. 2019, doi: 10.1152/PHYSREV.00012.2018.
- [91] H. R. Jang and H. Rabb, "The innate immune response in ischemic acute kidney injury," *Clin Immunol*, vol. 130, no. 1, pp. 41–50, Jan. 2009, doi: 10.1016/J.CLIM.2008.08.016.
- [92] A. Bonavia and K. Singbartl, "A review of the role of immune cells in acute kidney injury," *Pediatr Nephrol*, vol. 33, no. 10, pp. 1629–1639, Oct. 2018, doi: 10.1007/S00467-017-3774-5.
- [93] V. Papayannopoulos, "Neutrophil extracellular traps in immunity and disease," *Nat Rev Immunol*, vol. 18, no. 2, pp. 134–147, Feb. 2018, doi: 10.1038/NRI.2017.105.
- [94] J. Zhang *et al.*, "HMGB1-TLR4-IL-23-IL-17A axis accelerates renal ischemia-reperfusion injury via the recruitment and migration of neutrophils," *Int Immunopharmacol*, vol. 94, May 2021, doi: 10.1016/J.INTIMP.2021.107433.
- [95] Z. Li *et al.*, "The Pathogenesis of Ischemia-Reperfusion Induced Acute Kidney Injury Depends on Renal Neutrophil Recruitment Whereas Sepsis-Induced AKI Does Not," *Front Immunol*, vol. 13, Apr. 2022, doi: 10.3389/FIMMU.2022.843782.
- [96] D. Nakazawa *et al.*, "Histones and Neutrophil Extracellular Traps Enhance Tubular Necrosis and Remote Organ Injury in Ischemic AKI," *J Am Soc Nephrol*, vol. 28, no. 6, pp. 1753–1768, Jun. 2017, doi: 10.1681/ASN.2016080925.

- [97] T. A. Wynn and K. M. Vannella, "Macrophages in Tissue Repair, Regeneration, and Fibrosis," *Immunity*, vol. 44, no. 3, pp. 450–462, Mar. 2016, doi: 10.1016/J.IMMUNI.2016.02.015.
- [98] A. Zuk and J. V. Bonventre, "Acute Kidney Injury," <https://doi.org/10.1146/annurev-med-050214-013407>, vol. 67, pp. 293–307, Jan. 2016, doi: 10.1146/ANNUREV-MED-050214-013407.
- [99] S. C. Huen and L. G. Cantley, "Macrophages in Renal Injury and Repair," *Annu Rev Physiol*, vol. 79, pp. 449–469, Feb. 2017, doi: 10.1146/ANNUREV-PHYSIOL-022516-034219.
- [100] M. Collin and F. Ginhoux, "Human dendritic cells," *Semin Cell Dev Biol*, vol. 86, pp. 1–2, Feb. 2019, doi: 10.1016/J.SEMCDB.2018.04.015.
- [101] C. Kurts, F. Ginhoux, and U. Panzer, "Kidney dendritic cells: fundamental biology and functional roles in health and disease," *Nat Rev Nephrol*, vol. 16, no. 7, pp. 391–407, Jul. 2020, doi: 10.1038/S41581-020-0272-Y.
- [102] L. Li and M. D. Okusa, "Macrophages, dendritic cells, and kidney ischemia-reperfusion injury," *Semin Nephrol*, vol. 30, no. 3, pp. 268–277, May 2010, doi: 10.1016/J.SEMNEPHROL.2010.03.005.
- [103] T. Takano, H. Elimam, and A. V. Cybulsky, "Complement-mediated cellular injury," *Semin Nephrol*, vol. 33, no. 6, pp. 586–601, 2013, doi: 10.1016/J.SEMNEPHROL.2013.08.009.
- [104] E. Rodríguez *et al.*, "Membrane Attack Complex and Factor H in Humans with Acute Kidney Injury," *Kidney Blood Press Res*, vol. 43, no. 5, pp. 1655–1665, Nov. 2018, doi: 10.1159/000494680.
- [105] J. M. Thurman, M. S. Lucia, D. Ljubanovic, and V. M. Holers, "Acute tubular necrosis is characterized by activation of the alternative pathway of complement," *Kidney Int*, vol. 67, no. 2, pp. 524–530, 2005, doi: 10.1111/J.1523-1755.2005.67109.X.
- [106] J. W. McCullough, B. Renner, and J. M. Thurman, "The Role of the Complement System in Acute Kidney Injury," *Semin Nephrol*, vol. 33, no. 6, pp. 543–556, Nov. 2013, doi: 10.1016/J.SEMNEPHROL.2013.08.005.
- [107] R. Franzin *et al.*, "Inflammaging and Complement System: A Link Between Acute Kidney Injury and Chronic Graft Damage," *Front Immunol*, vol. 11, p. 734, May 2020, doi: 10.3389/FIMMU.2020.00734.

- [108] N. M. Jager, F. Poppelaars, M. R. Daha, and M. A. Seelen, "Complement in renal transplantation: The road to translation," *Mol Immunol*, vol. 89, pp. 22–35, Sep. 2017, doi: 10.1016/J.MOLIMM.2017.05.014.
- [109] E. K. Stenson, J. Kendrick, B. Dixon, and J. M. Thurman, "The complement system in pediatric acute kidney injury," *Pediatr Nephrol*, vol. 38, no. 5, p. 1411, May 2023, doi: 10.1007/S00467-022-05755-3.
- [110] C. Zoja, S. Buelli, and M. Morigi, "Shiga toxin triggers endothelial and podocyte injury: the role of complement activation," *Pediatric Nephrology*, vol. 34, no. 3, pp. 379–388, Mar. 2019, doi: 10.1007/S00467-017-3850-X/METRICS.
- [111] B. Renner *et al.*, "Factor H related proteins modulate complement activation on kidney cells," *Kidney Int*, vol. 102, no. 6, pp. 1331–1344, Dec. 2022, doi: 10.1016/J.KINT.2022.07.035.
- [112] T. Wada and M. Nangaku, "Novel roles of complement in renal diseases and their therapeutic consequences," *Kidney Int*, vol. 84, no. 3, pp. 441–450, 2013, doi: 10.1038/KI.2013.134.
- [113] J. S. Danobeitia *et al.*, "Complement inhibition attenuates acute kidney injury after ischemia-reperfusion and limits progression to renal fibrosis in mice," *PLoS One*, vol. 12, no. 8, Aug. 2017, doi: 10.1371/JOURNAL.PONE.0183701.
- [114] T. Freiwald and B. Afzali, "Renal diseases and the role of complement: Linking complement to immune effector pathways and therapeutics," *Adv Immunol*, vol. 152, pp. 1–81, Jan. 2021, doi: 10.1016/BS.AI.2021.09.001.
- [115] C. Shi, E. Mammadova-Bach, C. Li, D. Liu, and H. J. Anders, "Pathophysiology and targeted treatment of cholesterol crystal embolism and the related thrombotic angiopathy," *FASEB J*, vol. 37, no. 10, p. e23179, Oct. 2023, doi: 10.1096/FJ.202301316R.
- [116] I. Kronzon and M. Saric, "Cholesterol embolization syndrome," *Circulation*, vol. 122, no. 6, pp. 631–641, Aug. 2010, doi: 10.1161/CIRCULATIONAHA.109.886465.
- [117] K. Takahashi *et al.*, "Incidence, Risk Factors, and Prognosis of Cholesterol Crystal Embolism Because of Percutaneous Coronary Intervention," *American Journal of Cardiology*, vol. 167, pp. 15–19, Mar. 2022, doi: 10.1016/j.amjcard.2021.11.039.
- [118] R. D. Frank, "[Cholesterol embolism syndrome: a rare, but severe complication in patients with atherosclerosis]," *Dtsch Med Wochenschr*, vol. 137, no. 21, pp. 1130–1134, 2012, doi: 10.1055/S-0032-1305005.

- [119] M. Nakayama *et al.*, "The effect of low-dose corticosteroids on short- and long-term renal outcome in patients with cholesterol crystal embolism," *Ren Fail*, vol. 33, no. 3, pp. 298–306, Apr. 2011, doi: 10.3109/0886022X.2011.560403.
- [120] K. Ishiyama and T. Sato, "Efficacy of LDL apheresis for the treatment of cholesterol crystal embolism: A prospective, controlled study," *Ther Apher Dial*, vol. 26, no. 2, pp. 456–464, Apr. 2022, doi: 10.1111/1744-9987.13706.
- [121] C. Shi *et al.*, "Crystal clots as therapeutic target in cholesterol crystal embolism," *Circ Res*, pp. E37–E52, 2020, doi: 10.1161/CIRCRESAHA.119.315625.
- [122] J. A. Marschner, H. Schäfer, A. Holderied, and H. J. Anders, "Optimizing Mouse Surgery with Online Rectal Temperature Monitoring and Preoperative Heat Supply. Effects on Post-Ischemic Acute Kidney Injury," *PLoS One*, vol. 11, no. 2, p. e0149489, Feb. 2016, doi: 10.1371/JOURNAL.PONE.0149489.
- [123] A. Schreiber *et al.*, "Transcutaneous measurement of renal function in conscious mice," *Am J Physiol Renal Physiol*, vol. 303, no. 5, 2012, doi: 10.1152/AJPRENAL.00279.2012.
- [124] J. Friedemann *et al.*, "Improved kinetic model for the transcutaneous measurement of glomerular filtration rate in experimental animals," *Kidney Int*, vol. 90, no. 6, pp. 1377–1385, Dec. 2016, doi: 10.1016/J.KINT.2016.07.024.
- [125] N. Anggorowati *et al.*, "Histochemical and Immunohistochemical Study of α -SMA, Collagen, and PCNA in Epithelial Ovarian Neoplasm," *Asian Pac J Cancer Prev*, vol. 18, no. 3, p. 667, Mar. 2017, doi: 10.22034/APJCP.2017.18.3.667.
- [126] J. W. Weisel and R. I. Litvinov, "Fibrin Formation, Structure and Properties," *Subcell Biochem*, vol. 82, pp. 405–456, Jan. 2017, doi: 10.1007/978-3-319-49674-0_13.
- [127] R. I. Litvinov and J. W. Weisel, "Fibrin mechanical properties and their structural origins," *Matrix Biol*, vol. 60–61, p. 110, Jul. 2017, doi: 10.1016/J.MATBIO.2016.08.003.
- [128] S. T. Lord, "Fibrinogen and fibrin: scaffold proteins in hemostasis," *Curr Opin Hematol*, vol. 14, no. 3, pp. 236–241, May 2007, doi: 10.1097/MOH.0B013E3280DCE58C.
- [129] M. Nesheim, J. Walker, W. E. I. Wang, M. Boffa, A. Horrevoets, and L. Bajzar, "Modulation of fibrin cofactor activity in plasminogen activation," *Ann N Y Acad Sci*, vol. 936, pp. 247–260, 2001, doi: 10.1111/J.1749-6632.2001.TB03513.X.
- [130] P. Lertkiatmongkol, D. Liao, H. Mei, Y. Hu, and P. J. Newman, "Endothelial functions of platelet/endothelial cell adhesion molecule-1 (CD31)," *Curr Opin Hematol*, vol. 23, no. 3, pp. 253–259, 2016, doi: 10.1097/MOH.000000000000239.

- [131] P. Y. Lee, J.-X. Wang, E. Parisini, C. C. Dascher, and P. A. Nigrovic, "Ly6 family proteins in neutrophil biology," *J Leukoc Biol*, vol. 94, no. 4, pp. 585–594, Oct. 2013, doi: 10.1189/JLB.0113014.
- [132] K. Bujko, S. Rzeszotek, K. Hoehlig, J. Yan, A. Vater, and M. Z. Ratajczak, "Signaling of the Complement Cleavage Product Anaphylatoxin C5a Through C5aR (CD88) Contributes to Pharmacological Hematopoietic Stem Cell Mobilization," *Stem Cell Rev*, vol. 13, no. 6, p. 793, Dec. 2017, doi: 10.1007/S12015-017-9769-6.
- [133] M. Metzemaekers, M. Gouwy, and P. Proost, "Neutrophil chemoattractant receptors in health and disease: double-edged swords," *Cell Mol Immunol*, vol. 17, no. 5, pp. 433–450, May 2020, doi: 10.1038/S41423-020-0412-0.
- [134] R. B. Pouw and D. Ricklin, "Tipping the balance: intricate roles of the complement system in disease and therapy," *Semin Immunopathol*, vol. 43, no. 6, pp. 757–771, Dec. 2021, doi: 10.1007/S00281-021-00892-7.
- [135] L. Caroti *et al.*, "Hemolytic uremic syndrome and kidney transplantation in uncontrolled donation after circulatory death (DCD): A two-case report," *Clin Nephrol Case Stud*, vol. 9, no. 1, pp. 59–66, Jan. 2021, doi: 10.5414/CNCS110434.
- [136] A. Spasiano *et al.*, "Underlying Genetics of aHUS: Which Connection with Outcome and Treatment Discontinuation?," *Int J Mol Sci*, vol. 24, no. 19, p. 14496, Sep. 2023, doi: 10.3390/IJMS241914496.
- [137] P. Skendros *et al.*, "Complement and tissue factor-enriched neutrophil extracellular traps are key drivers in COVID-19 immunothrombosis," *J Clin Invest*, vol. 130, no. 11, pp. 6151–6157, Nov. 2020, doi: 10.1172/JCI141374.
- [138] F. Bruni *et al.*, "Complement and endothelial cell activation in COVID-19 patients compared to controls with suspected SARS-CoV-2 infection: A prospective cohort study," *Front Immunol*, vol. 13, Sep. 2022, doi: 10.3389/FIMMU.2022.941742.
- [139] K. N. Ekdahl, Y. Teramura, S. Asif, N. Jonsson, P. U. Magnusson, and B. Nilsson, "Thromboinflammation in Therapeutic Medicine," *Adv Exp Med Biol*, vol. 865, pp. 3–17, Aug. 2015, doi: 10.1007/978-3-319-18603-0_1.
- [140] H. Kozarcanin *et al.*, "The lectin complement pathway serine proteases (MASPs) represent a possible crossroad between the coagulation and complement systems in thromboinflammation," *J Thromb Haemost*, vol. 14, no. 3, pp. 531–545, Mar. 2016, doi: 10.1111/JTH.13208.

- [141] D. C. Mastellos *et al.*, “Complement C3 vs C5 inhibition in severe COVID-19: Early clinical findings reveal differential biological efficacy,” *Clin Immunol*, vol. 220, Nov. 2020, doi: 10.1016/J.CLIM.2020.108598.
- [142] A. Zarantonello, M. Revel, A. Grunenwald, and L. T. Roumenina, “C3-dependent effector functions of complement,” *Immunol Rev*, vol. 313, no. 1, pp. 120–138, Jan. 2023, doi: 10.1111/IMR.13147.
- [143] A. Ghannam *et al.*, “Human C3 Deficiency Associated with Impairments in Dendritic Cell Differentiation, Memory B Cells, and Regulatory T Cells,” *The Journal of Immunology*, vol. 181, no. 7, pp. 5158–5166, Oct. 2008, doi: 10.4049/JIMMUNOL.181.7.5158.
- [144] X. X. Li, D. M. Gorman, J. D. Lee, R. J. Clark, and T. M. Woodruff, “Unexpected Off-Target Activities for Recombinant C5a in Human Macrophages,” *The Journal of Immunology*, vol. 208, no. 1, pp. 133–142, Jan. 2022, doi: 10.4049/JIMMUNOL.2100444.
- [145] G. P. An, G. R. Ren, F. S. An, and C. Zhang, “Role of C5a-C5aR axis in the development of atherosclerosis,” *Sci China Life Sci*, vol. 57, no. 8, pp. 790–794, 2014, doi: 10.1007/S11427-014-4711-5.
- [146] K. Hoehlig *et al.*, “A Novel C5a-neutralizing Mirror-image (l-)Aptamer Prevents Organ Failure and Improves Survival in Experimental Sepsis,” *Molecular Therapy*, vol. 21, no. 12, p. 2236, 2013, doi: 10.1038/MT.2013.178.
- [147] L. Yatime, C. Maasch, K. Hoehlig, S. Klussmann, G. R. Andersen, and A. Vater, “Structural basis for the targeting of complement anaphylatoxin C5a using a mixed L-RNA/L-DNA aptamer,” *Nature Communications 2015 6:1*, vol. 6, no. 1, pp. 1–13, Apr. 2015, doi: 10.1038/ncomms7481.
- [148] K. Bujko, S. Rzeszotek, K. Hoehlig, J. Yan, A. Vater, and M. Z. Ratajczak, “Signaling of the Complement Cleavage Product Anaphylatoxin C5a Through C5aR (CD88) Contributes to Pharmacological Hematopoietic Stem Cell Mobilization,” *Stem Cell Rev Rep*, vol. 13, no. 6, pp. 793–800, Dec. 2017, doi: 10.1007/S12015-017-9769-6.
- [149] A. Schreiber, H. Xiao, J. C. Jennette, W. Schneider, F. C. Luft, and R. Kettritz, “C5a receptor mediates neutrophil activation and ANCA-induced glomerulonephritis,” *J Am Soc Nephrol*, vol. 20, no. 2, pp. 289–298, 2009, doi: 10.1681/ASN.2008050497.
- [150] J. Dick *et al.*, “C5a receptor 1 promotes autoimmunity, neutrophil dysfunction and injury in experimental anti-myeloperoxidase glomerulonephritis,” *Kidney Int*, vol. 93, no. 3, pp. 615–625, Mar. 2018, doi: 10.1016/J.KINT.2017.09.018.

- [151] A. R. Kitching *et al.*, “ANCA-associated vasculitis,” *Nat Rev Dis Primers*, vol. 6, no. 1, Dec. 2020, doi: 10.1038/S41572-020-0204-Y.
- [152] X. Liu *et al.*, “Differential contributions of the C5b-9 and C5a/C5aR pathways to microvascular and macrovascular thrombosis in complement-mediated thrombotic microangiopathy patients,” *Clin Immunol*, vol. 259, p. 109871, Feb. 2023, doi: 10.1016/J.CLIM.2023.109871.
- [153] S. V. Seshan, C. W. Franzke, P. Redecha, M. Monestier, N. Mackman, and G. Girardi, “Role of tissue factor in a mouse model of thrombotic microangiopathy induced by antiphospholipid antibodies,” *Blood*, vol. 114, no. 8, pp. 1675–1683, 2009, doi: 10.1182/BLOOD-2009-01-199117.
- [154] K. Zhang *et al.*, “C5a/C5aR pathway accelerates renal ischemia-reperfusion injury by downregulating PGRN expression,” *Int Immunopharmacol*, vol. 53, pp. 17–23, Dec. 2017, doi: 10.1016/J.INTIMP.2017.10.006.
- [155] M. Blasco, E. Guillén-Olmos, M. Diaz-Ricart, and M. Palomo, “Complement Mediated Endothelial Damage in Thrombotic Microangiopathies,” *Front Med (Lausanne)*, vol. 9, Apr. 2022, doi: 10.3389/FMED.2022.811504.
- [156] N. J. Gloude *et al.*, “Circulating dsDNA, endothelial injury, and complement activation in thrombotic microangiopathy and GVHD,” *Blood*, vol. 130, no. 10, pp. 1259–1266, Sep. 2017, doi: 10.1182/BLOOD-2017-05-782870.
- [157] E. Gavriilaki *et al.*, “Role of the lectin pathway of complement in hematopoietic stem cell transplantation-associated endothelial injury and thrombotic microangiopathy,” *Exp Hematol Oncol*, vol. 10, no. 1, Dec. 2021, doi: 10.1186/S40164-021-00249-8.
- [158] P. Shivshankar, Y. D. Li, S. L. Mueller-Ortiz, and R. A. Wetsel, “In response to complement anaphylatoxin peptides C3a and C5a, human vascular endothelial cells migrate and mediate the activation of B-cells and polarization of T-cells,” *FASEB J*, vol. 34, no. 6, pp. 7540–7560, Jun. 2020, doi: 10.1096/FJ.201902397R.
- [159] C. W. van den Berg, D. V. Tambourgi, H. W. Clark, S. J. Hoong, O. B. Spiller, and E. P. McGreal, “Mechanism of neutrophil dysfunction: neutrophil serine proteases cleave and inactivate the C5a receptor,” *J Immunol*, vol. 192, no. 4, pp. 1787–1795, Feb. 2014, doi: 10.4049/JIMMUNOL.1301920.

- [160] S. Ortiz-Espinosa *et al.*, “Complement C5a induces the formation of neutrophil extracellular traps by myeloid-derived suppressor cells to promote metastasis,” *Cancer Lett*, vol. 529, pp. 70–84, Mar. 2022, doi: 10.1016/J.CANLET.2021.12.027.
- [161] S. A. Apostolidis *et al.*, “Signaling Through FcγRIIA and the C5a-C5aR Pathway Mediate Platelet Hyperactivation in COVID-19,” *Front Immunol*, vol. 13, Mar. 2022, doi: 10.3389/FIMMU.2022.834988.
- [162] H. Nording *et al.*, “Platelets regulate ischemia-induced revascularization and angiogenesis by secretion of growth factor-modulating factors,” *Blood Adv*, vol. 7, no. 21, pp. 6411–6427, Nov. 2023, doi: 10.1182/BLOODADVANCES.2021006891.
- [163] C. Grossklaus, B. Damerou, E. Lemgo, and W. Vogt, “Induction of platelet aggregation by the complement-derived peptides C3a and C5a,” *Naunyn Schmiedebergs Arch Pharmacol*, vol. 295, no. 1, pp. 71–76, Oct. 1976, doi: 10.1007/BF00509775.
- [164] S. Aiello *et al.*, “C5a and C5aR1 are key drivers of microvascular platelet aggregation in clinical entities spanning from aHUS to COVID-19,” *Blood Adv*, vol. 6, no. 3, pp. 866–881, Feb. 2022, doi: 10.1182/BLOODADVANCES.2021005246.
- [165] C. Q. Schmidt, H. Schrezenmeier, and D. Kavanagh, “Complement and the prothrombotic state,” *Blood*, vol. 139, no. 13, pp. 1954–1972, Mar. 2022, doi: 10.1182/BLOOD.2020007206.
- [166] S. F. Chen and M. Chen, “Complement Activation in Progression of Chronic Kidney Disease,” *Adv Exp Med Biol*, vol. 1165, pp. 423–441, 2019, doi: 10.1007/978-981-13-8871-2_20.
- [167] D. Jalal *et al.*, “Endothelial Microparticles and Systemic Complement Activation in Patients With Chronic Kidney Disease,” *J Am Heart Assoc*, vol. 7, no. 14, Jul. 2018, doi: 10.1161/JAHA.117.007818.
- [168] C. Kurts, F. Ginhoux, and U. Panzer, “Kidney dendritic cells: fundamental biology and functional roles in health and disease,” *Nature Reviews Nephrology* 2020 16:7, vol. 16, no. 7, pp. 391–407, May 2020, doi: 10.1038/s41581-020-0272-y.
- [169] A. Zaal, B. Nota, K. S. Moore, M. Dieker, S. M. van Ham, and A. ten Brinke, “TLR4 and C5aR crosstalk in dendritic cells induces a core regulatory network of RSK2, PI3Kβ, SGK1, and FOXO transcription factors,” *J Leukoc Biol*, vol. 102, no. 4, pp. 1035–1054, Oct. 2017, doi: 10.1189/JLB.2MA0217-058R.

8.Acknowledgement

There are so many people who guide me and inspired me throughout my doctoral studies, I would like to express my sincere gratitude to all those lovely people.

I would like to extend heartfelt gratitude to my mentor Prof.Hans-Joachim Anders who gave the valuable opportunity to join our loving kidney laboratory. Thank you for your exceptional guidance with your professional knowledge, providing constructive advice during the process of my whole PHD program. He has helped me to develop my research ideas, edit my work and connect with other researchers in my field. I am especially grateful for his encouragement and during tough times. Your supports with transition to a new professional perspective is invaluable to me and inspire my academic career. In addition I would also like to acknowledge the supports of Dr.Elmina Mammadova-Bach, Dr.Stefanie Steiger for your continuous advices and suggestions for my research work and life at laboratory of the renal Division at LMU. And I would also like to give my gratitude to Dr. Seven Klussmann, Dr. Axel Vater, Aptarion Biotech, for sharing their generosity in sharing their knowledge and cooperation to fulfill this thesis.

I would like to give my sincere appreciations to my colleagues, Tamisa Seeko Bandeira Honda, Kanako Watanabe-Kusunaki, Chongxu Shi who thoughtfully not just teach me experimental approaches but also helped me to critical thinking, how to handle troubleshooting, and countless discussions. To Anna Anfimiadou and Janina Mandelbaum also thanks for their preparation of immunohistology kidney sections, thank you very much for your supports. I would also like to take this opportunity to be grateful to my other colleagues Qiuyue, Meisi, Qiubo, Chenyu, Li for their love and encouragements. I would like to extend my appreciation for the countless discussions, brainstorming sessions, and moments of shared enthusiasm that made the research process both enjoyable and enlightening.

I owe my deepest appreciations to express my heartfelt gratitude for my family for their unwavering support and love. Their encouragement has been my strength, and I am truly blessed to have such an amazing family.

I am grateful to everyone who appear in my life for your unwavering support and friendship throughout this challenging but rewarding journey. In the end, I must express my deep appreciations to the animals for the scarification of human beings.

Date:

Danyang Zhao

Affidavit



Affidavit

Danyang Zhao
Surname, first name

Goethestrasse 31
Street

80336 ,Munich, Germany
Zip code, town, country

I hereby declare, that the submitted thesis entitled:

.Complement C5a blockade is sufficient to resolve crystalline thrombotic microangiopathy.....

is my own work. I have only used the sources indicated and have not made unauthorised use of services of a third party. Where the work of others has been quoted or reproduced, the source is always given.

I further declare that the dissertation presented here has not been submitted in the same or similar form to any other institution for the purpose of obtaining an academic degree.

Munich 26.03.2024
place, date

Danyang Zhao
Signature doctoral candidate